

D-GCCA: Decomposition-based Generalized Canonical Correlation Analysis for Multi-view High-dimensional Data

Hai Shu*

HS120@NYU.EDU

*Department of Biostatistics
School of Global Public Health
New York University
New York, NY 10003, USA*

Zhe Qu

ZQU2@TULANE.EDU

*Department of Mathematics
Tulane University
New Orleans, LA 70118, USA*

Hongtu Zhu

HTZHU@EMAIL.UNC.EDU

*Departments of Biostatistics, Statistics, Computer Science, and Genetics
The University of North Carolina at Chapel Hill
Chapel Hill, NC 27599, USA*

Editor: Qiaozhu Mei

Abstract

Modern biomedical studies often collect multi-view data, that is, multiple types of data measured on the same set of objects. A popular model in high-dimensional multi-view data analysis is to decompose each view's data matrix into a low-rank common-source matrix generated by latent factors common across all data views, a low-rank distinctive-source matrix corresponding to each view, and an additive noise matrix. We propose a novel decomposition method for this model, called decomposition-based generalized canonical correlation analysis (D-GCCA). The D-GCCA rigorously defines the decomposition on the \mathcal{L}^2 space of random variables in contrast to the Euclidean dot product space used by most existing methods, thereby being able to provide the estimation consistency for the low-rank matrix recovery. Moreover, to well calibrate common latent factors, we impose a desirable orthogonality constraint on distinctive latent factors. Existing methods, however, inadequately consider such orthogonality and may thus suffer from substantial loss of undetected common-source variation. Our D-GCCA takes one step further than generalized canonical correlation analysis by separating common and distinctive components among canonical variables, while enjoying an appealing interpretation from the perspective of principal component analysis. Furthermore, we propose to use the variable-level proportion of signal variance explained by common or distinctive latent factors for selecting the variables most influenced. Consistent estimators of our D-GCCA method are established with good finite-sample numerical performance, and have closed-form expressions leading to efficient computation especially for large-scale data. The superiority of D-GCCA over state-of-the-art methods is also corroborated in simulations and real-world data examples.

Keywords: Canonical variable, common and distinctive variation structures, data integration, high-dimensional data, multi-view data.

*. Corresponding author.

1. Introduction

Data integration is widely used in biomedical studies to combine multi-view data, which are multiple types (i.e., views) of data obtained from the same set of objects, into meaningful and valuable information. Such studies include The Cancer Genome Atlas (TCGA; Hoadley et al., 2018) with multi-platform genomic data for tumor samples, and Human Connectome Project (HCP; Van Essen et al., 2013) with multi-modal brain images of healthy adults, among many others (Crawford et al., 2016; Jensen et al., 2017). The use of multi-view data can allow us to enhance understanding the etiology of many complex diseases, such as cancers (Ciriello et al., 2015; Campbell et al., 2018) and neurodegenerative diseases (Weiner et al., 2013; Saeed et al., 2017). Researchers hence have become highly interested in studying the shared and individual information across multi-view data through separating their common and distinctive variation structures (van der Kloet et al., 2016; Smilde et al., 2017).

Let $\mathbf{Y}_k \in \mathbb{R}^{p_k \times n}$ ($k = 1, \dots, K$) be the row-mean centered data matrix of the k th view of K -view data obtained on a common set of n objects, where p_k is the number of variables. One popular approach for disentangling their common and distinctive variation structures is to decompose each data matrix into

$$\mathbf{Y}_k = \mathbf{X}_k + \mathbf{E}_k = \mathbf{C}_k + \mathbf{D}_k + \mathbf{E}_k \quad \text{for } k = 1, \dots, K, \quad (1)$$

where \mathbf{X}_k is a low-rank signal matrix with an additive noise matrix \mathbf{E}_k , \mathbf{C}_k is a low-rank *common-source matrix* that represents the part of \mathbf{X}_k coming from the underlying source of variation (a.k.a. latent factors) common across all views, and \mathbf{D}_k is a low-rank *distinctive-source matrix* from distinctive latent factors of the corresponding view. In other words, the common-source and distinctive-source matrices contain the variation information in each view, respectively, explained by the common and distinctive latent factors of the K views.

There is a growing literature on developing decomposition methods for model (1). Throughout this paper, we will consider six state-of-the-art methods, including orthogonal n-block partial least squares (OnPLS; Löfstedt and Trygg, 2011), distinctive and common components with simultaneous component analysis (DISCO-SCA; Schouteden et al., 2013), common orthogonal basis extraction (COBE; Zhou et al., 2016), joint and individual variation explained (JIVE; Lock et al., 2013) and its variant R.JIVE (O'Connell and Lock, 2016), and the angle-based JIVE (AJIVE; Feng et al., 2018). The decomposition differs per method. OnPLS is developed from a multi-block partial least squares (PLS) method that is equivalent to the generalized canonical correlation analysis (GCCA) using the sum of covariances criterion (Tenenhaus and Tenenhaus, 2011). Both DISCO-SCA and JIVE are based on the simultaneous component analysis (SCA; Smilde et al., 2003) that applies the principal component analysis (PCA) to the concatenation of all observed data matrices, but DISCO-SCA imposes more orthogonality constraints. R.JIVE is a JIVE variant with an additional orthogonality constraint. Both AJIVE and COBE can be regarded as extensions of the maximum-variance based GCCA (Kettenring, 1971), but with different denoising strategies. Although PLS, SCA, and GCCA are widely-used data integration methods, they solve problems different from (1) and are only used as one step of the above methods. Problem (1) belongs to the scope of multi-block or multi-view data analysis that covers a wide spectrum of topics, on which we refer readers to Zhao et al. (2017), Li et al. (2018) and Mishra et al. (2021) for reviews.

The six state-of-the-art methods for model (1) can be applied to data with $K \geq 2$ views, but suffer from two major issues. (i) They are built on the inappropriate Euclidean dot product space (\mathbb{R}^n, \cdot) , which simply approximates the \mathcal{L}^2 space of random variables. (ii) They inadequately consider orthogonality (i.e., uncorrelatedness) constraints among distinctive-source matrices $\{\mathbf{D}_k\}_{k=1}^K$, so there is no guarantee against the risk that $\{\mathbf{D}_k\}_{k=1}^K$ are all pairwise correlated and thus retain some undiscovered common latent factors and their explained variation. To address these issues, a nice decomposition, called decomposition-based canonical correlation analysis (D-CCA), is recently proposed in Shu et al. (2020) based on the canonical correlation analysis (CCA; Hotelling, 1936), but unfortunately, it is limited to two data views, $K = 2$.

The aim of this paper is to address issues (i) and (ii) for data with $K \geq 2$ views. We assume that the columns of each matrix in (1) are n independent copies of the corresponding random vector in

$$\mathbf{y}_k = \mathbf{x}_k + \mathbf{e}_k = \mathbf{c}_k + \mathbf{d}_k + \mathbf{e}_k \in \mathbb{R}^{p_k}, \quad (2)$$

with entries of \mathbf{c}_k , \mathbf{d}_k and \mathbf{e}_k belonging to \mathcal{L}_0^2 , where \mathbf{c}_k and \mathbf{d}_k are called the *common-source random vector* and the *distinctive-source random vector*, respectively, generated by common and distinctive latent factors. Here, \mathcal{L}_0^2 is the vector space composed of all real-valued random variables with zero mean and finite variance. We denote $(\mathcal{L}_0^2, \text{cov})$ as the inner product space of \mathcal{L}_0^2 that is endowed with the covariance operator as the inner product.

A major drawback of the six existing methods is that their decompositions are defined with respect to the orthogonality of (\mathbb{R}^n, \cdot) rather than the more precise orthogonality of $(\mathcal{L}_0^2, \text{cov})$. Obviously, the orthogonality of (\mathbb{R}^n, \cdot) (i.e., zero sample covariance) is not equivalent to that of $(\mathcal{L}_0^2, \text{cov})$ (i.e., zero covariance), and on the contrary, the former excludes any jointly continuous, uncorrelated random variables. Specifically, if $v_1, v_2 \in \mathcal{L}_0^2$ are jointly continuous with $\text{cov}(v_1, v_2) = 0$, then their n independent paired observations $\mathbf{v}_1, \mathbf{v}_2 \in \mathbb{R}^n$ have $P(\mathbf{v}_1 \cdot \mathbf{v}_2 = \mathbf{v}_1^\top \mathbf{v}_2 \neq 0) = 1$ (Rohatgi and Saleh, 2015, p. 134). Hence, (\mathbb{R}^n, \cdot) is not a correct space to define a decomposition for model (1). Moreover, our decomposition defined from $(\mathcal{L}_0^2, \text{cov})$ enables us to investigate the asymptotic consistency of estimating unobservable $\{\mathbf{C}_k, \mathbf{D}_k\}_{k=1}^K$ and their explained proportions of signal variance. In contrast, the six existing methods are unable to establish the estimation consistency.

Furthermore, based on $(\mathcal{L}_0^2, \text{cov})$, we can naturally use the variable-level proportion of signal variance explained by either common or distinctive latent factors in order to quantify their influence on each variable for the purpose of variable selection. In contrast, the existing decomposition methods based on (\mathbb{R}^n, \cdot) only consider the proportion of explained variation at the view level and barely discuss it at the variable level (Smilde et al., 2017). At the view level, they measure the variation of data by the sum of squares of data points; thus, their proportion of signal variation explained, for example, by common latent factors is $\|\mathbf{C}_k\|_F^2 / \|\mathbf{X}_k\|_F^2$, which essentially approximates the statistical quantity $\text{tr}\{\text{cov}(\mathbf{c}_k)\} / \text{tr}\{\text{cov}(\mathbf{x}_k)\}$ in $(\mathcal{L}_0^2, \text{cov})$. More clearly seen at the variable level, variance is superior over the Euclidean sum of squares to measure the variation of a random variable, but with the inevitable, challenging question on the uniform consistency in estimation under high-dimensional settings (Fan et al., 2018). This might be a reason that hinders the use of the variable-level proportion of explained variation in the existing decomposition methods.

Even translated into $(\mathcal{L}_0^2, \text{cov})$, the six competing methods focus on the orthogonality (i.e., uncorrelatedness) between \mathbf{c}_k and \mathbf{d}_k , but they inadequately consider orthogonality

constraints among $\{\mathbf{d}_k\}_{k=1}^K$. Specifically, OnPLS, COBE, JIVE, and AJIVE do not impose any orthogonality on $\{\mathbf{d}_k\}_{k=1}^K$. R.JIVE enforces such orthogonality at the price of relegating its unexplained portion of signal \mathbf{x}_k into noise \mathbf{e}_k . DISCO-SCA often only approximates, but not exactly achieves its target orthogonality for $\{\mathbf{d}_k\}_{k=1}^K$ (van der Kloet et al., 2016). When $K = 2$, the orthogonality between \mathbf{d}_1 and \mathbf{d}_2 desirably assures no common latent factors retained between them. For $K > 2$, with the same aim to well capture the common latent factors, a similar desirable orthogonality constraint on $\{\mathbf{d}_k\}_{k=1}^K$ is that at least one pair among them are uncorrelated. However, it is unclear how to build a decomposition for all $K \geq 2$ that can ensure both the above desirable orthogonality among $\{\mathbf{d}_k\}_{k=1}^K$ and the interpretability of associated $\{\mathbf{c}_k\}_{k=1}^K$.

We propose a novel method, called decomposition-based generalized canonical correlation analysis (D-GCCA), to handle model (1)-(2) with $K \geq 2$ views. Our method is equivalent to D-CCA when $K = 2$. The key idea of D-GCCA is to divide the decomposition problem (2) into multiple sub-problems via Carroll's GCCA (Carroll, 1968). We slightly relax the aforementioned desirable orthogonality of $\{\mathbf{d}_k\}_{k=1}^K$ by enforcing it for each sub-problem. This in turn leads to a geometrically interpretable definition of $\{\mathbf{c}_k\}_{k=1}^K$ on space $(\mathcal{L}_0^2, \text{cov})$ by connecting Carroll's GCCA with PCA. In particular, our defined common latent factors of $\{\mathbf{x}_k\}_{k=1}^K$ represent the same contribution made by the principal basis of the entire signal space $\sum_{k=1}^K \text{span}(\mathbf{x}_k^\top)$ in generating each of the K signal subspaces $\{\text{span}(\mathbf{x}_k^\top)\}_{k=1}^K$. Here, for any random vectors \mathbf{v}_1 and \mathbf{v}_2 with entries in $(\mathcal{L}_0^2, \text{cov})$, $\text{span}(\mathbf{v}_1^\top)$ denotes the subspace of $(\mathcal{L}_0^2, \text{cov})$ that is spanned by entries of \mathbf{v}_1 , and $\text{span}(\mathbf{v}_1^\top) + \text{span}(\mathbf{v}_2^\top) = \text{span}((\mathbf{v}_1^\top, \mathbf{v}_2^\top))$.

Estimating matrices $\{\mathbf{C}_k, \mathbf{D}_k\}_{k=1}^K$ and their proportions of explained signal variance poses theoretical and computational difficulties for high-dimensional data. The observed high-dimensional matrices $\{\mathbf{Y}_k\}_{k=1}^K$ are often high-rank in practice. If the high-rank \mathbf{Y}_k is directly treated as the signal, its associated high-rank covariance matrix can be inconsistently estimated by the traditional sample covariance matrix due to the curse of "intrinsic" high dimensionality (Yin et al., 1988; Vershynin, 2012). Low-rank signal \mathbf{X}_k or equivalently low-rank $\text{cov}(\mathbf{x}_k)$ is thus often assumed to facilitate the construction of consistent estimates (Shu et al., 2020). Fortunately, big data matrices are often approximately low-rank in many real-world applications (Udell and Townsend, 2019), and their low-rank approximations render feasible or more efficient computation, while retaining the major portion of information (Kishore Kumar and Schneider, 2017). We consider the low-rank plus noise structure given in (1)-(2) under the widely used high-dimensional spiked covariance model (Fan et al., 2013; Wang and Fan, 2017; Shu et al., 2020). Subsequently, we propose soft-thresholding based estimators for $\{\mathbf{C}_k, \mathbf{D}_k\}_{k=1}^K$ and therefrom derive estimators for the proportions of signal variance explained by either common or distinctive latent factors. Convergence properties of our estimators are established with reasonably good finite-sample performance shown by simulations. The proposed estimators have closed-form expressions and thus are more computationally efficient than most existing methods that use time-expensive iterative optimization algorithms. For example, to decompose three $91,282 \times 1080$ data matrices in our HCP application, our approach can complete in 18 seconds on a single computing node, whereas some state-of-the-art methods cannot converge within 5 hours.

The contributions of this paper are summarized below:

- We propose a novel decomposition method, called D-GCCA, for tackling $K \geq 2$ data views under model (1), based on $(\mathcal{L}_0^2, \text{cov})$ instead of (\mathbb{R}^n, \cdot) . Our distinctive-source matrices are especially imposed with an orthogonality constraint to avoid substantial loss of undetected common-source variation. The proposed common-source matrices exhibit a geometric interpretation from the perspective of PCA. Our D-GCCA reduces to D-CCA when $K = 2$.
- We establish consistent estimators for our defined common-source and distinctive-source matrices under high-dimensional settings with convergence rates in both the Frobenius norm and the spectral norm. The proposed estimators have closed-form expressions and thus are computationally efficient. To the best of our knowledge, this is the first work that establishes the high-dimensional estimation consistency under model (1) with $K \geq 2$.
- We propose to use the variable-level proportion of signal variance explained by either common or distinctive latent factors for selecting the most influenced variables. Consistent estimators are theoretically established and numerically verified.
- We compare our D-GCCA with the six competing methods on both simulated and real-world data to show the superiority of proposed method for separating the common-source and distinctive-source variations across multi-view data.
- As a byproduct, we reformulate Carroll's GCCA from the traditional (\mathbb{R}^n, \cdot) to the more precise $(\mathcal{L}_0^2, \text{cov})$ and provide some useful properties, which may facilitate the use of GCCA in statistical data integration.

The rest of this paper is organized as follows. We introduce our random-variable version of Carroll's GCCA and propose our D-GCCA method in Section 2. We propose our estimation approach of high-dimensional D-GCCA and establish its asymptotic properties in Section 3. Section 4 evaluates the finite-sample performance of proposed estimators via simulations. We also compare D-GCCA with the six competing methods through simulated data in Section 4 and through two real-world data examples from TCGA and HCP in Section 5. Concluding remarks are made in Section 6. All theoretical proofs and additional simulation results are presented in Appendices. A Python package for the proposed D-GCCA method is available at <https://github.com/shu-hai/D-GCCA>.

We now introduce some notation. For a real matrix $\mathbf{M} = (M_{ij})_{1 \leq i \leq p, 1 \leq j \leq n}$, the ℓ th largest singular value is denoted by $\sigma_\ell(\mathbf{M})$, the ℓ th largest eigenvalue when $p = n$ is $\lambda_\ell(\mathbf{M})$, the spectral norm is $\|\mathbf{M}\|_2 = \sigma_1(\mathbf{M})$, the Frobenius norm is $\|\mathbf{M}\|_F = (\sum_{i=1}^p \sum_{j=1}^n M_{ij}^2)^{1/2}$, the matrix \mathcal{L}^∞ norm is $\|\mathbf{M}\|_\infty = \max_{1 \leq i \leq p} \sum_{j=1}^n |M_{ij}|$, the max norm is $\|\mathbf{M}\|_{\max} = \max_{1 \leq i \leq p, 1 \leq j \leq n} |M_{ij}|$, and the Moore-Penrose pseudoinverse is \mathbf{M}^\dagger . Denote $\mathbf{M}^{[s:t,u:v]}$, $\mathbf{M}^{[s:t,:]}$, and $\mathbf{M}^{[:,u:v]}$ as the submatrices $(M_{ij})_{s \leq i \leq t, u \leq j \leq v}$, $(M_{ij})_{s \leq i \leq t, 1 \leq j \leq n}$, and $(M_{ij})_{1 \leq i \leq p, u \leq j \leq v}$ of \mathbf{M} , respectively. Let $[\mathbf{M}_1; \dots; \mathbf{M}_N] = (\mathbf{M}_1^\top, \dots, \mathbf{M}_N^\top)^\top$ be the row-wise concatenation of matrices $\mathbf{M}_1, \dots, \mathbf{M}_N$ that have the same number of columns. We write the j th entry of a vector \mathbf{v} by $\mathbf{v}^{[j]}$, and $\mathbf{v}^{[s:t]} = (\mathbf{v}^{[s]}, \mathbf{v}^{[s+1]}, \dots, \mathbf{v}^{[t]})^\top$. For any random vectors \mathbf{v}_1 and \mathbf{v}_2 , denote $\text{cov}(\mathbf{v}_1, \mathbf{v}_2)$ as the covariance matrix of \mathbf{v}_1 and \mathbf{v}_2 whose (i, j) th entry is $\text{cov}(\mathbf{v}_1^{[i]}, \mathbf{v}_2^{[j]})$, and write $\text{cov}(\mathbf{v}_1) = \text{cov}(\mathbf{v}_1, \mathbf{v}_1)$. Define $(v_i)_{i \in \mathcal{I}}$ by $(v_{i_1}, \dots, v_{i_q})$ with $\mathcal{I} = \{i_1, \dots, i_q\}$

and $i_1 < \dots < i_q$. The angle between any $x, y \in (\mathcal{L}_0^2, \text{cov})$ is denoted by $\theta(x, y)$, and the norm of x is $\|x\| = \sqrt{\text{var}(x)}$. We use $\cos\{\theta(x, y)\}$ and $\text{corr}(x, y)$ exchangeably, and define $\text{corr}(x, 0) = 0$. The symbol \perp used between two subspaces, sets, and/or random variables in $(\mathcal{L}_0^2, \text{cov})$ means their orthogonality, i.e., uncorrelatedness. Define $r_0 = 0$, $r_k = \text{rank}\{\text{cov}(\mathbf{x}_k)\}$, and $r_f = \text{rank}\{\text{cov}([\mathbf{x}_1; \dots; \mathbf{x}_K])\}$. Note that $r_k = \dim\{\text{span}(\mathbf{x}_k^\top)\}$ and $r_f = \dim\{\text{span}([\mathbf{x}_1; \dots; \mathbf{x}_K]^\top)\}$. For two sequences, write $a_n \asymp b_n$ iff $a_n = O(b_n)$ and $b_n = O(a_n)$, and $a_n \lesssim_P b_n$ iff $a_n = O_P(b_n)$. Throughout the paper, the asymptotic arguments are by default under $n \rightarrow \infty$.

2. Methodology

We first develop the random-variable version of Carroll's GCCA in $(\mathcal{L}_0^2, \text{cov})$ and then use it to derive our D-GCCA decomposition.

2.1 Generalized canonical correlation analysis

In the literature, many GCCA methods extend CCA to more than two data views based on different optimization criteria, such as the sum of correlations, the maximum variance (MAXVAR), and the minimum variance (MINVAR) (Horst, 1961; Carroll, 1968; Kettenring, 1971). We derive our D-GCCA for model (1)-(2) by using Carroll's GCCA (Carroll, 1968).

We first translate Carroll's GCCA into the space $(\mathcal{L}_0^2, \text{cov})$. Carroll's GCCA was originally proposed and is often studied in (\mathbb{R}^n, \cdot) using data samples (e.g., Carroll, 1968; van de Velden, 2011; Draper et al., 2014). Kettenring (1971) briefly mentioned that the random-variable version of Carroll's GCCA is a mixture of the MAXVAR and MINVAR methods. We provide the solution to the optimization problem of Carroll's GCCA in $(\mathcal{L}_0^2, \text{cov})$ as well as some important properties.

For subspaces $\{\text{span}(\mathbf{x}_k^\top)\}_{k=1}^K$, the Carroll's GCCA in $(\mathcal{L}_0^2, \text{cov})$ sequentially finds the closest elements among the K subspaces. The method has r_f stages. The ℓ th stage finds the closest elements, denoted as $z_1^{(\ell)}, \dots, z_K^{(\ell)}$, among the K subspaces, which are called the ℓ th-stage canonical variables, along with an auxiliary variable $w^{(\ell)}$ as follows:

$$\begin{aligned} \{z_1^{(\ell)}, \dots, z_K^{(\ell)}, w^{(\ell)}\} &= \arg \max_{\{z_1, \dots, z_K, w\}} \sum_{k=1}^K \cos^2\{\theta(z_k, w)\} \\ \text{subject to } &\begin{cases} z_k \in \text{span}(\mathbf{x}_k^\top), \|z_k\| = 1, \\ w \perp \{w^{(j)}\}_{j=0}^{\ell-1}, w \in \mathcal{L}_0^2, \|w\| = 1, w^{(0)} = 0. \end{cases} \end{aligned} \tag{3}$$

In $(\mathcal{L}_0^2, \text{cov})$, the cosine similarity $\cos\{\theta(\cdot, \cdot)\}$ is equal to $\text{corr}(\cdot, \cdot)$. The auxiliary variable $w^{(\ell)}$ is the variable closest to all $\{z_k^{(\ell)}\}_{k=1}^K$, and the sum of its squared cosine similarities with $\{z_k^{(\ell)}\}_{k=1}^K$ is used to measure the closeness of $\{z_k^{(\ell)}\}_{k=1}^K$. The variable $w^{(\ell)}$ is also called the consensus variable of $\{z_k^{(\ell)}\}_{k=1}^K$ in the literature (Kiers et al., 1994; Dahl and Næs, 2006). Figure 2 (a) illustrates the Carroll's GCCA.

Let \mathbf{f}_k^\top be an arbitrary orthonormal basis of $\text{span}(\mathbf{x}_k^\top)$, $\mathbf{f} = [\mathbf{f}_1; \dots; \mathbf{f}_K]$, and $\{\boldsymbol{\eta}^{(\ell)}\}_{1 \leq \ell \leq r_f}$ be any r_f orthonormal eigenvectors of $\text{cov}(\mathbf{f})$, where $\boldsymbol{\eta}^{(\ell)} = [\boldsymbol{\eta}_1^{(\ell)}; \dots; \boldsymbol{\eta}_K^{(\ell)}]$ corresponds to

eigenvalue $\lambda_\ell(\text{cov}(\mathbf{f}))$ with $\boldsymbol{\eta}_k^{(\ell)} \in \mathbb{R}^{r_k}$. We have $r_f = \text{rank}\{\text{cov}(\mathbf{f})\}$. The following theorem presents the solution to (3) as well as some useful properties for our decomposition method.

Theorem 1 *The following results hold.*

(i) *For $\ell \leq r_f$ and $k \leq K$, the solution of (3) is given by*

$$z_k^{(\ell)} = \begin{cases} \text{any standardized variable in } \text{span}(\mathbf{x}_k^\top), & \text{if } \boldsymbol{\eta}_k^{(\ell)} = \mathbf{0}, \\ \pm(\boldsymbol{\eta}_k^{(\ell)} / \|\boldsymbol{\eta}_k^{(\ell)}\|_F)^\top \mathbf{f}_k, & \text{if } \boldsymbol{\eta}_k^{(\ell)} \neq \mathbf{0}, \end{cases} \quad (4)$$

$$w^{(\ell)} = [\lambda_\ell(\text{cov}(\mathbf{f}))]^{-1/2} (\boldsymbol{\eta}^{(\ell)})^\top \mathbf{f}. \quad (5)$$

Moreover, we have

$$\begin{aligned} \cos\{\theta(z_k^{(\ell)}, w^{(\ell)})\} &= \pm[\lambda_\ell(\text{cov}(\mathbf{f}))]^{1/2} \|\boldsymbol{\eta}_k^{(\ell)}\|_F, \\ \sum_{k=1}^K \cos^2\{\theta(z_k^{(\ell)}, w^{(\ell)})\} &= \lambda_\ell(\text{cov}(\mathbf{f})), \end{aligned} \quad (6)$$

$$\sum_{k=1}^K \text{span}(\mathbf{x}_k^\top) = \text{span}(\{w^{(\ell)}\}_{\ell=1}^{r_f}). \quad (7)$$

(ii) *For $\ell \leq r_f$, re-define $z_k^{(\ell)}$ in (4) to be*

$$z_k^{(\ell)} = \begin{cases} 0, & \text{if } \boldsymbol{\eta}_k^{(\ell)} = \mathbf{0}, \text{ i.e., } w^{(\ell)} \perp \text{span}(\mathbf{x}_k^\top), \\ (\boldsymbol{\eta}_k^{(\ell)} / \|\boldsymbol{\eta}_k^{(\ell)}\|_F)^\top \mathbf{f}_k, & \text{otherwise.} \end{cases} \quad (8)$$

Then, we have $\theta(z_k^{(\ell)}, w^{(\ell)}) \in [0, \pi/2]$ and $\text{span}(\{z_k^{(\ell)}\}_{\ell=1}^{r_f}) = \text{span}(\mathbf{x}_k^\top)$.

(iii) *For $z_k^{(\ell)}$ in either (4) or (8), if $\lambda_\ell(\text{cov}(\mathbf{f})) \leq 1$ and $\text{span}(\{z_k^{(m)}\}_{m=1}^{\ell-1}) \neq \text{span}(\mathbf{x}_k^\top)$ for some ℓ and k , then there exists a $w^{(\ell)} \in \text{span}(\mathbf{x}_k^\top)$ such that $w^{(\ell)} \perp \sum_{1 \leq j \neq k \leq K} \text{span}(\mathbf{x}_j^\top)$.*

In the following text, if without further clarification, we refer $z_k^{(\ell)}$ to the one defined in (8) so that $\theta(z_k^{(\ell)}, w^{(\ell)})$ falls into $[0, \pi/2]$.

Unlike our D-GCCA for disentangling the common and distinctive latent factors and their explained variations among multiple data views, the existing GCCA methods (e.g., Horst, 1961; Carroll, 1968; Kettenring, 1971; Tenenhaus and Tenenhaus, 2011, 2014; Cai and Huo, 2020) often focus on finding the canonical variables $\{z_k^{(\ell)}\}_{k=1}^K$, which are merely the most correlated components among the multiple views, and studying the coefficients in their linear expressions formed by corresponding signal variables $\{\mathbf{x}_k^{[i]}\}_{i=1}^{p_k}$. The auxiliary variables $w^{(\ell)}$ s of Carroll's GCCA or its variant MAXVAR GCCA are also called as a consensus or common latent representation of multi-view data in the literature (Kiers et al., 1994; Dahl and Næs, 2006; Fu et al., 2017; Benton et al., 2019), but they do not solve our problem in (1)-(2), which also involves distinctive latent factors. As extensions of MAXVAR GCCA for (1)-(2), AJIVE and COBE treat the consensus variables $w^{(\ell)}$ s as the common latent factors and define \mathbf{c}_k as the projection of \mathbf{x}_k onto the space spanned by $w^{(\ell)}$ s. This simple approach

is undesirable even for $K = 2$ views, where both Carroll's GCCA and MAXVAR GCCA reduce to CCA. For example, if $\mathbf{x}_k = z_k^{(1)}$ for $k \leq K = 2$, then one only needs to consider the first-stage consensus variable $w^{(1)}$. Let \mathbf{c}_k be the projection of $\mathbf{x}_k = z_k^{(1)}$ onto $w^{(1)}$, then $\mathbf{c}_k = (z_1^{(1)} + z_2^{(1)})/2$ and $\mathbf{d}_1 = -\mathbf{d}_2 = (z_1^{(1)} - z_2^{(1)})/2$, but the distinctive-source random vectors \mathbf{d}_1 and \mathbf{d}_2 now share the same latent factor $(z_1^{(1)} - z_2^{(1)})/2$, contradicting their definition that they are generated from distinctive latent factors. In contrast, our D-GCCA, detailed in the next subsection, yields $\mathbf{d}_1 \perp \mathbf{d}_2$ with $\mathbf{c}_k = [1 - \tan\{\theta(z_1^{(1)}, z_2^{(1)})/2\}](z_1^{(1)} + z_2^{(1)})/2$. See Guo and Wu (2019) and Wong et al. (2021) for an overview and recent progress in GCCA-based multi-view data analysis.

2.2 Decomposition-based generalized canonical correlation analysis

2.2.1 COMMON-SOURCE AND DISTINCTIVE-SOURCE MATRICES AND RANDOM VECTORS

In the model given by (1)-(2), the columns of each common-source matrix \mathbf{C}_k or distinctive-source matrix \mathbf{D}_k are assumed to be n independent copies of its corresponding random vector \mathbf{c}_k or \mathbf{d}_k . We thus consider the following decomposition with noise excluded:

$$\mathbf{x}_k = \mathbf{c}_k + \mathbf{d}_k \quad \text{for } k = 1, \dots, K. \quad (9)$$

The estimation of $\{\mathbf{C}_k, \mathbf{D}_k\}_{k=1}^K$ from noisy data $\{\mathbf{Y}_k\}_{k=1}^K$ will be given in Section 3.

Like the divide-and-conquer strategy of D-CCA, our D-GCCA first breaks down decomposition problem (9) into multiple sub-problems. Each ℓ th sub-problem is solved by finding a common variable $c^{(\ell)}$ and K distinctive variables $\{d_k^{(\ell)}\}_{k=1}^K$ for the ℓ th-stage canonical variables $\{z_k^{(\ell)}\}_{k=1}^K$ such that

$$z_k^{(\ell)} = c^{(\ell)} + d_k^{(\ell)} \quad \text{for } k = 1, \dots, K. \quad (10)$$

The ideal orthogonality among $\{\mathbf{d}_k\}_{k=1}^K$ and its reduced version on $\{d_k^{(\ell)}\}_{k=1}^K$ are given below.

(O.1) At least one pair among $\{\text{span}(\mathbf{d}_k^\top)\}_{k=1}^K$ is orthogonal.

(O.2) At least one pair among $\{d_k^{(\ell)}\}_{k=1}^K$ is orthogonal.

The auxiliary variable $w^{(\ell)}$ in (3) naturally serves as the direction variable of our common variable $c^{(\ell)}$ of $\{z_k^{(\ell)}\}_{k=1}^K$. We define $c^{(\ell)}$ by

$$c^{(\ell)} = \alpha^{(\ell)} w^{(\ell)}, \quad (11)$$

where $\alpha^{(\ell)}$ satisfies

(C.1) $|\alpha^{(\ell)}|$ is the smallest value such that (O.2) holds;

(C.2) $\alpha^{(\ell)} < 0$ if (C.1) has two solutions with respect to $\alpha^{(\ell)}$.

The rationale of setting constraints (C.1) and (C.2) is given as follows. Let $\alpha_1^{(\ell)}$ and $\alpha_2^{(\ell)}$ be two candidate values of $\alpha^{(\ell)}$, each of which leads to the required orthogonality (O.2). If $|\alpha_1^{(\ell)}| < |\alpha_2^{(\ell)}|$, then the extra variance ($|\alpha_2^{(\ell)}|^2 - |\alpha_1^{(\ell)}|^2$) for the variable $c^{(\ell)}$ of $\alpha_2^{(\ell)}$ can

be alternatively explained by the variables $\{d_k^{(\ell)}\}_{k=1}^K$ of $\alpha_1^{(\ell)}$. Figure 1 shows a motivating example with $K = 3$ and equal angles among $\{z_k^{(1)}\}_{k=1}^3$; $\alpha^{(1)} = \alpha_1^{(1)}$ is more sensible, because as $\text{corr}(z_1^{(1)}, z_2^{(1)}) = \cos\{\theta(z_1^{(1)}, z_2^{(1)})\}$ increases from 0 to 1, the variance of $c^{(1)} = \alpha_1^{(1)}w^{(1)}$ also increases from 0 to 1, reflecting the strength of the correlation, whereas the variance of $c^{(1)} = \alpha_2^{(1)}w^{(1)}$ is not monotonic. If $\alpha_1^{(\ell)} < 0 < \alpha_2^{(\ell)}$ and $|\alpha_1^{(\ell)}| = |\alpha_2^{(\ell)}|$, then the $d_k^{(\ell)}$ corresponding to $\alpha_1^{(\ell)}$, for $k = 1, \dots, K$, has a larger variance than that to $\alpha_2^{(\ell)}$.

We provide the existence and explicit formula of $\alpha^{(\ell)}$ in the theorem below.

Theorem 2 For $\ell \leq r_f$, $w^{(\ell)}$ in (5), and $\{z_k^{(\ell)}\}_{k=1}^K$ in (8), we have that $\alpha^{(\ell)}$ in (11) exists and satisfies

$$\begin{aligned} \alpha^{(\ell)} \in \arg \min_{\alpha_{jk}^{(\ell)}} \left\{ \left| \alpha_{jk}^{(\ell)} \right| : \alpha_{jk}^{(\ell)} = \frac{1}{2} \left[\cos\{\theta(w^{(\ell)}, z_j^{(\ell)})\} + \cos\{\theta(w^{(\ell)}, z_k^{(\ell)})\} - (\Delta_{jk}^{(\ell)})^{1/2} \right] \right. \\ \left. \text{for } \Delta_{jk}^{(\ell)} \geq 0 \quad \text{and} \quad 1 \leq j < k \leq K \right\} \end{aligned}$$

with $\Delta_{jk}^{(\ell)} = [\cos\{\theta(w^{(\ell)}, z_j^{(\ell)})\} + \cos\{\theta(w^{(\ell)}, z_k^{(\ell)})\}]^2 - 4 \cos\{\theta(z_j^{(\ell)}, z_k^{(\ell)})\}$.

Remark 1 We interpret the decomposition given in (10)-(11) via analyzing the relationship between the entire signal space $\sum_{k=1}^K \text{span}(\mathbf{x}_k^\top)$ and its subspaces $\{\text{span}(\mathbf{x}_k^\top)\}_{k=1}^K$. First, from the perspective of PCA, we consider how the K signal subspaces $\{\text{span}(\mathbf{x}_k^\top)\}_{k=1}^K$ contribute to forming the whole signal space $\sum_{k=1}^K \text{span}(\mathbf{x}_k^\top)$. We use an arbitrary orthonormal basis \mathbf{f}_k^\top of $\text{span}(\mathbf{x}_k^\top)$ to represent its contribution to $\sum_{k=1}^K \text{span}(\mathbf{x}_k^\top)$, because \mathbf{f}_k^\top fully

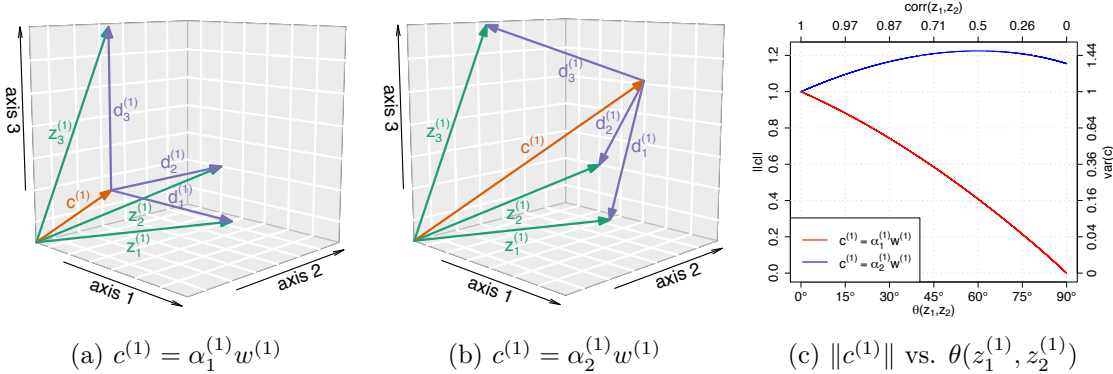


Figure 1: The geometry of D-GCCA for $K = 3$ data views with $\theta(z_1^{(1)}, z_2^{(1)}) = \theta(z_1^{(1)}, z_3^{(1)}) = \theta(z_2^{(1)}, z_3^{(1)}) \in (0^\circ, 90^\circ)$. There are only two possible choices of $\alpha^{(1)}$ for the common variable $c^{(1)} = \alpha^{(1)}w^{(1)}$ such that at least one pair among $\{d_k^{(1)}\}_{k=1}^3$ is orthogonal: $c^{(1)} = \alpha_1^{(1)}w^{(1)}$ in panel (a) and $c^{(1)} = \alpha_2^{(1)}w^{(1)}$ in panel (b), where $\alpha_1^{(1)} < \alpha_2^{(1)}$, and $d_1^{(1)}, d_2^{(1)}$ and $d_3^{(1)}$ are mutually orthogonal. Panel (c) shows that as $\theta(z_1^{(1)}, z_2^{(1)})$ increases or equivalently as $\text{corr}(z_1^{(1)}, z_2^{(1)}) = \cos\{\theta(z_1^{(1)}, z_2^{(1)})\}$ decreases, $\|c^{(1)}\| = \sqrt{\text{var}(c^{(1)})}$ decreases if $c^{(1)} = \alpha_1^{(1)}w^{(1)}$, but is not monotonic if $c^{(1)} = \alpha_2^{(1)}w^{(1)}$. D-GCCA chooses $c^{(1)} = \alpha_1^{(1)}w^{(1)}$.

characterizes $\text{span}(\mathbf{x}_k^\top)$ due to $\text{span}(\mathbf{x}_k^\top) = \{\mathbf{f}_k^\top \mathbf{b} : \forall \mathbf{b} \in \mathbb{R}^{r_k}\}$, and its entries, all of which are standardized variables, provide a fair comparison among subspaces $\{\text{span}(\mathbf{x}_k^\top)\}_{k=1}^K$. By (5) and (7), $\{w^{(\ell)} \sqrt{\lambda_\ell(\text{cov}(\mathbf{f}))}\}_{\ell=1}^{r_f}$ are the r_f principal components of $\mathbf{f}^\top = (\mathbf{f}_1^\top, \dots, \mathbf{f}_K^\top)$, which fully capture the variance of \mathbf{f} , that is, the accumulated contribution to $\sum_{k=1}^K \text{span}(\mathbf{x}_k^\top)$ from all subspaces $\{\text{span}(\mathbf{x}_k^\top)\}_{k=1}^K$. They also constitute an orthogonal basis of $\sum_{k=1}^K \text{span}(\mathbf{x}_k^\top)$ that is the closest to these subspaces in the sense of (3). We thus call standardized variables $\{w^{(\ell)}\}_{\ell=1}^{r_f}$ as the principal basis of $\sum_{k=1}^K \text{span}(\mathbf{x}_k^\top)$ with respect to $\{\text{span}(\mathbf{x}_k^\top)\}_{k=1}^K$. Next, from the perspective of the principal basis $\{w^{(\ell)}\}_{\ell=1}^{r_f}$, we conversely deduce how the entire signal space $\sum_{k=1}^K \text{span}(\mathbf{x}_k^\top)$ generates its subspaces $\{\text{span}(\mathbf{x}_k^\top)\}_{k=1}^K$. With $0/0 := 0$, $z_k^{(\ell)}$ is the normalized projection of $w^{(\ell)}$ onto $\text{span}(\mathbf{x}_k^\top)$. Theorem 1 (ii) shows that the normalized projections $\{z_k^{(\ell)}\}_{\ell=1}^{r_f}$ of $\{w^{(\ell)}\}_{\ell=1}^{r_f}$ span the subspace $\text{span}(\mathbf{x}_k^\top)$ for each $k \leq K$. Hence, the decomposition in (10)-(11) essentially measures the same contribution of the principal-basis component $w^{(\ell)}$ in generating each of the K signal subspaces $\{\text{span}(\mathbf{x}_k^\top)\}_{k=1}^K$.

Remark 2 Let $L = \max\{\ell \in \{1, \dots, r_f\} : \lambda_\ell(\text{cov}(\mathbf{f})) > 1\}$. We only need to consider the first L principal-basis components $\{w^{(\ell)}\}_{\ell=1}^L$ due to the following reasons. For $\ell > L$, by Theorem 1 (iii), either there exists a $w^{(\ell)} \in \text{span}(\mathbf{x}_k^\top)$ for some k that is orthogonal to all the other signal subspaces $\{\text{span}(\mathbf{x}_j^\top)\}_{j \neq k}$, or otherwise, $\{z_k^{(m)}\}_{m=1}^{\ell-1}$ has spanned the subspace $\text{span}(\mathbf{x}_k^\top)$ for all $k = 1, \dots, K$. The first scenario results in $c^{(\ell)} = 0$, and the second one indicates that the contribution of $w^{(\ell)}$ to each signal subspace has already been accomplished by the preceding components $\{w^{(m)}\}_{m=1}^{\ell-1}$. Our stopping rule $\ell \leq L$ for Carroll's GCCA when $K \geq 2$ is an extension from the stopping rule $\ell \leq r_{12}$ of the CCA with $K = 2$, where $r_{12} = \max\{\ell \in \{1, \dots, r_f\} : \text{corr}(z_1^{(\ell)}, z_2^{(\ell)}) > 0\}$ is the number of positive canonical correlations. The number $L = r_{12}$ when $K = 2$, because $\lambda_\ell(\text{cov}(\mathbf{f})) = 1 + \text{corr}(z_1^{(\ell)}, z_2^{(\ell)}) > 1$ if $\ell \leq r_{12}$, and otherwise $\lambda_\ell(\text{cov}(\mathbf{f})) \leq 1$ (Kettenring, 1971, Lemma 2).

We now combine the decompositions for all $\ell = 1, \dots, L$ in (10) to form the original decomposition (9). Define the index set of nonzero $c^{(\ell)}$ s by $\mathcal{I}_0 = \{\ell \in \{1, \dots, L\} : c^{(\ell)} \neq 0$, i.e., $a^{(\ell)} \neq 0\}$. We set $\mathbf{c}_k = \mathbf{0}_{p_k \times 1}$ and $\mathbf{C}_k = \mathbf{0}_{p_k \times n}$ for all k when $\mathcal{I}_0 = \emptyset$, so we only consider $\mathcal{I}_0 \neq \emptyset$ as follows. Let $\mathbf{z}_k^{\mathcal{I}_0} = (z_k^{(\ell)})_{\ell \in \mathcal{I}_0}^\top$. The portion of \mathbf{x}_k generated from latent factors $\mathbf{z}_k^{\mathcal{I}_0}$ is equivalent to the projection of \mathbf{x}_k onto $\text{span}\{(\mathbf{z}_k^{\mathcal{I}_0})^\top\}$ given by

$$\text{cov}(\mathbf{x}_k, \mathbf{z}_k^{\mathcal{I}_0}) \{ \text{cov}(\mathbf{z}_k^{\mathcal{I}_0}) \}^\dagger \mathbf{z}_k^{\mathcal{I}_0} = \text{cov}(\mathbf{x}_k, \mathbf{z}_k^{\mathcal{I}_0}) \{ \text{cov}(\mathbf{z}_k^{\mathcal{I}_0}) \}^\dagger (c^{(\ell)} + d_k^{(\ell)})_{\ell \in \mathcal{I}_0}^\top. \quad (12)$$

Here, $\text{cov}(\mathbf{x}_k, \mathbf{z}_k^{\mathcal{I}_0}) \{ \text{cov}(\mathbf{z}_k^{\mathcal{I}_0}) \}^\dagger$ is a deterministic coefficient matrix. We define the common-source vector \mathbf{c}_k of \mathbf{x}_k as

$$\mathbf{c}_k = \text{cov}(\mathbf{x}_k, \mathbf{z}_k^{\mathcal{I}_0}) \{ \text{cov}(\mathbf{z}_k^{\mathcal{I}_0}) \}^\dagger \mathbf{c}^{\mathcal{I}_0}, \quad (13)$$

which is the portion of (12) comes from the common latent factors $(\mathbf{c}^{\mathcal{I}_0})^\top := (c^{(\ell)})_{\ell \in \mathcal{I}_0}$.

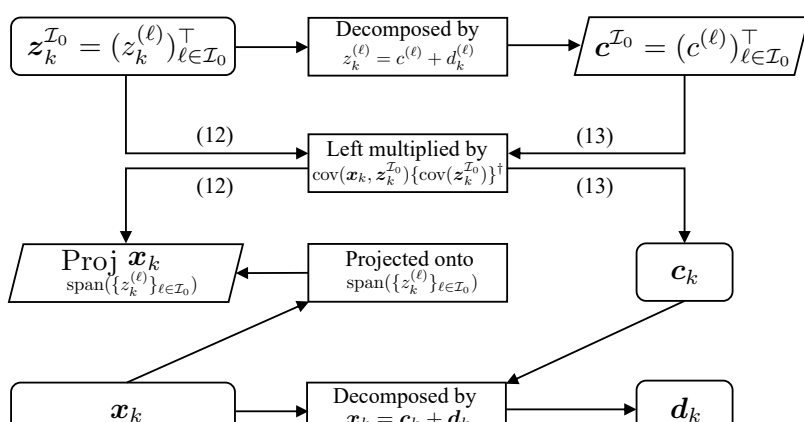
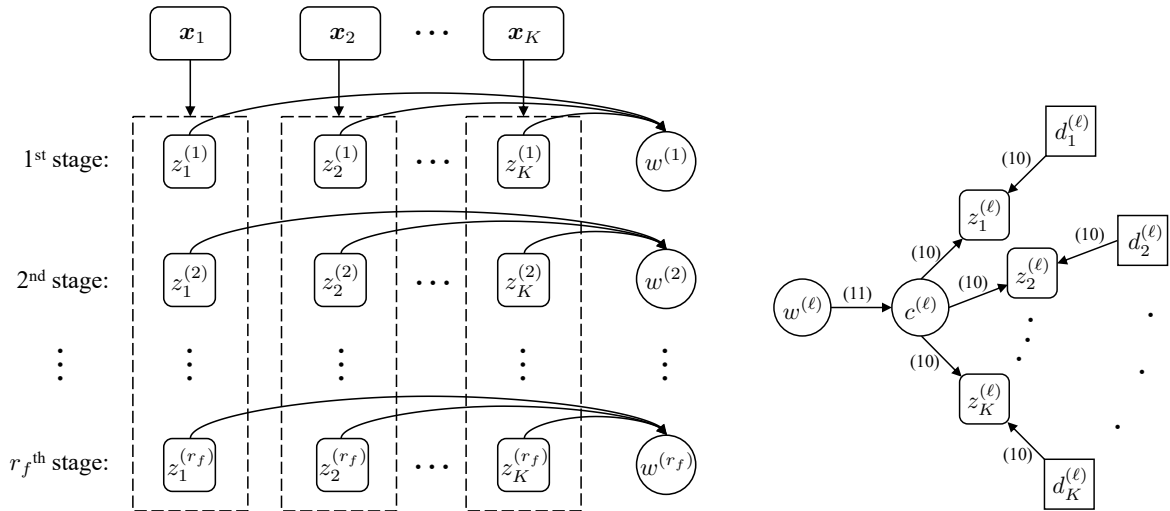
Definition 3 For D-GCCA, we define the common-source random vector \mathbf{c}_k of \mathbf{x}_k as (13) and the distinctive-source random vector $\mathbf{d}_k = \mathbf{x}_k - \mathbf{c}_k$. The common-source matrix \mathbf{C}_k and distinctive-source matrix \mathbf{D}_k are the corresponding sample matrices of \mathbf{c}_k and \mathbf{d}_k , respectively. The $\{c^{(\ell)}\}_{\ell \in \mathcal{I}_0}$ in (11) are called the common latent factors of $\{\mathbf{x}_k\}_{k=1}^K$, and $\{d_k^{(\ell)}\}_{\ell=1}^{r_f}$ in (10) are called the distinctive latent factors of \mathbf{x}_k .

Figure 2 illustrates the steps of the proposed D-GCCA. When $K = 2$, the following theorem shows that our D-GCCA is equivalent to D-CCA.

Theorem 3 When $K = 2$, $\{\mathbf{c}_k\}_{k=1}^K$ in (13) are the same as those of D-CCA in (16) of Shu et al. (2020).

We further investigate the uniqueness of $\{\mathbf{c}_k\}_{k=1}^K$.

Theorem 4 For $L \geq 1$, if $\lambda_1(\text{cov}(\mathbf{f})), \dots, \lambda_L(\text{cov}(\mathbf{f}))$ are distinct, then $\{\mathbf{c}_k\}_{k=1}^K$ are uniquely defined by (13) regardless of the non-unique choice of \mathbf{f} and $\{\boldsymbol{\eta}^{(\ell)}\}_{1 \leq \ell \leq L}$.



(c) Step 3: Eqns. (12) and (13)

Figure 2: Illustration of D-GCCA steps.

The largest L eigenvalues of $\text{cov}(\mathbf{f})$ are invariant to the choice of \mathbf{f} . For a given \mathbf{f} , the distinctness of these L eigenvalues ensures the identifiability of $\{\boldsymbol{\eta}^{(\ell)}\}_{1 \leq \ell \leq L}$ up to a sign change and thus simplifies the analysis. Analogous assumptions are often made in the literature (Zhou and He, 2008; Birnbaum et al., 2013; Wang and Fan, 2017). If the joint distribution of the n ($\geq L$) samples of \mathbf{f} is absolutely continuous or elliptically contoured, then the largest L eigenvalues of its sample covariance matrix are distinct with probability one (Okamoto, 1973; Gupta and Varga, 1991). Hence, our distinct eigenvalues assumption is plausible in practice.

2.2.2 PROPORTION OF SIGNAL VARIANCE EXPLAINED

The contribution of common latent factors $\{c^{(\ell)}\}_{\ell \in \mathcal{I}_0}$ in generating the signal vector \mathbf{x}_k of the k th data view, or the influence of $\{c^{(\ell)}\}_{\ell \in \mathcal{I}_0}$ on \mathbf{x}_k , can be measured by

$$\text{PVE}_c(\mathbf{x}_k) = \frac{\text{tr}\{\text{cov}(\mathbf{c}_k)\}}{\text{tr}\{\text{cov}(\mathbf{x}_k)\}}, \quad (14)$$

which is the proportion of \mathbf{x}_k 's variance explained by their generated common-source vector \mathbf{c}_k . The influence of distinctive latent factors $\{d_k^{(\ell)}\}_{\ell=1}^{r_f}$ on \mathbf{x}_k can be quantified by

$$\text{PVE}_d(\mathbf{x}_k) = 1 - \text{PVE}_c(\mathbf{x}_k), \quad (15)$$

which is interpreted as the extra proportion of \mathbf{x}_k 's variance that is explained by adding their generated distinctive-source vector \mathbf{d}_k (Smilde et al., 2017). The above two quantities are the view-level proportions of signal variance explained in the k th data view.

Similarly, the influences of $\{c^{(\ell)}\}_{\ell \in \mathcal{I}_0}$ and $\{d_k^{(\ell)}\}_{\ell=1}^{r_f}$ on the signal variable $\mathbf{x}_k^{[i]}$ can be assessed by the explained proportions

$$\text{PVE}_c(\mathbf{x}_k^{[i]}) = \frac{\text{var}(\mathbf{c}_k^{[i]})}{\text{var}(\mathbf{x}_k^{[i]})} \quad \text{and} \quad \text{PVE}_d(\mathbf{x}_k^{[i]}) = 1 - \text{PVE}_c(\mathbf{x}_k^{[i]}), \quad (16)$$

respectively. The variable-level proportions of explained signal variance are useful in selecting variables within each data view that are highly influenced by $\{c^{(\ell)}\}_{\ell \in \mathcal{I}_0}$ and $\{d_k^{(\ell)}\}_{\ell=1}^{r_f}$, respectively. With more easily interpretable feature definitions (e.g., name or location) from original data views, these selected variables are concrete representatives of the common and distinctive latent factors. In contrast, the variables selected by the sparse GCCA (Tenenhaus et al., 2014; Cai and Huo, 2020) are only linked to the canonical variables, which are merely the most correlated components between the multiple data views, not linked to their common or distinctive latent factors.

2.2.3 ADDITIONAL REMARKS

Unlike the $K = 2$ case, for $K \geq 3$ data views, it is highly difficult to build a decomposition in the form of (2) that simultaneously enjoys both the ideal orthogonality (O.1) of distinctive-source vectors $\{\mathbf{d}_k\}_{k=1}^K$ and a sensible interpretation of the associated common-source vectors $\{\mathbf{c}_k\}_{k=1}^K$. We thus relax (O.1) to (O.2). That is, we impose (O.1) on distinctive latent factors $\{d_k^{(\ell)}\}_{k=1}^K$ for each ℓ th stage of GCCA. This leads to a nice interpretation

of common latent factor $c^{(\ell)}$ given in Remark 1 as the contribution of the principal-basis component $w^{(\ell)}$ made uniformly to generating all signal subspaces $\{\text{span}(\mathbf{x}_k^\top)\}_{k=1}^K$. Our \mathbf{c}_k defined in (13) is the part of \mathbf{x}_k that is generated by $\{c^{(\ell)}\}_{\ell \in \mathcal{I}_0}$.

Due to the relaxation from (O.1) to (O.2), it is possible that our $\mathbf{d}_1, \dots, \mathbf{d}_K$ are all pairwise correlated and thus retain some common underlying source of variation. In other words, one may continue to apply D-GCCA to $\{\mathbf{d}_k\}_{k=1}^K$ to obtain their common latent factors. One solution to fix this issue is to uncover these remaining common latent factors sequentially and treat them hierarchically. Specifically, denote $\{(\mathbf{d}_k^{(0)}, \mathbf{c}_k^{(1)}, \mathbf{d}_k^{(1)})\}_{k=1}^K = \{(\mathbf{x}_k, \mathbf{c}_k, \mathbf{d}_k)\}_{k=1}^K$ and $\{c^{(\ell,1)}\}_{\ell \in \mathcal{I}_0^{(1)}} = \{c^{(\ell)}\}_{\ell \in \mathcal{I}_0}$. One may iteratively apply D-GCCA to $\{\mathbf{d}_k^{(t)} := \mathbf{d}_k^{(t-1)} - \mathbf{c}_k^{(t)}\}_{k=1}^K$ to obtain their common latent factors $\{c^{(\ell,t+1)}\}_{\ell \in \mathcal{I}_0^{(t+1)}}$ and common-source random vectors $\{\mathbf{c}_k^{(t+1)}\}_{k=1}^K$ from $t = 1$ up to a given number $T \geq 1$, or until $\{c^{(\ell,t+1)}\}_{\ell \in \mathcal{I}_0^{(t+1)}} = \emptyset$ or $\text{PVE}_c(\mathbf{d}_k^{(t)}) \prod_{i=0}^{t-1} \text{PVE}_d(\mathbf{d}_k^{(i)}) \leq \varepsilon$ for a given tolerance $\varepsilon > 0$. This iterative procedure yields a hierarchical decomposition structure for each \mathbf{x}_k , where $\mathbf{c}_k^{(t)}$ and $\mathbf{d}_k^{(t)}$ can be called the t th-level common-source and distinctive-source random vectors of \mathbf{x}_k , and the common and distinctive latent factors of $\{\mathbf{d}_k^{(t-1)}\}_{k=1}^K$ can be called the t th-level common and distinctive latent factors of $\{\mathbf{x}_k\}_{k=1}^K$. The importance of the t th-level common latent factors $\{c^{(\ell,t)}\}_{\ell \in \mathcal{I}_0^{(t)}}$ to $\{\mathbf{x}_k\}_{k=1}^K$ decreases as t increases, because the more important common latent factors are supposed to be uncovered earlier due to Remark 1. We thus focus on the first-level decomposition in this paper. More details about the hierarchical structure are given in Appendix A. Note that when $K = 2$ or each \mathbf{x}_k follows a single-factor model (i.e., $r_k = 1$), the first-level distinctive-source vectors $\{\mathbf{d}_k\}_{k=1}^K$ satisfy (O.1).

The difficulties of imposing (O.1) on GCCA for $K \geq 3$ views are as follows. First, the inter-stage orthogonality of canonical variables, the key to realizing (O.1) in CCA by D-CCA for $K = 2$, may not exist in GCCA for $K \geq 3$. Specifically, let $r_1 \leq \dots \leq r_K$, and augment canonical variables $\{z_k^{(\ell)}\}_{\ell=1}^{r_1}$ of CCA/GCCA with standardized variables $\{z_k^{(\ell)}\}_{r_1 < \ell \leq r_k}$ and zeros $\{z_k^{(\ell)}\}_{r_k < \ell \leq r_K}$ so that $\text{span}(\mathbf{x}_k^\top) = \text{span}(\{z_k^{(\ell)}\}_{\ell=1}^{r_K})$. When $K = 2$, CCA satisfies the inter-stage orthogonality that $\text{span}(\{z_k^{(i)}\}_{k=1}^K) \perp \text{span}(\{z_k^{(j)}\}_{k=1}^K)$ for $1 \leq i \neq j \leq r_K$. This enables D-CCA to divide the problem $\mathbf{x}_k = \mathbf{c}_k + \mathbf{d}_k$ ($k \leq K$) into the r_K mutually uncorrelated sub-problems $z_k^{(\ell)} = c^{(\ell)} + d_k^{(\ell)}$ ($k \leq K$), $\ell = 1, \dots, r_K$, and conquer (O.1) by imposing (O.2). Nevertheless, when $K \geq 3$, the inter-stage orthogonality is not guaranteed for GCCA. For example, it does not hold for $K = 3$ when $\text{span}(\mathbf{x}_k^\top) = \text{span}(z_k)$ with $k = 1, 2$ and $\text{span}(\mathbf{x}_3^\top) = \text{span}(\{z_1, z_2\})$ with $z_1, z_2 \in \mathcal{L}_0^2$ and $\theta(z_1, z_2) \in (0, \pi/2)$, even if $\{z_k^{(\ell)}\}_{\ell=1}^{r_K}$ are not canonical variables. Second, even under the inter-stage orthogonality, (O.2) for all ℓ does not ensure (O.1). For instance, (O.1) fails for $K = 3$ when $\text{span}(\mathbf{d}_k^\top) = \text{span}(\{d_k^{(\ell)}\}_{\ell=1}^2)$ for $k \leq 3$, $\{d_k^{(1)}\}_{k=1}^3 \perp \{d_k^{(2)}\}_{k=1}^3$, $d_1^{(1)} \perp d_2^{(1)} \not\perp d_3^{(1)} \not\perp d_1^{(1)}$, and $d_1^{(2)} \not\perp d_2^{(2)} \perp d_3^{(2)}$. Third, to satisfy (O.1), one may alternatively attempt to design an inner product space with the subspaces of $\sum_{k=1}^K \text{span}(\mathbf{x}_k^\top)$ as elements and then apply the Carroll's GCCA (3) and our decomposition (10) directly to it for $\ell = 1$. However, the existence of such an inner product space, particularly with a meaningful geometric interpretation, is unknown. A close example is the Grassmann algebra of $\sum_{k=1}^K \text{span}(\mathbf{x}_k^\top)$, which is spanned by the blades algebraically representing the subspaces of $\sum_{k=1}^K \text{span}(\mathbf{x}_k^\top)$ (Hestenes and Sobczyk, 1984; Dorst et al., 2010), but a sum of blades may be a multivector not equivalent to a vector space and thus the resulting $\{d_k^{(1)}\}_{k=1}^K$ may not represent $\{\text{span}(\mathbf{d}_k^\top)\}_{k=1}^K$.

3. Estimation

3.1 Estimators

We derive the estimators of common-source and distinctive-source matrices $\{\mathbf{C}_k, \mathbf{D}_k\}_{k=1}^K$ by starting with the estimation of signal matrices $\{\mathbf{X}_k\}_{k=1}^K$ from the observed data $\{\mathbf{Y}_k\}_{k=1}^K$.

Suppose that the low-rank plus noise structure in (1)-(2) follows the factor model:

$$\mathbf{Y}_k = \mathbf{X}_k + \mathbf{E}_k = \mathbf{B}_k \mathbf{F}_k + \mathbf{E}_k, \quad \mathbf{y}_k = \mathbf{x}_k + \mathbf{e}_k = \mathbf{B}_k \mathbf{f}_k + \mathbf{e}_k, \quad (17)$$

where $\mathbf{B}_k \in \mathbb{R}^{p_k \times r_k}$ is a real deterministic matrix, the columns of \mathbf{F}_k and \mathbf{E}_k are, respectively, the n independent copies of \mathbf{f}_k and \mathbf{e}_k , \mathbf{f}_k^\top is an orthonormal basis of $\text{span}(\mathbf{x}_k^\top)$ with $\text{cov}(\mathbf{f}_k, \mathbf{e}_k) = \mathbf{0}_{r_k \times p_k}$, $\text{span}(\mathbf{x}_k^\top)$ is a fixed space that is independent of $\{p_k\}_{k=1}^K$ and n , and $\mathbf{F} := [\mathbf{F}_1; \dots; \mathbf{F}_K]$ has independent columns. We assume that $\text{cov}(\mathbf{y}_k)$ is a spiked covariance matrix, for which the largest r_k eigenvalues are significantly larger than the rest, namely, signals are distinguishably stronger than noises. The r_k spiked eigenvalues are majorly contributed by signal \mathbf{x}_k , whereas the rest small eigenvalues are induced by noise \mathbf{e}_k . The spiked covariance model has been widely used in various fields, such as signal processing (Nadakuditi and Silverstein, 2010), machine learning (Huang, 2017), and economics (Chamberlain and Rothschild, 1983).

For simplicity, we define the estimators of $\{\mathbf{X}_k, \mathbf{C}_k, \mathbf{D}_k\}_{k=1}^K$ using the true $\{r_k\}_{k=1}^K$, \mathcal{I}_0 , $r_k^* = \text{rank}\{\text{cov}(\mathbf{z}_k^{\mathcal{I}_0})\}$, $\mathcal{I}_{\Delta_+}^{(\ell)} = \{(j, k) : \Delta_{jk}^{(\ell)} > 0, 1 \leq j < k \leq K\}$, $\mathcal{I}_{\Delta_0}^{(\ell)} = \{(j, k) : \Delta_{jk}^{(\ell)} = 0, 1 \leq j < k \leq K\}$, and $\text{sign}(\alpha^{(\ell)})$ for all $\ell \in \mathcal{I}_0$. The practical selection of these nuisance parameters is discussed in Section 3.3.

We use the following soft-thresholding estimator of \mathbf{X}_k proposed in Shu et al. (2020). This estimator is originally inspired by the method of Wang and Fan (2017) for spiked covariance matrix estimation:

$$\widehat{\mathbf{X}}_k = \mathbf{U}_{k1} \text{diag}\{\widehat{\sigma}_1^S(\mathbf{Y}_k), \dots, \widehat{\sigma}_{r_k}^S(\mathbf{Y}_k)\} \mathbf{U}_{k2}^\top, \quad (18)$$

where $\widehat{\sigma}_\ell^S(\mathbf{Y}_k) = [\max\{\sigma_\ell^2(\mathbf{Y}_k) - \tau_k p_k, 0\}]^{1/2}$, $\tau_k = \sum_{\ell=r_k+1}^{p_k} \sigma_\ell^2(\mathbf{Y}_k) / (np_k - nr_k - p_k r_k)$, and $\mathbf{U}_{k1} \text{diag}\{\sigma_1(\mathbf{Y}_k), \dots, \sigma_{r_k}(\mathbf{Y}_k)\} \mathbf{U}_{k2}^\top$ is the top- r_k singular value decomposition (SVD) of \mathbf{Y}_k .

We next use $\widehat{\mathbf{X}}_k$ to develop estimators for \mathbf{C}_k and $\mathbf{D}_k = \mathbf{X}_k - \mathbf{C}_k$. Recall from (13) that we have the random variable $\mathbf{c}_k = \text{cov}(\mathbf{x}_k, \mathbf{z}_k^{\mathcal{I}_0}) \{\text{cov}(\mathbf{z}_k^{\mathcal{I}_0})\}^\dagger \mathbf{c}^{\mathcal{I}_0}$.

We begin with the estimation of $\text{cov}(\mathbf{x}_k, \mathbf{z}_k^{\mathcal{I}_0})$. Define an estimator of $\text{cov}(\mathbf{x}_k)$ by $\widehat{\text{cov}}(\mathbf{x}_k) = \widehat{\mathbf{X}}_k \widehat{\mathbf{X}}_k^\top / n$ whose SVD is denoted as $\widehat{\text{cov}}(\mathbf{x}_k) = \widehat{\mathbf{V}}_{xk} \widehat{\Lambda}_{xk} \widehat{\mathbf{V}}_{xk}^\top$, where $\widehat{\Lambda}_{xk} = \text{diag}\{\lambda_1(\widehat{\text{cov}}(\mathbf{x}_k)), \dots, \lambda_{r_k}(\widehat{\text{cov}}(\mathbf{x}_k))\}$ and $\widehat{\mathbf{V}}_{xk}$ has r_k orthonormal columns. We can obtain $\lambda_\ell(\widehat{\text{cov}}(\mathbf{x}_k)) = [\widehat{\sigma}_\ell^S(\mathbf{Y}_k)]^2 / n$ and $\widehat{\mathbf{V}}_{xk} = \mathbf{U}_{k1}$. Define the estimators of \mathbf{F}_k and \mathbf{F} by $\widehat{\mathbf{F}}_k = (\widehat{\Lambda}_{xk}^{1/2})^\dagger \widehat{\mathbf{V}}_{xk}^\top \widehat{\mathbf{X}}_k$ and $\widehat{\mathbf{F}} = [\widehat{\mathbf{F}}_1; \dots; \widehat{\mathbf{F}}_K]$, respectively. We estimate $\text{cov}(\mathbf{f})$ by $\widehat{\text{cov}}(\mathbf{f}) = \widehat{\mathbf{F}} \widehat{\mathbf{F}}^\top / n$. Let $\widehat{\boldsymbol{\eta}}^{(\ell)} = [\widehat{\boldsymbol{\eta}}_1^{(\ell)}; \dots; \widehat{\boldsymbol{\eta}}_K^{(\ell)}]$, with $\widehat{\boldsymbol{\eta}}_k^{(\ell)} \in \mathbb{R}^{r_k}$, be a normalized eigenvector of $\widehat{\text{cov}}(\mathbf{f})$ corresponding to $\lambda_\ell(\widehat{\text{cov}}(\mathbf{f}))$. We also let different $\widehat{\boldsymbol{\eta}}^{(\ell)}$ s be orthogonal. Our estimated sample vector of the variable $w^{(\ell)}$ in (5) is defined by

$$(\widehat{\mathbf{w}}^{(\ell)})^\top = \begin{cases} [\lambda_\ell(\widehat{\text{cov}}(\mathbf{f}))]^{-1/2} (\widehat{\boldsymbol{\eta}}^{(\ell)})^\top \widehat{\mathbf{F}}, & \text{if } \lambda_\ell(\widehat{\text{cov}}(\mathbf{f})) \neq 0, \\ \mathbf{0}_{1 \times n}, & \text{otherwise,} \end{cases} \quad (19)$$

and that of the variable $z_k^{(\ell)}$ in (8) is $(\hat{\mathbf{z}}_k^{(\ell)})^\top = (\hat{\boldsymbol{\eta}}_k^{(\ell)} / \|\hat{\boldsymbol{\eta}}_k^{(\ell)}\|_F)^\top \hat{\mathbf{F}}_k$ if $\|\hat{\boldsymbol{\eta}}_k^{(\ell)}\|_F \neq 0$ and otherwise $\hat{\mathbf{z}}_k^{(\ell)} = \mathbf{0}_{n \times 1}$. Then, $\text{cov}(\mathbf{x}_k, \mathbf{z}_k^{\mathcal{I}_0})$ is estimated by

$$\widehat{\text{cov}}(\mathbf{x}_k, \mathbf{z}_k^{\mathcal{I}_0}) = n^{-1} \hat{\mathbf{X}}_k (\hat{\mathbf{z}}_k^{(\ell)})_{\ell \in \mathcal{I}_0} = \hat{\mathbf{V}}_{xk} \hat{\boldsymbol{\Lambda}}_{xk}^{1/2} \hat{\mathbf{H}}_k^\top, \quad (20)$$

where $\hat{\mathbf{H}}_k = (\hat{\boldsymbol{\eta}}_k^{(\ell)} / \|\hat{\boldsymbol{\eta}}_k^{(\ell)}\|_F)_{\ell \in \mathcal{I}_0}^\top$ with $\mathbf{0}/0 := \mathbf{0}$.

The matrix $\text{cov}(\mathbf{z}_k^{\mathcal{I}_0})$ is initially estimated by $\widehat{\text{cov}}(\mathbf{z}_k^{\mathcal{I}_0}) = \hat{\mathbf{H}}_k \hat{\mathbf{H}}_k^\top$. Let $\widehat{\text{cov}}(\mathbf{z}_k^{\mathcal{I}_0}) = \hat{\mathbf{V}}_{zk} \hat{\boldsymbol{\Lambda}}_{zk} \hat{\mathbf{V}}_{zk}^\top$ be its compact SVD, where $\hat{\boldsymbol{\Lambda}}_{zk}$ has nonincreasing diagonal elements. With $\check{r}_k := \min(r_k^*, \text{rank}\{\widehat{\text{cov}}(\mathbf{z}_k^{\mathcal{I}_0})\})$, our estimator of $\text{cov}(\mathbf{z}_k^{\mathcal{I}_0})$ is defined by the top- \check{r}_k SVD of $\widehat{\text{cov}}(\mathbf{z}_k^{\mathcal{I}_0})$ as

$$\widehat{\text{cov}}(\mathbf{z}_k^{\mathcal{I}_0}) = \hat{\mathbf{V}}_{zk}^{[:, 1:\check{r}_k]} \hat{\boldsymbol{\Lambda}}_{zk}^{[1:\check{r}_k, 1:\check{r}_k]} (\hat{\mathbf{V}}_{zk}^{[:, 1:\check{r}_k]})^\top. \quad (21)$$

To approximate the sample matrix $\mathbf{C}^{\mathcal{I}_0}$ of latent factors $\mathbf{c}^{\mathcal{I}_0} = (c^{(\ell)})_{\ell \in \mathcal{I}_0}^\top = (\alpha^{(\ell)} w^{(\ell)})_{\ell \in \mathcal{I}_0}^\top$, the key is the estimation of the value $\alpha^{(\ell)}$ given in Theorem 2. Replacing $\cos\{\theta(w^{(\ell)}, z_k^{(\ell)})\}$ and $\cos\{\theta(z_j^{(\ell)}, z_k^{(\ell)})\}$ by $\widehat{\cos}\{\theta(w^{(\ell)}, z_k^{(\ell)})\} = (\hat{\mathbf{w}}^{(\ell)})^\top \hat{\mathbf{z}}_k^{(\ell)} / n$ and $\widehat{\cos}\{\theta(z_j^{(\ell)}, z_k^{(\ell)})\} = (\hat{\mathbf{z}}_j^{(\ell)})^\top \hat{\mathbf{z}}_k^{(\ell)} / n$ in $\Delta_{jk}^{(\ell)}$ yields its initial estimator $\tilde{\Delta}_{jk}^{(\ell)}$. For $(j, k) \in \mathcal{I}_{\Delta+}^{(\ell)} \cup \mathcal{I}_{\Delta_0}^{(\ell)}$, define

$$\hat{\alpha}_{jk}^{(\ell)} = \frac{1}{2} \left[\widehat{\cos}\{\theta(w^{(\ell)}, z_j^{(\ell)})\} + \widehat{\cos}\{\theta(w^{(\ell)}, z_k^{(\ell)})\} - (\tilde{\Delta}_{jk}^{(\ell)})^{1/2} \right] \quad (22)$$

where $\tilde{\Delta}_{jk}^{(\ell)} = \max(\tilde{\Delta}_{jk}^{(\ell)}, 0)[(j, k) \in \mathcal{I}_{\Delta+}^{(\ell)}]$ with $[\cdot]$ being the Iverson bracket. For $\ell \in \mathcal{I}_0$, we define

$$\hat{\alpha}^{(\ell)} = \arg \min_{\hat{\alpha}_{jk}^{(\ell)}} \left\{ |\hat{\alpha}_{jk}^{(\ell)}| : \hat{\alpha}_{jk}^{(\ell)} \text{sign}(\alpha^{(\ell)}) > 0, (j, k) \in \mathcal{I}_{\Delta+}^{(\ell)} \cup \mathcal{I}_{\Delta_0}^{(\ell)} \right\}.$$

Then, $\mathbf{C}^{\mathcal{I}_0}$ is estimated with $\hat{\mathbf{w}}^{(\ell)}$ in (19) by

$$\hat{\mathbf{C}}^{\mathcal{I}_0} = (\hat{\alpha}^{(\ell)} \hat{\mathbf{w}}^{(\ell)})_{\ell \in \mathcal{I}_0}^\top. \quad (23)$$

Combining (20), (21) and (23) yields our estimator of the common-source matrix \mathbf{C}_k :

$$\hat{\mathbf{C}}_k = \widehat{\text{cov}}(\mathbf{x}_k, \mathbf{z}_k^{\mathcal{I}_0}) \{ \widehat{\text{cov}}(\mathbf{z}_k^{\mathcal{I}_0}) \}^\dagger \hat{\mathbf{C}}^{\mathcal{I}_0}. \quad (24)$$

Our estimator of the distinctive-source matrix \mathbf{D}_k is defined by

$$\hat{\mathbf{D}}_k = \hat{\mathbf{X}}_k - \hat{\mathbf{C}}_k. \quad (25)$$

The major time cost of proposed matrix estimators comes from the SVD of each \mathbf{Y}_k with complexity $O(\min\{np_k^2, n^2 p_k\})$.

We define the estimators for the view-level and the variable-level proportions of explained signal variance $\text{PVE}_c(\mathbf{x}_k) = 1 - \text{PVE}_d(\mathbf{x}_k)$ and $\text{PVE}_c(\mathbf{x}_k^{[i]}) = 1 - \text{PVE}_d(\mathbf{x}_k^{[i]})$ by

$$\widehat{\text{PVE}}_c(\mathbf{x}_k) = 1 - \widehat{\text{PVE}}_d(\mathbf{x}_k) = \|\hat{\mathbf{C}}_k\|_F^2 / \|\hat{\mathbf{X}}_k\|_F^2, \quad (26)$$

$$\widehat{\text{PVE}}_c(\mathbf{x}_k^{[i]}) = 1 - \widehat{\text{PVE}}_d(\mathbf{x}_k^{[i]}) = \|\hat{\mathbf{C}}_k^{[i,:]}\|_F^2 / \|\hat{\mathbf{X}}_k^{[i,:]}\|_F^2. \quad (27)$$

3.2 Asymptotic properties

We introduce an assumption used in Wang and Fan (2017) and Shu et al. (2020).

Assumption 1 *We assume the following conditions for model (17).*

- (i) *Let $\lambda_{k,1} > \dots > \lambda_{k,r_k} > \lambda_{k,r_k+1} \geq \dots \geq \lambda_{k,p_k} > 0$ be the eigenvalues of $\text{cov}(\mathbf{y}_k)$. There exist positive constants κ_1, κ_2 and δ_0 such that $\kappa_1 \leq \lambda_{k,\ell} \leq \kappa_2$ for $\ell > r_k$ and $\min_{\ell \leq r_k} (\lambda_{k,\ell} - \lambda_{k,\ell+1})/\lambda_{k,\ell} \geq \delta_0$.*
- (ii) *Assume that $p_k > \kappa_0 n$ with a constant $\kappa_0 > 0$. When $n \rightarrow \infty$, assume $\lambda_{k,r_k} \rightarrow \infty$, $p_k/(n\lambda_{k,\ell})$ is upper bounded for $\ell \leq r_k$, $\lambda_{k,1}/\lambda_{k,r_k}$ is bounded from above and below, and $p_k^{1/2}(\log n)^{1/\gamma_{k2}} = o(\lambda_{k,r_k})$ with γ_{k2} given in (v).*
- (iii) *The columns of $\mathbf{Z}_{y_k} = \Lambda_{y_k}^{-1/2} \mathbf{V}_{y_k}^\top \mathbf{Y}_k$ are independent copies of $\mathbf{z}_{y_k} = \Lambda_{y_k}^{-1/2} \mathbf{V}_{y_k}^\top \mathbf{y}_k$, where $\mathbf{V}_{y_k} \Lambda_{y_k} \mathbf{V}_{y_k}^\top$ is the full SVD of $\text{cov}(\mathbf{y}_k)$ with $\Lambda_{y_k} = \text{diag}(\lambda_{k,1}, \dots, \lambda_{k,p_k})$. Vector \mathbf{z}_{y_k} 's entries $\{z_{y_k}^{[i]}\}_{i=1}^{p_k}$ are independent with $E(z_{y_k}^{[i]}) = 0$, $\text{var}(z_{y_k}^{[i]}) = 1$, and the sub-Gaussian norm $\sup_{q \geq 1} q^{-1/2} [E(|z_{y_k}^{[i]}|^q)]^{1/q} \leq \kappa_s$ with a constant $\kappa_s > 0$ for all $i \leq p_k$.*
- (iv) *Matrix $\mathbf{B}_k^\top \mathbf{B}_k$ is a diagonal matrix. For all $i \leq p_k$ and $\ell \leq r_k$, $|\mathbf{B}_k^{[i,\ell]}| \leq \kappa_B (\lambda_{k,\ell}/p_k)^{1/2}$ with a constant $\kappa_B > 0$.*
- (v) *Denote $\mathbf{e}_k = (e_{k,1}, \dots, e_{k,p_k})^\top$ and $\mathbf{f}_k = (f_{k,1}, \dots, f_{k,r_k})^\top$. Let $\|\text{cov}(\mathbf{e}_k)\|_\infty < s_0$ with a constant $s_0 > 0$. For all $i \leq p_k$ and $\ell \leq r_k$, there exist positive constants $\gamma_{k1}, \gamma_{k2}, b_{k1}$ and b_{k2} such that for $t > 0$, $P(|e_{k,i}| > t) \leq \exp\{-(t/b_{k1})^{\gamma_{k1}}\}$ and $P(|f_{k,\ell}| > t) \leq \exp\{-(t/b_{k2})^{\gamma_{k2}}\}$.*

Assumption 1 follows Assumptions 2.1-2.3 and 4.1-4.2 of Wang and Fan (2017) which guarantee the consistency of each signal estimator $\widehat{\mathbf{X}}_k$ given in (18). The diverging leading eigenvalues and bounded nonspiked eigenvalues of $\text{cov}(\mathbf{y}_k)$ in conditions (i) and (ii), together with the approximate sparsity constraint $\|\text{cov}(\mathbf{e}_k)\|_\infty < s_0$ in condition (v), ensure sufficiently strong signals for thresholding. These conditions are common in the literature of high-dimensional factor models (Bai, 2003; Bai et al., 2008; Fan et al., 2013). The sub-Gaussian constraint in (iii) and the exponential-type tails in (v) generalize Gaussian distributions, while allowing the use of the large deviation theory to establish concentration bounds. For condition (iv), letting $\mathbf{f}_k = \Lambda_{xk}^{-1/2} \mathbf{V}_{xk}^\top \mathbf{x}_k$ with the compact SVD $\text{cov}(\mathbf{x}_k) = \mathbf{V}_{xk} \Lambda_{xk} \mathbf{V}_{xk}^\top$, we have $\mathbf{B}_k = \text{cov}(\mathbf{x}_k, \mathbf{f}_k) = \mathbf{V}_{xk} \Lambda_{xk}^{1/2}$. Hence, $\mathbf{B}_k^\top \mathbf{B}_k = \Lambda_{xk}$ is a diagonal matrix. Then, it follows from Weyl's inequality that $\max_{\ell \leq r_k} \|\mathbf{B}_k^{[i,\ell]}\|_F^2 / \lambda_{k,\ell} \leq 1 + \|\text{cov}(\mathbf{e}_k)\|_2 / \lambda_{k,\ell} = 1 + o(1)$. It is thus reasonable to assume $|\mathbf{B}_k^{[i,\ell]}| = O(\sqrt{\lambda_{k,\ell}/p_k})$. See Wang and Fan (2017) and Shu et al. (2020) for more discussions on Assumption 1.

We have the following asymptotic properties for estimators defined in (18) and (24)-(27).

Theorem 5 *Suppose that Assumption 1 holds and true $\{r_k\}_{k=1}^K$ are given. Then for each $k \leq K$, we have*

$$\frac{\|\widehat{\mathbf{X}}_k - \mathbf{X}_k\|_*^2}{\|\mathbf{X}_k\|_*^2} = O_P \left(\min \left\{ \frac{1}{n^2} + \frac{\log p_k}{n \text{SNR}_k}, 1 \right\} \right),$$

where $\|\cdot\|_\star$ denotes either the Frobenius norm or the spectral norm and $\text{SNR}_k = \frac{\text{tr}\{\text{cov}(\mathbf{x}_k)\}}{\text{tr}\{\text{cov}(\mathbf{e}_k)\}}$ is the signal-to-noise ratio of \mathbf{y}_k . Additionally assume that K is a constant, $\mathcal{I}_0 \neq \emptyset$, $\{\lambda_\ell(\text{cov}(\mathbf{f}))\}_{\ell=1}^L$ are distinct, and true $\{\mathcal{I}_0, \{r_k^*\}_{k=1}^K, \{\mathcal{I}_{\Delta_+}^{(\ell)}, \mathcal{I}_{\Delta_0}^{(\ell)}, \text{sign}(\alpha^{(\ell)})\}_{\ell \in \mathcal{I}_0}\}$ are given. If $\delta_\eta := \frac{1}{\sqrt{n}} + \sum_{k=1}^K \sqrt{\frac{\log p_k}{n \text{SNR}_k}} = o(1)$, then

$$\max \left\{ \frac{\|\widehat{\mathbf{C}}_k - \mathbf{C}_k\|_\star^2}{\|\mathbf{X}_k\|_\star^2}, \frac{\|\widehat{\mathbf{D}}_k - \mathbf{D}_k\|_\star^2}{\|\mathbf{X}_k\|_\star^2} \right\} = O_P(\delta_\eta^2) \quad (28)$$

and

$$\left| \widehat{\text{PVE}}_c(\mathbf{x}_k) - \text{PVE}_c(\mathbf{x}_k) \right| = O_P(\delta_\eta). \quad (29)$$

Furthermore, if $\delta_k := (1 + \frac{1}{\text{SNR}_k}) \sqrt{\frac{\log p_k}{n}} = o(1)$ and $\min_{i \leq p_k} \text{var}(\mathbf{x}_k^{[i]}) \geq M_k \lambda_{r_k}(\text{cov}(\mathbf{x}_k)) / p_k$ with a constant $M_k > 0$, then we have

$$\max_{1 \leq i \leq p_k} \left| \widehat{\text{PVE}}_c(\mathbf{x}_k^{[i]}) - \text{PVE}_c(\mathbf{x}_k^{[i]}) \right| = O_P(\delta_\eta + \delta_k). \quad (30)$$

Under Assumption 1, the signal-to-noise ratio $\text{SNR}_k \asymp \lambda_{k,1}/p_k$. For pervasive factor models that have leading eigenvalues $\lambda_{k,\ell} \asymp p_k$ for $\ell \leq r_k$ (Fan et al., 2013; Wang and Fan, 2017), we have $\text{SNR}_k \asymp 1$, and thus $\delta_\eta \asymp \sum_{k=1}^K \sqrt{(\log p_k)/n}$ and $\delta_k \asymp \sqrt{(\log p_k)/n}$. It is commonly assumed that $\sqrt{(\log p_k)/n} = o(1)$ in the literature of high-dimensional statistics (Bickel and Levina, 2008; Rothman et al., 2009). Hence, $\delta_\eta = o(1) = \delta_k$ holds at least for pervasive factor models. Note that $\sum_{i=1}^{p_k} \text{var}(\mathbf{x}_k^{[i]}) = \text{tr}(\text{cov}(\mathbf{x}_k)) = \sum_{\ell=1}^{r_k} \lambda_\ell(\text{cov}(\mathbf{x}_k))$. Thus, it is reasonable to assume $\min_{i \leq p_k} \text{var}(\mathbf{x}_k^{[i]}) \geq M_k \lambda_{r_k}(\text{cov}(\mathbf{x}_k)) / p_k$.

When $K = 2$, the convergence rates of $\widehat{\mathbf{C}}_k$ and $\widehat{\mathbf{D}}_k$ in (28) are faster than those in Theorem 3 of the D-CCA paper (Shu et al., 2020). This benefits from the predetermination of the nuisance parameters $\{\mathcal{I}_{\Delta_+}^{(\ell)}, \mathcal{I}_{\Delta_0}^{(\ell)}\}_{\ell \in \mathcal{I}_0}$ (e.g., by the approach in the next subsection). The same convergence rates can be obtained in the proof of Shu et al. (2020) if $\max\{\ell : \lambda_\ell(\text{cov}(\mathbf{x}_1, \mathbf{x}_2)) = 1\} = r_1 + r_2 - \text{rank}\{\text{cov}([\mathbf{x}_1; \mathbf{x}_2])\}$ is predetermined (e.g., by the two-step test of Chen and Fang (2019)). To the best of our knowledge, the results in (29)-(30) are the first work to show the high-dimensional estimation consistency of the view-level and variable-level proportions of explained signal variance for the decomposition model in (1)-(2) for $K \geq 2$, which are not seen in Shu et al. (2020) even when $K = 2$.

The convergence rates of our estimators in (28)–(30) depend on the information of all the K data views and decrease when K increases. The estimation involves denoising all signals $\{\mathbf{X}_k\}_{k=1}^K$ and accumulates the estimation errors of $\{\mathbf{X}_k\}_{k=1}^K$, since the common latent factors generally change as K increases and thus cannot be determined by fewer data views. For example, consider the case where $\mathbf{x}_k = z_k^{(1)}$ ($k = 1, \dots, K$) with $\text{corr}(z_i^{(1)}, z_j^{(1)}) = \rho \in (0, 1)$ for $1 \leq i \neq j \leq K$. As used in AJIVE, COBE and our D-GCCA, the desirable direction variable of the common latent factor is the consensus variable $w^{(1)}$ of GCCA, which is $w^{(1)} = \sum_{k=1}^2 z_k^{(1)} / \sqrt{2 + 2\rho}$ when $K = 2$, and $w^{(1)} = (\sum_{k=1}^3 z_k^{(1)}) / \sqrt{3 + 6\rho}$ when $K = 3$, thereby resulting in different common latent factors for $K = 2$ and $K = 3$.

3.3 Selection of nuisance parameters

We discuss how to practically select the parameters $\{r_k\}_{k=1}^K$, \mathcal{I}_0 , $\{r_k^*\}_{k=1}^K$, $\{\mathcal{I}_{\Delta_+}^{(\ell)}, \mathcal{I}_{\Delta_0}^{(\ell)}\}_{\ell \in \mathcal{I}_0}$, and $\{\text{sign}(\alpha^{(\ell)})\}_{\ell \in \mathcal{I}_0}$. Denote $\widehat{r}_k, \widehat{L}, \widehat{\mathcal{I}}_0, \widehat{r}_k^*, \widehat{\mathcal{I}}_{\Delta_+}^{(\ell)}, \widehat{\mathcal{I}}_{\Delta_0}^{(\ell)}$, and $\widehat{\text{sign}}(\alpha^{(\ell)})$ to be estimators of their true counterparts.

We select $\{\widehat{r}_k\}_{k=1}^K$ by using the edge distribution method of Onatski (2010) that consistently estimates the rank for the factor model in (17) under mild conditions. To determine the other parameters, we use hypothesis tests based on the denoised data $\{\widehat{\mathbf{X}}_k\}_{k=1}^K$. Testing procedures have been widely used in the literature of CCA (Bartlett, 1941; Lawley, 1959; Caliński and Krzyśko, 2005; Song et al., 2016) to select similar parameters.

Consider the selection of $L = \max\{\ell \in \{1, \dots, r_f\} : \lambda_\ell(\text{cov}(\mathbf{f})) > 1\}$. Left-multiplying the both sides of $[\text{cov}(\mathbf{f})\boldsymbol{\eta}^{(\ell)}]^{[\sum_{i=0}^{k-1} r_i : \sum_{i=1}^k r_i]} = [\lambda_\ell(\text{cov}(\mathbf{f}))\boldsymbol{\eta}^{(\ell)}]^{[\sum_{i=0}^{k-1} r_i : \sum_{i=1}^k r_i]}$ by $\boldsymbol{\eta}_k^{(\ell)}$ can obtain $\text{cov}((\boldsymbol{\eta}_k^{(\ell)})^\top \mathbf{f}_k, \sum_{j \neq k} (\boldsymbol{\eta}_j^{(\ell)})^\top \mathbf{f}_j) = [\lambda_\ell(\text{cov}(\mathbf{f})) - 1] \|\boldsymbol{\eta}_k^{(\ell)}\|_F^2$ for all $k \leq K$. Let \widehat{L} be the largest $\ell \in [0, \text{rank}(\widehat{\text{cov}}(\mathbf{f}))]$ such that for at least one k , both $\text{corr}(w^{(\ell)}, z_k^{(\ell)}) = 0$ and $\text{corr}((\boldsymbol{\eta}_k^{(\ell)})^\top \mathbf{f}_k, \sum_{j \neq k} (\boldsymbol{\eta}_j^{(\ell)})^\top \mathbf{f}_j) = 0$ are rejected by a right-tailed test for zero correlation. The two tests indicate $\|\boldsymbol{\eta}_k^{(\ell)}\|_F \neq 0$ and $\text{cov}((\boldsymbol{\eta}_k^{(\ell)})^\top \mathbf{f}_k, \sum_{j \neq k} (\boldsymbol{\eta}_j^{(\ell)})^\top \mathbf{f}_j) > 0$, respectively, thereby implying $\lambda_\ell(\text{cov}(\mathbf{f})) - 1 = \text{cov}((\boldsymbol{\eta}_k^{(\ell)})^\top \mathbf{f}_k, \sum_{j \neq k} (\boldsymbol{\eta}_j^{(\ell)})^\top \mathbf{f}_j) / \|\boldsymbol{\eta}_k^{(\ell)}\|_F^2 > 0$. We use the normal approximation test of DiCiccio and Romano (2017) for testing zero correlation.

To determine $\mathcal{I}_0 = \{\ell \in \{1, \dots, L\} : \alpha^{(\ell)} \neq 0\}$, we retain index $\ell \leq \widehat{L}$ in $\widehat{\mathcal{I}}_0$ if $\text{corr}(w^{(\ell)}, z_k^{(\ell)}) = 0$ and $\text{corr}(z_j^{(\ell)}, z_k^{(\ell)}) = 0$ are rejected respectively by the right-tailed and the two-tailed zero-correlation tests for all $k \leq K$ and all $j \neq k$.

The rank estimate \widehat{r}_k^* of $r_k^* = \text{rank}\{\text{cov}(z_k^{\mathcal{I}_0})\}$ is obtained by the two-step test of Chen and Fang (2019) for the rank of matrix $\text{cov}(z_k^{\widehat{\mathcal{I}}_0})$.

We next select $\mathcal{I}_{\Delta_+}^{(\ell)} = \{(j, k) : \Delta_{jk}^{(\ell)} > 0, 1 \leq j < k \leq K\}$ and $\mathcal{I}_{\Delta_0}^{(\ell)} = \{(j, k) : \Delta_{jk}^{(\ell)} = 0, 1 \leq j < k \leq K\}$. Note that $\Delta_{jk}^{(\ell)} = -4 \text{cov}(z_{j,k}^{(\ell)}, z_{k,j}^{(\ell)})$ with $z_{j,k}^{(\ell)} = z_j^{(\ell)} - \frac{1}{2}[\cos\{\theta(w^{(\ell)}, z_j^{(\ell)})\} + \cos\{\theta(w^{(\ell)}, z_k^{(\ell)})\}]w^{(\ell)}$. For $\ell \in \widehat{\mathcal{I}}_0$, we include (j, k) into $\widehat{\mathcal{I}}_{\Delta_+}^{(\ell)}$ if $\text{corr}(z_{j,k}^{(\ell)}, z_{k,j}^{(\ell)}) = 0$ is rejected by the left-tailed zero-correlation test, and then include the remaining (j, k) into $\widehat{\mathcal{I}}_{\Delta_0}^{(\ell)}$ if $\text{corr}(z_{j,k}^{(\ell)}, z_{k,j}^{(\ell)}) = 0$ is not rejected by the right-tailed zero-correlation test.

Finally, consider to determine the sign of $\alpha^{(\ell)}$. Define $\alpha_+^{(\ell)} = \min\{\alpha_{jk}^{(\ell)} : \alpha_{jk}^{(\ell)} > 0, (j, k) \in \widehat{\mathcal{I}}_\Delta^{(\ell)}\}$ and $\alpha_-^{(\ell)} = \max\{\alpha_{jk}^{(\ell)} : \alpha_{jk}^{(\ell)} < 0, (j, k) \in \widehat{\mathcal{I}}_\Delta^{(\ell)}\}$, and define $\widehat{\alpha}_+^{(\ell)}$ and $\widehat{\alpha}_-^{(\ell)}$ in the same way by using $\widehat{\alpha}_{jk}^{(\ell)}$ instead. Let $\widehat{\text{sign}}(\alpha^{(\ell)})$ be the sign of the existing one of $\widehat{\alpha}_+^{(\ell)}$ and $\widehat{\alpha}_-^{(\ell)}$ if the other does not exist. Otherwise, first test $|\alpha_+^{(\ell)}| - |\alpha_-^{(\ell)}| = 0$ by applying the bias-corrected and accelerated bootstrap interval (Efron and Tibshirani, 1993). Let $\widehat{\text{sign}}(\alpha^{(\ell)}) = 1$ if zero is outside the bootstrap interval and $|\widehat{\alpha}_+^{(\ell)}| < |\widehat{\alpha}_-^{(\ell)}|$, and otherwise let $\widehat{\text{sign}}(\alpha^{(\ell)}) = -1$.

4. Simulation studies

In this section, we evaluate the finite-sample performance of proposed D-GCCA estimation via simulations, comparing with the six competing methods mentioned in Section 1.

4.1 Simulation setups

We consider $K = 3$ data views with signals $\{\mathbf{x}_k\}_{k=1}^3$ following the four simulation setups below, and generate signal-independent Gaussian noises $\{e_{k,i}\}_{i=1}^{p_k} \stackrel{iid}{\sim} N(0, \sigma_{e_k}^2)$ that are independent across data views. Simulations are conducted with sample size $n = 300$, variable dimension p_1 ranging from 100 to 1500, noise variance $\sigma_{e_1}^2$ from 0.25 to 9, and 1000 independent replications under each setting.

- Setup 1.1: Let $\mathbf{x}_1 \stackrel{d}{=} \mathbf{x}_2 \stackrel{d}{=} \mathbf{x}_3$ and $r_1 = r_2 = r_3 = 1$. Set standardized canonical variables $z_1^{(1)}, z_2^{(1)}, z_3^{(1)}$ to be jointly Gaussian with $\theta_z := \theta(z_j^{(1)}, z_k^{(1)})$ for all $j \neq k$. Let $\Lambda_k = 500$ for $k = 1, 2, 3$. Randomly generate three unit vectors $\{\mathbf{V}_{xk}\}_{k=1}^3$ that are equal if with the same size and are fixed for all simulation replications of the same (p_1, p_2, p_3) . Let $\mathbf{x}_k = \mathbf{V}_{xk} \Lambda_{xk}^{1/2} z_k^{(1)}$. We vary θ_z from 10° to 70° , resulting in D-GCCA's $\{\text{PVE}_c(\mathbf{x}_k)\}_{k=1}^3$ all from 0.853 to 0.079 invariant to $\{p_k\}_{k=1}^3$; see Appendix C. Let $\sigma_{e_1}^2 = \sigma_{e_2}^2 = \sigma_{e_3}^2$.
- Setup 1.2: Fix variable dimensions $(p_2, p_3) = (300, 900)$ and noise variances $\sigma_{e_2}^2 = \sigma_{e_3}^2 = 1$. The other settings are the same as in Setup 1.1.
- Setup 2.1: Let $p_1 = p_2 = p_3$ and $r_1 = r_2 = r_3 = 5$. Design $\text{cov}(\mathbf{f})$ with eigenvalues $(3, 2.8, 2.25, 1.5, 1, 1, 1, 1, 0.635, 0.415, 0.4, 0, 0, 0, 0)$ such that, respectively for $\ell = 1, \dots, 4$, $\{\theta(w^{(\ell)}, z_k^{(\ell)})\}_{k \leq 3}$ are all approximately $0^\circ, 15^\circ, 30^\circ$, and 45° , and $\{\theta(z_j^{(\ell)}, z_k^{(\ell)})\}_{j < k \leq 3}$ are all close to $0^\circ, 25^\circ, 50^\circ$ and 75° . Matrix $\text{cov}(\mathbf{f})$ is given in Appendix C. Set \mathbf{f} to be multivariate Gaussian with mean zero and covariance matrix $\text{cov}(\mathbf{f})$. Let $\Lambda_k = \text{diag}(500, 400, 300, 200, 100)$ for all $k \leq 3$. Randomly generate three matrices $\{\mathbf{V}_{xk}\}_{k=1}^3$, each with orthonormal columns, which are equal if with the same size and are fixed for all simulation replications of the same (p_1, p_2, p_3) . Let $\mathbf{x}_k = \mathbf{V}_{xk} \Lambda_{xk}^{1/2} \mathbf{f}_k$. D-GCCA has $(\text{PVE}_c(\mathbf{x}_1), \text{PVE}_c(\mathbf{x}_2), \text{PVE}_c(\mathbf{x}_3)) = (0.387, 0.324, 0.427)$ invariant to $\{p_k\}_{k=1}^3$. Let $\sigma_{e_1}^2 = \sigma_{e_2}^2 = \sigma_{e_3}^2$.
- Setup 2.2: Fix $(p_2, p_3) = (300, 900)$ and $\sigma_{e_2}^2 = \sigma_{e_3}^2 = 1$. The other settings are the same as in Setup 2.1.

4.2 Finite-sample performance of D-GCCA estimators

We first evaluate the performance of the D-GCCA estimation that uses true nuisance parameters $\{\{r_k, r_k^*\}_{k=1}^K, \mathcal{I}_0, \{\mathcal{I}_{\Delta_+}^{(\ell)}, \mathcal{I}_{\Delta_0}^{(\ell)}, \text{sign}(\alpha^{(\ell)})\}_{\ell \in \mathcal{I}_0}\}$. The practical selection of these nuisance parameters has been discussed in Section 3.3 and its performance is investigated later in this subsection. It is easily seen that $\text{SNR}_k = \text{tr}(\Lambda_k)/(p_k \sigma_{e_k}^2)$ in the above simulation setups. For simplicity, we hence examine the trend of estimation errors in Theorem 5 with respect to $(p_k, \sigma_{e_k}^2)$ instead of (p_k, SNR_k) .

Figure 3 shows the estimation errors of D-GCCA under Setups 1.1 and 1.2 with $\theta_z = 50^\circ$. Similar results are observed and provided in Appendix C for the other values of θ_z . For Setup 1.1 in Figure 3 (a), the average estimation errors are almost the same for the three identically distributed data views, indicating the fair treatment of proposed estimation to each view. As expected in Theorem 5, the errors generally increase as either dimension p_1 or noise variance $\sigma_{e_1}^2$ grows, and the relatively slower error trend of $\widehat{\text{PVE}}_c(\mathbf{x}_k)$ reflects its slower

convergence rate as compared with those of $\{\widehat{\mathbf{X}}_k, \widehat{\mathbf{C}}_k, \widehat{\mathbf{D}}_k\}$. The errors are acceptable even for some cases when p_1 or $\sigma_{e_1}^2$ is large along with very low SNR_k . For example, the errors are smaller than 0.05 at $(p_1, \sigma_{e_1}^2) = (1500, 4)$ with $\text{SNR}_k = 0.083$. In Figure 3 (b) for Setup 1.2, the estimation result of the first data view is similar to that in Figure 3 (a). As for the second and third data views with fixed variable dimensions and noise variances, when $(p_1, \sigma_{e_1}^2)$ the parameters of the first data view grow, the signal matrix estimation is not affected, while the estimation errors of the other three quantities are observed with slight increasing trends. These results are consistent with those shown in Theorem 5. Because Setups 1.1 and 1.2 are single-factor models, we have $\text{PVE}_c(\mathbf{x}_k^{[i]}) = \text{PVE}_c(\mathbf{x}_k)$ and $\widehat{\text{PVE}}_c(\mathbf{x}_k^{[i]}) = \widehat{\text{PVE}}_c(\mathbf{x}_k)$ for all $i \leq p_k$. The max absolute error of $\{\widehat{\text{PVE}}_c(\mathbf{x}_k^{[i]})\}_{i=1}^{p_k}$ hence coincides with the absolute error of $\widehat{\text{PVE}}_c(\mathbf{x}_k)$ shown in the seventh row of Figure 3.

Now we consider Setups 2.1 and 2.2 that are multi-factor models. Figure 4 presents similar results as in Figure 3 for the estimation of $\{\mathbf{X}_k, \mathbf{C}_k, \mathbf{D}_k, \text{PVE}_c(\mathbf{x}_k)\}_{k=1}^3$. Figure 5 shows the performance of $\{\widehat{\text{PVE}}_c(\mathbf{x}_k^{[i]})\}_{i=1}^{p_k}$. The first three rows of Figure 5 summarize the maximum, the third quartile, and the median of their absolute errors. As in Theorem 5, those errors increase as either dimension p_1 or noise variance $\sigma_{e_1}^2$ grows. For large p_1 or $\sigma_{e_1}^2$, although the estimated PVE values have large maximum absolute errors, the fourth row of Figure 5 shows strong average correlations (> 0.75) between the true and estimated PVEs. In terms of variable selection, the consequent ranking of variables may be more informative. We evaluate the ranking quality by the Spearman's ρ coefficient (Spearman, 1904) and the normalized discounted cumulative gain (nDCG; Wang et al., 2013). Spearman's $\rho \in [-1, 1]$ computes the correlation between the rank values of the true and estimated PVEs. The considered nDCG ranges on $[0, 1]$ and uses the true PVE as the degree of relevancy with the logarithmic discount. For both metrics, a higher value indicates better concordance between the rankings of variables from the true and estimated PVEs. The fifth row of Figure 5 shows high average Spearman's ρ values mostly above 0.95 for low noise $\sigma_{e_1}^2 \leq 1$, above 0.85 for modest to moderate dimension $p_1 \leq 600$, and nearly all above 0.75 for strong noise $\sigma_{e_1}^2 \in \{4, 9\}$ or large dimension $p_1 \in [900, 1500]$. For the ranking of variables based on either $\{\widehat{\text{PVE}}_c(\mathbf{x}_k^{[i]})\}_{i=1}^{p_k}$ or $\{\widehat{\text{PVE}}_d(\mathbf{x}_k^{[i]})\}_{i=1}^{p_k}$, strong agreement with that based on their estimands is observed in the last two rows of Figure 5 with the average nDCG above 0.97 for considering all ranks and above 0.86 for only the top $p_k/10$ ranks.

We also numerically evaluate the selection approach of nuisance parameters that is proposed in Section 3.3. Figures 6, 13 and 14 show the accuracy of the selection approach for the four simulation setups. For simplicity, we apply the same significance level α , ranging from 0.5 down to 0.0001, to all hypothesis tests involved in the selection approach. For Setups 1.1 and 1.2, $\alpha \in [0.0001, 0.5]$ and $\alpha \in [0.005, 0.5]$ perform the same well for $\theta_z \in [10^\circ, 60^\circ]$ and $\theta_z = 70^\circ$, respectively, with accuracy values all above 90% and most around or above 95%. As for Setups 2.1 and 2.2, as shown in Figure 6 (e) and (f), when the significance level is 0.1, the accuracy achieves nearly 90% for most considered cases. There is no dramatic change when the significance level is down from 0.2 to 0.05. In practice, it is worth trying several significance levels to monitor the change of nuisance parameters, and also suggested to report the used significance level along with the obtained decomposition. One may also expect to potentially improve the accuracy by additionally using the Bagging technique (Hastie et al., 2009), that is, for each nuisance parameter applying the selection

approach to a large number of resampled data sets and then combining the results by majority voting. We leave this to interested readers.

4.3 Comparison with related methods

We now compare the performance of D-GCCA and the six competing methods (JIVE, R.JIVE, AJIVE, COBE, OnPLS, and DISCO-SCA) under the four simulation setups.

Since the decompositions defined by the seven methods are different, it is unfair to compare the errors of their matrix estimates to D-GCCA's true matrices. Alternatively, under the general model given in (1) and (2), for each method we consider whether at least one orthogonal pair among $\{\mathbf{d}_k\}_{k=1}^K$ exists, and otherwise how severe the common underlying source of variation is retained among $\{\mathbf{d}_k\}_{k=1}^K$.

The orthogonality between \mathbf{d}_j and \mathbf{d}_k is equivalent to $\sum_{m=1}^{r_d_j} \sum_{\ell=1}^{r_d_k} [\text{corr}(d_j^{(m)}, d_k^{(\ell)})] \neq 0$, where $\{d_k^{(\ell)}\}_{\ell=1}^{r_d_k}$ denote the latent factors of \mathbf{d}_k . We detect each $\text{corr}(d_j^{(m)}, d_k^{(\ell)}) \neq 0$ using the normal approximation test (DiCiccio and Romano, 2017), with false discovery rate controlled at 0.05 (Benjamini and Hochberg, 1995) and the ℓ th right-singular vector of $\widehat{\mathbf{D}}_k$ used as the n samples of $d_k^{(\ell)}$.

Let $\rho_\ell(\{\mathbf{x}_k\}_{k=1}^K)$ be the maximum of the objective function in (3). If no pairs in $\{\mathbf{d}_k\}_{k=1}^K$ are orthogonal, we use $\rho_1(\{\mathbf{d}_k\}_{k=1}^K) \in [1, K]$ to measure the severity of common underlying source retained by $\{\mathbf{d}_k\}_{k=1}^K$. From equation (6), we estimate $\rho_1(\{\mathbf{d}_k\}_{k=1}^K)$ by $\widehat{\rho}_1(\{\mathbf{d}_k\}_{k=1}^K) = \lambda_1(\widehat{\mathbf{F}}\widehat{\mathbf{F}}^\top/n)$ with the matrix $\widehat{\mathbf{F}}$ defined in Section 3.1 but uses $\{\widehat{\mathbf{D}}_k\}_{k=1}^K$ here instead of $\{\widehat{\mathbf{X}}_k\}_{k=1}^K$.

Table 1 reports the comparison results for Setups 1.1 and 1.2 with $(p_1, \theta_z, \sigma_{e_1}^2) = (600, 50^\circ, 1)$ and Setups 2.1 and 2.2 with $(p_1, \sigma_{e_1}^2) = (600, 1)$. We first observe that all simulation replications of R.JIVE for the four setups have at least one orthogonal pair among $\{\mathbf{d}_k\}_{k=1}^3$, but its scaled squared errors of signal matrix estimates are much larger than those of JIVE (its original version with no orthogonality constraint on $\{\mathbf{d}_k\}_{k=1}^K$) and our D-GCCA. This agrees with the design of R.JIVE, which can discard some signal as noise to ensure the orthogonality of $\{\mathbf{d}_k\}_{k=1}^K$. For Setups 1.1 and 1.2 with three one-dimensional signal subspaces $\{\text{span}(\mathbf{x}_k^\top)\}_{k=1}^3$, our D-GCCA also has all its simulation replications satisfying the desirable orthogonality among $\{\mathbf{d}_k\}_{k=1}^3$, which is consistent with its decomposition in (10) for canonical variables. In contrast, the other five methods do not show the desirable orthogonality for nearly all replications under the four setups. For Setups 2.1 and 2.2 with higher-dimensional signal subspaces, neither does D-GCCA own the desirable orthogonality, as explained in Section 2.2.3 due to its relaxation into each sub-problem (10), but D-GCCA still has significantly smaller mean $\widehat{\rho}_1(\{\mathbf{d}_k\}_{k=1}^K)$ values than those available for the other five methods.

5. Real-world Data Examples

5.1 Application to TCGA breast cancer genomic data

We compare our D-GCCA with the six state-of-the-art methods in analyzing the TCGA breast cancer genomic data (Koboldt et al., 2012). We consider three types of genomic data on a common set of 664 tumor samples that contain mRNA expression data for the top

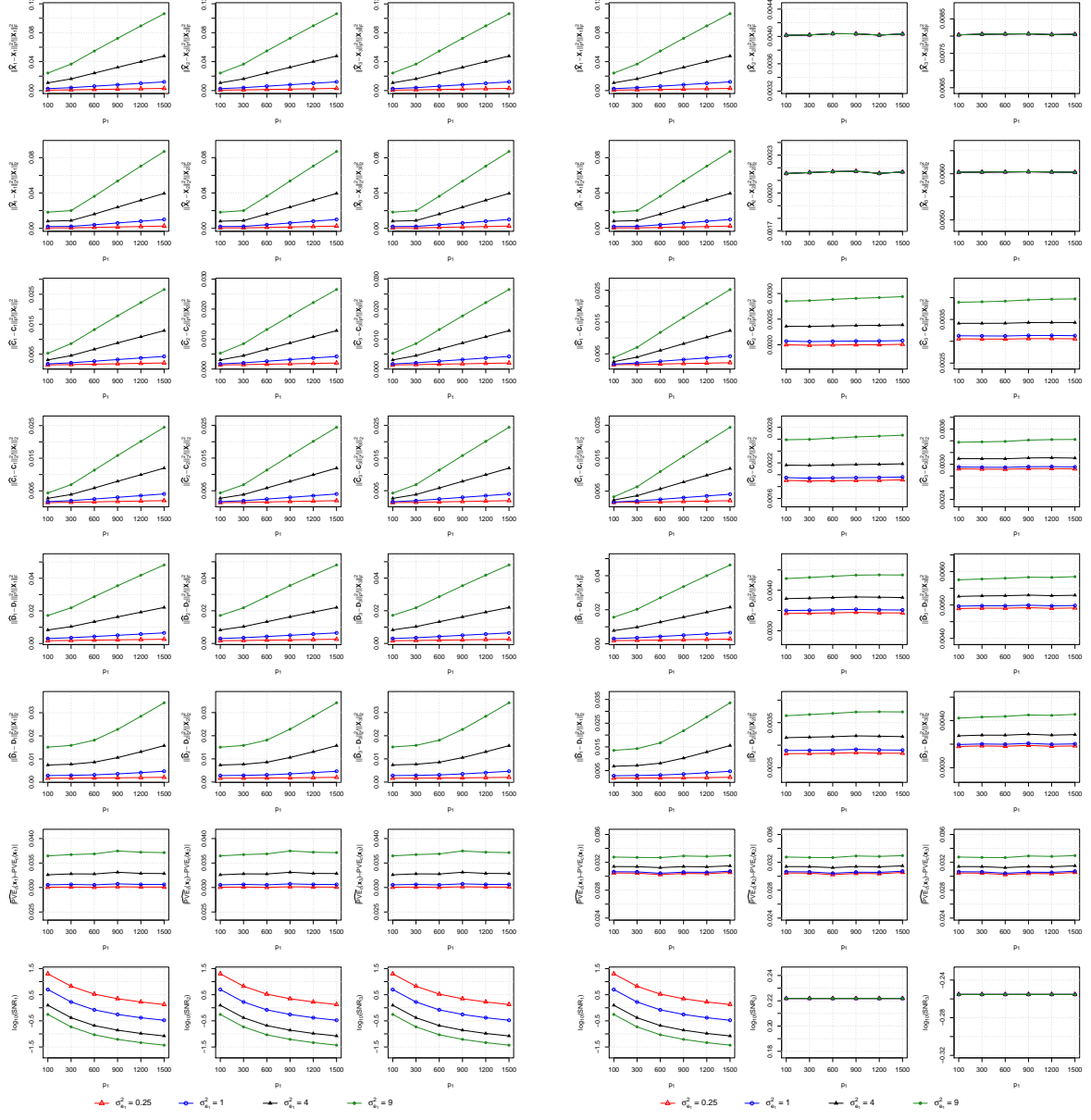


Figure 3: Average errors of D-GCCA estimates over 1000 replications for Setups 1.1 and 1.2.

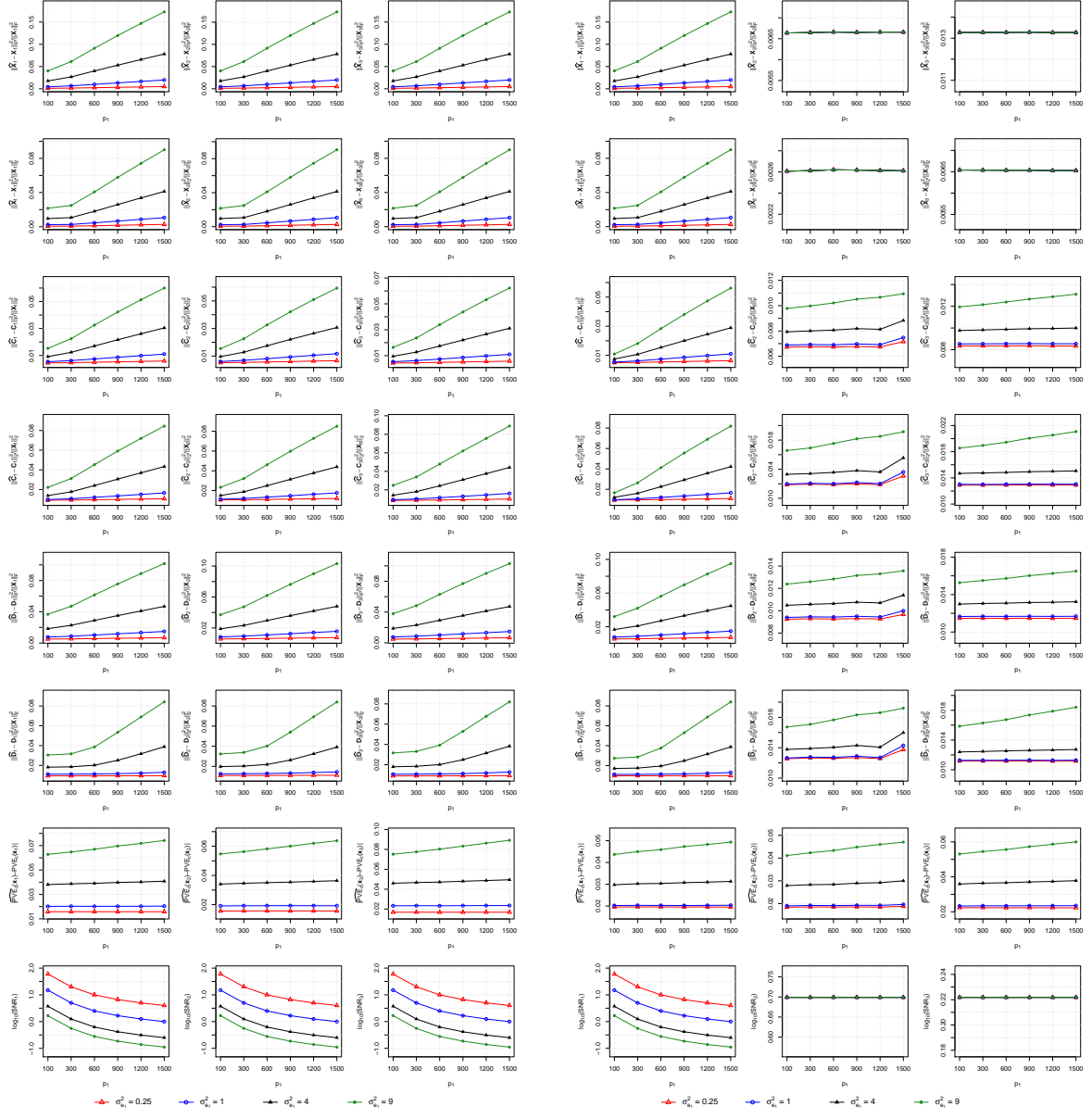


Figure 4: Average errors of D-GCCA estimates over 1000 replications for Setups 2.1 and 2.2.

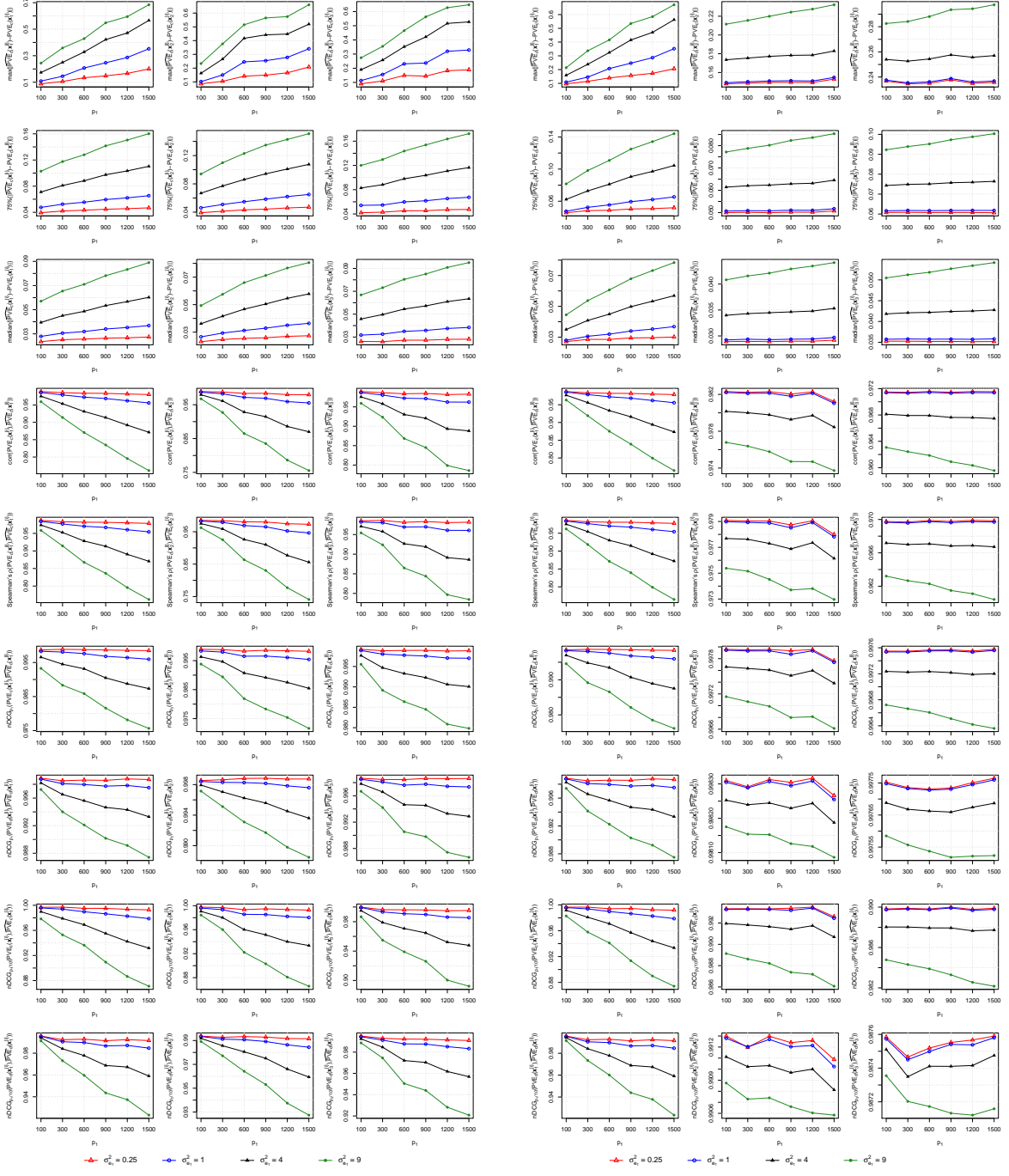


Figure 5: Average results of D-GCCA's variable-level PVE estimation over 1000 replications for Setups 2.1 and 2.2.

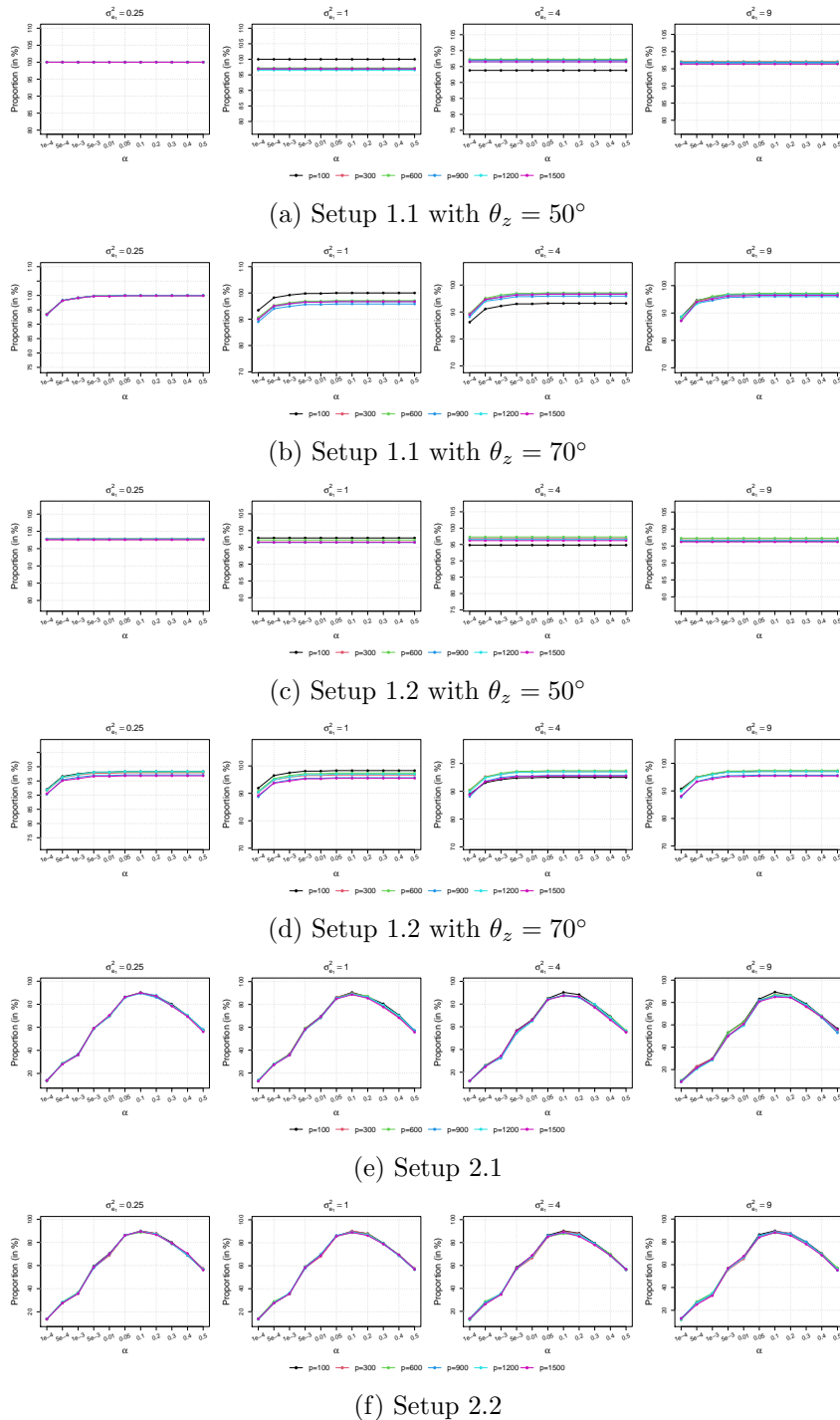


Figure 6: The proportion of 1000 simulation replications where all nuisance parameters of D-GCCA are correctly selected. The nuisance parameters are selected using the approach described in Section 3.3 with a significance level α uniformly applied to all tests.

Setup	Method	≥ 1 orth. pair	$\hat{\rho}_1(\{\mathbf{d}_k\}_{k=1}^3)$	$\frac{\ \hat{\mathbf{X}}_1 - \mathbf{X}_1\ _F^2}{\ \mathbf{X}_1\ _F^2}, \frac{\ \hat{\mathbf{X}}_2 - \mathbf{X}_2\ _F^2}{\ \mathbf{X}_2\ _F^2}, \frac{\ \hat{\mathbf{X}}_3 - \mathbf{X}_3\ _F^2}{\ \mathbf{X}_3\ _F^2}$
$(p_1 = 600, \theta_z = 50^\circ, \sigma_{e_1}^2 = 1)$	D-GCCA1	100%	1.10 (0.05)	0.006 (6.0e-4), 0.006 (5.9e-4), 0.006 (5.6e-4)
	D-GCCA2	100%	1.10 (0.05)	0.006 (1.0e-3), 0.006 (1.1e-3), 0.006 (1.6e-3)
	JIVE	0%	2.22 (0.06)	0.014 (1.4e-3), 0.014 (1.4e-3), 0.014 (1.3e-3)
	R.JIVE	100%	1.00 (0.00)	0.032(1.0e-2), 0.021(3.1e-3), 0.023(7.1e-3)
	AJIVE	0% (zero $\hat{\mathbf{C}}_{ks}$)	2.28 (0.05)	0.006 (6.0e-4), 0.006 (6.0e-4), 0.006 (5.6e-4)
	COBE	0% (zero $\hat{\mathbf{C}}_{ks}$)	2.28 (0.05)	0.006 (6.0e-4), 0.006 (6.0e-4), 0.006 (5.6e-4)
	OnPLS	1.1%	1.87 (0.05)	0.026 (2.3e-3), 0.026 (2.3e-3), 0.026 (2.2e-3)
	DISCO-SCA	0% (zero $\hat{\mathbf{C}}_{ks}$)	3.00 (0.00)	0.014 (1.3e-3), 0.014 (1.3e-3), 0.014 (1.3e-3)
	D-GCCA1	100%	1.10 (0.05)	0.006 (6.0e-4), 0.004 (4.1e-4), 0.008 (7.3e-4)
$(p_1 = 600, \theta_z = 50^\circ, \sigma_{e_1}^2 = 1)$	D-GCCA2	100%	1.10 (0.05)	0.006 (1.0e-3), 0.004 (7.9e-4), 0.008 (1.7e-3)
	JIVE	0%	2.20 (0.06)	0.014 (1.4e-3), 0.009 (1.0e-3), 0.018 (1.6e-3)
	R.JIVE	100%	1.00 (0.00)	0.033(1.0e-2), 0.014(2.3e-3), 0.029(6.7e-3)
	AJIVE	0% (zero $\hat{\mathbf{C}}_{ks}$)	2.28 (0.05)	0.006 (6.0e-4), 0.004 (4.1e-4), 0.008 (7.3e-4)
	COBE	0% (zero $\hat{\mathbf{C}}_{ks}$)	2.28 (0.05)	0.006 (6.0e-4), 0.004 (4.1e-4), 0.008 (7.3e-4)
	OnPLS	0.9%	1.83 (0.05)	0.026 (2.4e-3), 0.018 (1.6e-3), 0.026 (2.2e-3)
	DISCO-SCA	0% (zero $\hat{\mathbf{C}}_{ks}$)	3.00 (0.00)	0.014 (1.3e-3), 0.008 (7.6e-4), 0.020 (1.8e-3)
	D-GCCA1	0%	2.13 (0.05)	0.010 (4.5e-4), 0.010 (4.5e-4), 0.010 (4.8e-4)
	D-GCCA2	0%	2.14 (0.06)	0.010 (4.5e-4), 0.010 (4.5e-4), 0.010 (4.8e-4)
$(p_1 = 600, \sigma_{e_1}^2 = 1)$	Setup 2.1 JIVE	0%	2.52 (0.21)	0.016 (2.0e-3), 0.016 (2.2e-3), 0.016 (2.1e-3)
	R.JIVE	100%	1.00 (0.00)	0.076(4.3e-2), 0.080(4.9e-2), 0.065(3.4e-2)
	AJIVE	0%	2.80 (0.02)	0.010 (4.4e-4), 0.010 (4.3e-4), 0.010 (4.7e-4)
	COBE	0%	2.80 (0.02)	0.010 (4.6e-4), 0.010 (4.6e-4), 0.010 (4.8e-4)
	OnPLS	0.1%	2.65 (0.18)	0.014 (1.7e-3), 0.014 (3.1e-3), 0.015 (1.8e-3)
	DISCO-SCA	NA	NA	NA
	D-GCCA1	0%	2.13 (0.05)	0.010 (4.5e-4), 0.007 (3.2e-4), 0.013 (6.1e-4)
	D-GCCA2	0%	2.14 (0.06)	0.010 (4.5e-4), 0.007 (3.2e-4), 0.013 (6.1e-4)
	Setup 2.2 JIVE	0%	2.41 (0.26)	0.016 (2.3e-3), 0.010 (1.4e-3), 0.021 (3.1e-3)
$(p_1 = 600, \sigma_{e_1}^2 = 1)$	R.JIVE	100%	1.00 (0.00)	0.064(4.0e-2), 0.063(5.0e-2), 0.079(4.3e-2)
	AJIVE	0%	2.80 (0.02)	0.010 (4.4e-4), 0.006 (3.0e-4), 0.013 (6.1e-4)
	COBE	0%	2.80 (0.02)	0.010 (4.6e-4), 0.007 (3.2e-4), 0.013 (6.2e-4)
	OnPLS	0.5%	2.51 (0.18)	0.015 (6.5e-3), 0.009 (1.3e-3), 0.020 (2.6e-3)
	DISCO-SCA	NA	NA	NA

Table 1: The proportions of replications with at least one orthogonal pair among $\{\mathbf{d}_k\}_{k=1}^3$, averages (standard deviations) of $\hat{\rho}_1(\{\mathbf{d}_k\}_{k=1}^3)$, and averages (standard deviations) of scaled squared errors of signal matrix estimates over 1000 simulation replications. D-GCCA1: the D-GCCA using true nuisance parameters. D-GCCA2: the D-GCCA using nuisance parameters selected by the approach in Section 3.3. NA: not available due to out of the 24-hour time limit on a CPU core (up to 3.0GHz) per simulation replication. By the paired t-test, both D-GCCA1 and D-GCCA2 have significantly different mean $\hat{\rho}_1(\{\mathbf{d}_k\}_{k=1}^3)$ values from those of all the other methods with p-values < 1e-10.

2642 variably expressed genes, miRNA expression data for 437 highly variant miRNAs, and DNA methylation data for 3298 most variable probes. The data have been preprocessed following the procedure of Lock and Dunson (2013). The tumor samples are categorized by the classic PAM50 model (Parker et al., 2009) into four intrinsic subtypes that are relevant with clinical outcomes, including 111 Basal-like, 56 HER2-enriched, 346 Luminal A, and 151 Luminal B tumors. The PAM50 intrinsic subtypes are defined by mRNA expression only. We investigate whether these intrinsic subtypes are also characterized by other genomic data types such as DNA methylation and miRNA expression that represent different biological components. In particular, we study the relationship between the PAM50 intrinsic subtypes and the common and distinctive underlying mechanisms of the three genomic data types by evaluating the ability of their corresponding matrices in model (1) to separate the four intrinsic subtypes.

Each observed data matrix is row-centered by subtracting the average within each row. The nuisance parameters of our D-GCCA method are selected by using the approach described in Section 3.3. The selection approach yields the same decomposition by the choices 0.2 and 0.0001 for the significance level uniformly applied to all involved hypothesis tests. The values ($\text{rank}(\hat{\mathbf{X}}_k)$, $\text{rank}(\hat{\mathbf{C}}_k)$, $\text{rank}(\hat{\mathbf{D}}_k)$, $\widehat{\text{PVE}}_c(\mathbf{x}_k)$) from the D-GCCA method are (4, 2, 4, 0.239), (3, 2, 3, 0.184) and (3, 2, 3, 0.147) for the mRNA, miRNA, and DNA data types, respectively. To quantify the subtype separation in a matrix, we adopt the SWISS

Method	$\hat{\mathbf{X}}_k$	$\hat{\mathbf{C}}_k$	$\hat{\mathbf{D}}_k$	$\hat{\mathbf{E}}_k$
D-GCCA	48.0, 62.7, 73.6	21.5[‡], 21.2, 26.8[#]	74.2, 84.9, 93.2	99.0, 98.4, 98.3
JIVE	74.0, 80.0, 82.5	65.6, 65.3, 58.9	86.1, 87.9, 92.1	99.8, 99.6, 99.7
R.JIVE	74.5, 74.7, 80.8	41.7, 38.1, 64.6	93.3, 99.7, 99.6	99.8, 97.0, 97.6
AJIVE	48.2, 62.7, 73.6	NA, NA, NA	48.2, 62.7, 73.6	99.0, 98.4, 98.3
COBE	48.2, 62.7, 73.6	NA, NA, NA	48.2, 62.7, 73.6	99.0, 98.4, 98.3
OnPLS	60.0, 70.8, 78.1	36.4, 34.1, 36.4	89.6, 95.8, 98.6	99.5, 98.9, 99.6
DISCO-SCA	56.7, 67.4, 75.0	52.6, 53.0, 48.5	99.0, 97.7, 99.3	99.4, 99.5, 99.6
JIVE*	48.0, 62.7, 73.6	35.0, 33.0, 50.8	89.0, 93.8, 97.3	NA, NA, NA
R.JIVE*	47.6, 60.2, 72.2	34.0, 28.5, 61.4	84.7, 98.7, 99.4	99.3, 84.7, 83.5
AJIVE*	48.0, 62.7, 73.6	NA, NA, NA	48.0, 62.7, 73.6	NA, NA, NA
COBE*	48.0, 62.7, 73.6	NA, NA, NA	48.0, 62.7, 73.6	NA, NA, NA
OnPLS*	48.0, 62.7, 73.6	22.6 [‡] , 26.4, 30.5	75.1, 87.8, 94.0	NA, NA, NA
DISCO-SCA*	48.0, 62.7, 73.6	28.0, 28.0, 28.0 [#]	77.9, 82.7, 94.9	NA, NA, NA
\mathbf{Y}_k	84.8, 87.8, 90.0			

Table 2: SWISS scores (in %) for TCGA breast cancer genomic data types ($k = \text{mRNA}$, miRNA, DNA). Lower SWISS scores indicate better subtype separation. Methods suffixed with * use D-GCCA’s $\hat{\mathbf{X}}_k$ s instead of \mathbf{Y}_k s as the input data. NA: not available due to a zero matrix estimate. All methods have $\text{SWISS}(\hat{\mathbf{X}}_k) < \text{SWISS}(\mathbf{Y}_k)$ for each k . Except AJIVE and COBE with $\hat{\mathbf{C}}_k = \mathbf{0}$, all the other methods have $\text{SWISS}(\hat{\mathbf{C}}_k) < \text{SWISS}(\hat{\mathbf{X}}_k) < \text{SWISS}(\hat{\mathbf{D}}_k)$ for each k . Our D-GCCA has the lowest $\text{SWISS}(\hat{\mathbf{C}}_k)$ for all k . By the test of Cabanski et al. (2010), all above comparisons of SWISS scores are significantly different with p-values < 0.001 , except for the two annotated respectively by ‡ and $^{\#}$ with p-values > 0.05 .

score of Cabanski et al. (2010) that calculates the standardized within-subtype sum of squares: For a matrix $\mathbf{M} = (M_{ij})_{p \times n}$,

$$\text{SWISS}(\mathbf{M}) = \frac{\sum_{i=1}^p \sum_{j=1}^n (M_{ij} - \bar{M}_{i,s(j)})^2}{\sum_{i=1}^p \sum_{j=1}^n (M_{ij} - \bar{M}_{i,\cdot})^2},$$

where $\bar{M}_{i,s(j)}$ is the average of the j th sample's subtype on the i th row, and $\bar{M}_{i,\cdot}$ is the average of the i th row's elements. The lower score indicates better subtype separation.

Table 2 shows the SWISS scores computed for the D-GCCA method and also the six competing methods mentioned in Section 1. The denoised signal matrix $\hat{\mathbf{X}}_k$ from all methods gains an improved ability on subtype separation with a smaller score, comparing to the noisy data matrix \mathbf{Y}_k . All methods, except AJIVE and COBE, discover nonzero common-source matrices, and show a clear pattern of decreasing SWISS scores from $\hat{\mathbf{D}}_k$ to $\hat{\mathbf{X}}_k$ and then to $\hat{\mathbf{C}}_k$. This pattern indicates that the four PAM50 intrinsic subtypes are more likely to be an inherent feature of the common mechanism underlying the three different genomic data types. Moreover, our D-GCCA method has the lowest scores for estimated common-source matrices when compared with the other methods. The result analysis remains the same even when our D-GCCA's $\hat{\mathbf{X}}_k$ s, which have the smallest SWISS scores among all signal estimates, are used as the input data for the other six methods.

The better SWISS scores of D-GCCA for common-source matrix estimates indicate its enhanced ability to capture the common latent factors than the other methods, which

Method	$d_{\text{mRNA}} \& d_{\text{miRNA}}$	$d_{\text{mRNA}} \& d_{\text{DNA}}$	$d_{\text{miRNA}} \& d_{\text{DNA}}$
D-GCCA	58.3%	58.3%	0%
JIVE	15.9%	21.0%	17.9%
R.JIVE	0%	0%	0%
AJIVE	75.0%	75.0%	77.8%
COBE	75.0%	75.0%	77.8%
OnPLS	41.3%	60.0%	36.1%
DISCO-SCA	62.5%	68.8%	56.3%
JIVE*	83.3%	75.0%	66.7%
R.JIVE*	0%	0%	0%
AJIVE*	75.0%	75.0%	77.8%
COBE*	75.0%	75.0%	77.8%
OnPLS*	83.3%	50.0%	25.0%
DISCO-SCA*	66.7%	83.3%	55.6%

Table 3: The proportions of significant nonzero correlations between distinctive latent factors across TCGA breast cancer genomic data types. The proportion is computed by $\frac{1}{d_j d_k} \sum_{m=1}^{r_{d_j}} \sum_{\ell=1}^{r_{d_k}} [\text{corr}(d_j^{(m)}, d_k^{(\ell)}) \neq 0]$ for $j \neq k$, where $\{d_k^{(\ell)}\}_{\ell=1}^{r_{d_k}}$ are latent factors of d_k , and $\text{corr}(d_j^{(m)}, d_k^{(\ell)}) \neq 0$ is detected by the normal approximation test (DiCiccio and Romano, 2017) with false discovery rate controlled at 0.05 (Benjamini and Hochberg, 1995) and the ℓ th right-singular vector of $\hat{\mathbf{D}}_k$ used as the n samples of $d_k^{(\ell)}$. Methods suffixed with * use D-GCCA's $\hat{\mathbf{X}}_k$ s instead of \mathbf{Y}_k s as the input data.

benefits from our well designed orthogonality constraint on distinctive latent factors. Table 3 further verifies this conclusion, and shows that significant nonzero correlations do not exist between D-GCCA's $\mathbf{d}_{\text{miRNA}}$ and \mathbf{d}_{DNA} but account for over 15% among all pairs of \mathbf{d}_k s from the other methods except R.JIVE. However, R.JIVE enforces the orthogonality of \mathbf{d}_k s by sacrificing its unexplained signal to be noise. This can be seen in Table 2, where R.JIVE has slightly lower SWISS scores for $\widehat{\mathbf{E}}_k$ s than JIVE, its original version with no orthogonality constraint on \mathbf{d}_k s, and moreover has nonzero $\widehat{\mathbf{E}}_k$ s when using low-rank D-GCCA's signal estimates as the input data.

For each genomic data type, Table 4 lists the top 10 variables most influenced by common latent factors and those by distinctive latent factors according to their explained variable-

Name	$\widehat{\text{PVE}}_c(\mathbf{x}_k^{[i]})$	SWISS score			Name	$\widehat{\text{PVE}}_d(\mathbf{x}_k^{[i]})$	SWISS score		
		$\widehat{\mathbf{X}}_k^{[i,:]}$	$\widehat{\mathbf{C}}_k^{[i,:]}$	$\widehat{\mathbf{D}}_k^{[i,:]}$			$\widehat{\mathbf{X}}_k^{[i,:]}$	$\widehat{\mathbf{C}}_k^{[i,:]}$	$\widehat{\mathbf{D}}_k^{[i,:]}$
Top 10 genes for $k = \text{mRNA}$									
AKR7A3	0.449	0.156	0.182	0.318	FGG	0.9999	0.750	0.253	0.750
RHCG	0.449	0.153	0.183	0.309	NEU4	0.9995	0.718	0.210	0.716
AADAT	0.448	0.136	0.179	0.281	TAS1R3	0.9995	0.738	0.745	0.732
GAL	0.448	0.145	0.180	0.300	PCSK1	0.9993	0.832	0.289	0.833
SLC26A9	0.448	0.175	0.185	0.363	HMGCLL1	0.9993	0.708	0.315	0.710
PLAC1	0.447	0.162	0.186	0.324	HNF4G	0.9993	0.774	0.248	0.776
KIAA1257	0.447	0.177	0.187	0.362	CRISP3	0.9991	0.725	0.469	0.723
FMO6P	0.447	0.133	0.176	0.281	TYRP1	0.9988	0.783	0.515	0.787
GDF15	0.447	0.166	0.184	0.345	LHFPL4	0.9987	0.775	0.335	0.778
TNNT2	0.445	0.131	0.178	0.287	NTS	0.9985	0.761	0.679	0.766
Top 10 miRNAs for $k = \text{miRNA}$									
hsa-mir-584	0.448	0.322	0.190	0.732	hsa-mir-34b	0.99995	0.924	0.233	0.923
hsa-mir-1468	0.444	0.276	0.174	0.657	hsa-mir-26a-2	0.9999	0.927	0.388	0.926
hsa-mir-203	0.443	0.346	0.196	0.763	hsa-mir-196a-1	0.9998	0.928	0.403	0.927
hsa-mir-135b	0.433	0.270	0.169	0.642	hsa-mir-874	0.9973	0.893	0.511	0.906
hsa-mir-519a-1	0.428	0.265	0.167	0.632	hsa-mir-193a	0.9953	0.881	0.539	0.899
hsa-mir-190b	0.420	0.384	0.210	0.782	hsa-mir-615	0.9947	0.872	0.667	0.892
hsa-mir-29c	0.415	0.341	0.193	0.747	hsa-mir-326	0.9944	0.882	0.444	0.901
hsa-mir-526b	0.413	0.371	0.182	0.797	hsa-mir-296	0.9934	0.943	0.291	0.936
hsa-mir-28	0.411	0.424	0.200	0.859	hsa-mir-26b	0.9912	0.856	0.663	0.882
hsa-mir-30e	0.409	0.299	0.166	0.681	hsa-let-7e	0.9877	0.854	0.537	0.884
Top 10 probes for $k = \text{DNA}$									
cg04220579	0.438	0.314	0.178	0.726	cg24030449	0.9999	0.981	0.424	0.980
cg02085507	0.437	0.309	0.190	0.700	cg17296078	0.9998	0.984	0.665	0.982
cg18055007	0.432	0.314	0.195	0.701	cg14009688	0.9997	0.984	0.684	0.983
cg26668713	0.432	0.319	0.182	0.732	cg00121904	0.9997	0.972	0.722	0.975
cg23178308	0.430	0.337	0.186	0.748	cg02789485	0.9997	0.982	0.281	0.981
cg12406559	0.428	0.329	0.176	0.756	cg07482936	0.9996	0.977	0.200	0.977
cg25167447	0.427	0.351	0.168	0.776	cg01817393	0.9996	0.977	0.197	0.978
cg14385738	0.422	0.337	0.176	0.770	cg10484958	0.9993	0.986	0.497	0.984
cg02433671	0.420	0.333	0.207	0.718	cg17532978	0.9986	0.969	0.383	0.974
cg00916635	0.420	0.346	0.171	0.786	cg08291098	0.9985	0.971	0.268	0.974

Table 4: Variables with top 10 largest $\widehat{\text{PVE}}_c(\mathbf{x}_k^{[i]})$ (the left half table) or $\widehat{\text{PVE}}_d(\mathbf{x}_k^{[i]})$ (the right half table) for each of the three TCGA breast cancer genomic data types. The SWISS score shows the separation of PAM50 subtypes; a lower score indicates a better separation.

level proportions of signal variance, $\{\widehat{\text{PVE}}_c(\mathbf{x}_k^{[i]})\}_{i=1}^{p_k}$ or $\{\widehat{\text{PVE}}_d(\mathbf{x}_k^{[i]})\}_{i=1}^{p_k}$. Table 4 also reports the SWISS scores for the data $\widehat{\mathbf{X}}_k^{[i,:]}$, $\widehat{\mathbf{C}}_k^{[i,:]}$ and $\widehat{\mathbf{D}}_k^{[i,:]}$ of each selected variable to corroborate the influences of those underlying mechanisms, because the PAM50 subtype separation has been shown above as a good indicator of the common underlying mechanism. Indeed, $\text{SWISS}(\widehat{\mathbf{C}}_k^{[i,:]})$ is significantly smaller than $\text{SWISS}(\widehat{\mathbf{D}}_k^{[i,:]})$ ($p\text{-value} < 0.05$) for all selected variables except for the gene TAS1R3 that has comparable scores 0.745 and 0.732. For the top 10 variables with largest $\widehat{\text{PVE}}_c(\mathbf{x}_k^{[i]})$ values $> 40\%$, their signal data $\widehat{\mathbf{X}}_k^{[i,:]}$'s well inherit from their $\widehat{\mathbf{C}}_k^{[i,:]}$'s the ability to separate the PAM50 subtypes with small SWISS scores ≤ 0.424 , confirming the considerable influence of the common underlying mechanism on these variables. The top 10 variables with largest $\widehat{\text{PVE}}_d(\mathbf{x}_k^{[i]})$ values all have much less informative $\text{SWISS}(\widehat{\mathbf{X}}_k^{[i,:]}) \geq 0.708$ nearly the same as $\text{SWISS}(\widehat{\mathbf{D}}_k^{[i,:]})$ and therefore are almost immune to the influence from the common underlying mechanism, which is consistent with their negligible $\widehat{\text{PVE}}_c(\mathbf{x}_k^{[i]})$ values $< 1.5\%$.

5.2 Application to HCP motor-task functional MRI

We consider the motor-task functional MRI data obtained from the HCP (Barch et al., 2013). During the image scanning, each of 1080 participants was asked by visual cues to either tap left or right fingers, or squeeze left or right toes, or move their tongue. From the acquired brain images, the HCP generated for every participant the z -statistic maps of the individual contrasts of the five tasks and also their average contrast against the fixation baseline. The average contrast represents the impact of the overall motor task. All the maps were computed at 91,282 grayordinates including 59,412 cortical surface vertices and 31,870 subcortical gray matter voxels. For each task, its z -statistic maps of all participants constitute a $91,282 \times 1080$ data matrix. We focus on the left-hand, right-hand, and overall motor tasks, and aim to discover the brain regions that are most affected by their common underlying mechanism.

The D-GCCA method is applied to the three data matrices of interest that are row-centered beforehand, with nuisance parameters selected by the approach discussed in Section 3.3. The selection approach yields the same decomposition by the choices 0.2 and 0.0001 for the significance level uniformly applied to all involved tests. All signal and common-source matrix estimates are rank-2. The distinctive-source random vectors of the left-hand and right-hand tasks are tested to be uncorrelated by the approach in Section 4.3, and thus the common-source variation of the three tasks is fully captured by their common-source random vectors. The estimated view-level proportion of signal variance explained by common latent factors, $\widehat{\text{PVE}}_c(\mathbf{x}_k)$, has values 0.122, 0.120 and 0.128, respectively, for the left-hand, right-hand and overall motor tasks. This quantity reflects the overall influence of the common underlying mechanism on the k th considered motor task.

To assess the local influence of the common underlying mechanism on the i th brain grayordinate of the k th task, we use $\widehat{\text{PVE}}_c(\mathbf{x}_k^{[i]})$ the estimated variable-level proportion of signal variance explained by common latent factors. Figure 7 illustrates the map of $\{\widehat{\text{PVE}}_c(\mathbf{x}_k^{[i]})\}_{i=1}^{91282}$ for each task. In Figure 7 (a) for the left-hand task, we see that the common underlying mechanism has stronger impacts on the right cortical surface, particularly, the somatomotor cortex in the right green circle, whereas it affects more on the left sub-

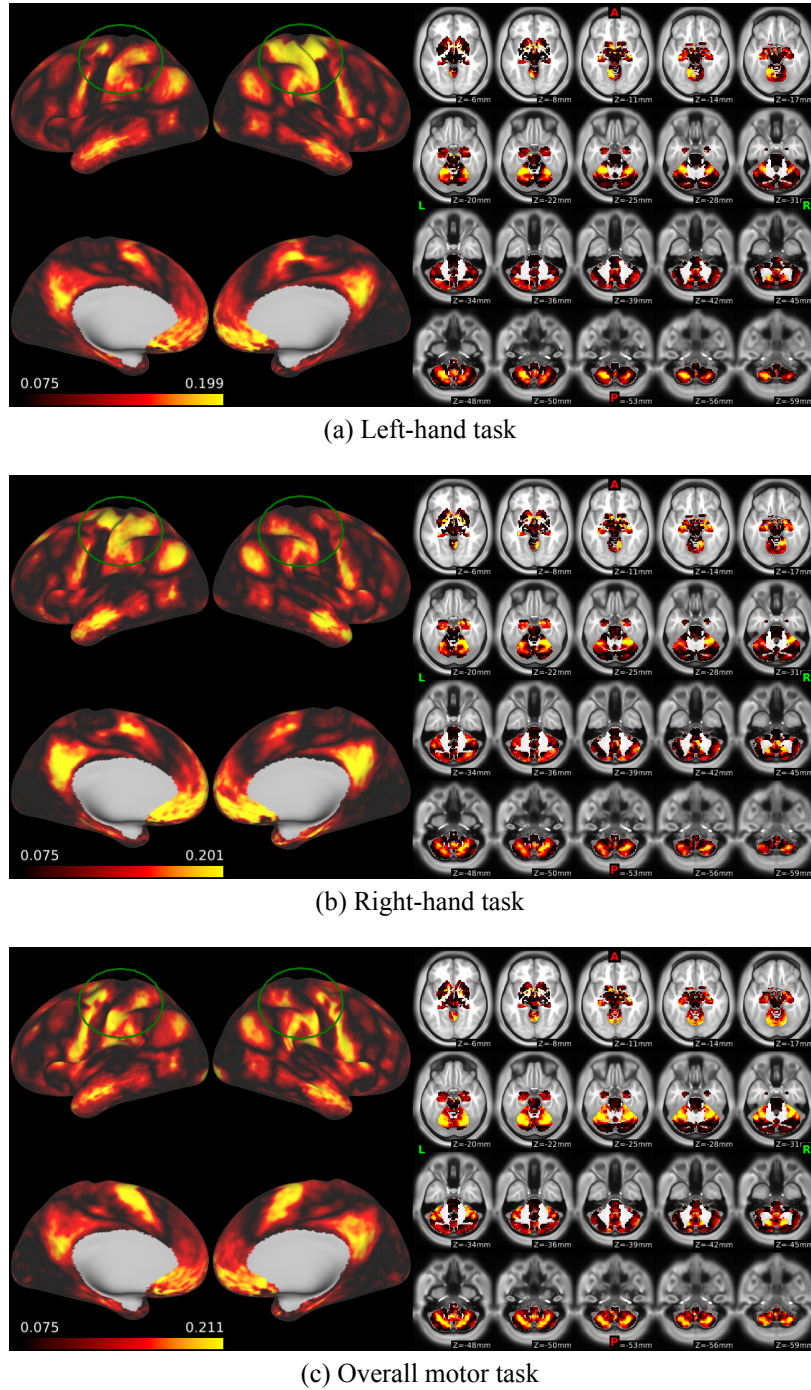


Figure 7: Maps of $\{\widehat{\text{PVE}}_c(\mathbf{x}_k^{[i]})\}_{i=1}^{91282}$ from D-GCCA for the three HCP motor tasks. In each subfigure, the left part displays the cortical surface with the outer side shown in the first row and the inner side in the second row; the right part shows the subcortical area on 20 xy slides at the z axis. The somatomotor cortex is annotated by green circles.

cortical regions such as the cerebellum shown in the first and last rows of the right part of the figure. The influence pattern is almost opposite for the right-hand task, and is nearly symmetric on the two sides of the brain for the overall motor task. The contralateral change in the somatomotor cortex and the cerebellum is consistent with their intrinsic functional connectivity shown in Buckner et al. (2011).

On this large-scale data, we also compare the computational performance of our D-GCCA and the six competing methods mentioned in Section 1. All methods were implemented separately on a computing node with two 10-core Intel Xeon E5-2690v2 3.0GHz CPUs, total 62GB memory, and 24-hour time limit. The three methods, JIVE (with 5.47 hours), R.JIVE (with 17.4 hours) and DISCO-SCA (out of 24 hours), all involving time-expensive iterative optimization, cannot converge within 5 hours. The OnPLS method ran out of memory due to computing the SVD of each large matrix $\mathbf{Y}_j \mathbf{Y}_k^\top$ for $j \neq k$. Both D-GCCA and AJIVE have closed-form expressions, and COBE uses a fast alternating optimization strategy. The computational time costs of the D-GCCA, AJIVE and COBE methods are 18.0, 180.5 and 25.3 seconds, respectively. However, the AJIVE and COBE methods were unable to identify nonzero common-source matrices.

6. Conclusion

In this paper, we propose a novel decomposition method, called D-GCCA, to separate the common and distinctive variation structures of two or more data views on the same objects. In contrast with existing methods, we build the decomposition on $(\mathcal{L}_0^2, \text{cov})$ rather than the traditional (\mathbb{R}^n, \cdot) , and particularly impose a certain orthogonality constraint on the distinctive latent factors to better capture the common-source variation, along with a geometric interpretation from PCA for the associated common latent factors. Asymptotic result of proposed estimation under high-dimensional settings is established and supported by simulations. Moreover, the D-GCCA decomposition has a closed-form expression and thus is more computationally efficient, especially for large-scale data, than most existing methods with time-expensive iterative optimization. Simulated and real-world data show the advantages of D-GCCA over state-of-the-art methods in capturing the common-source variation and also in the computational time cost.

Acknowledgments

Dr. Shu's work was partially supported by the NIH grant R21AG070303. Dr. Zhu's work was partially supported by NIH grants R01MH086633 and R01MH116527. The content is solely the responsibility of the authors and does not necessarily represent the official views of the NIH. We are grateful to the Action Editor Dr. Qiaozhu Mei and three anonymous reviewers for their constructive comments that greatly reshaped this article.

Appendix A. A Hierarchical Extension

The hierarchical decomposition structure in Section 2.2.3 is illustrated in Figure 8.

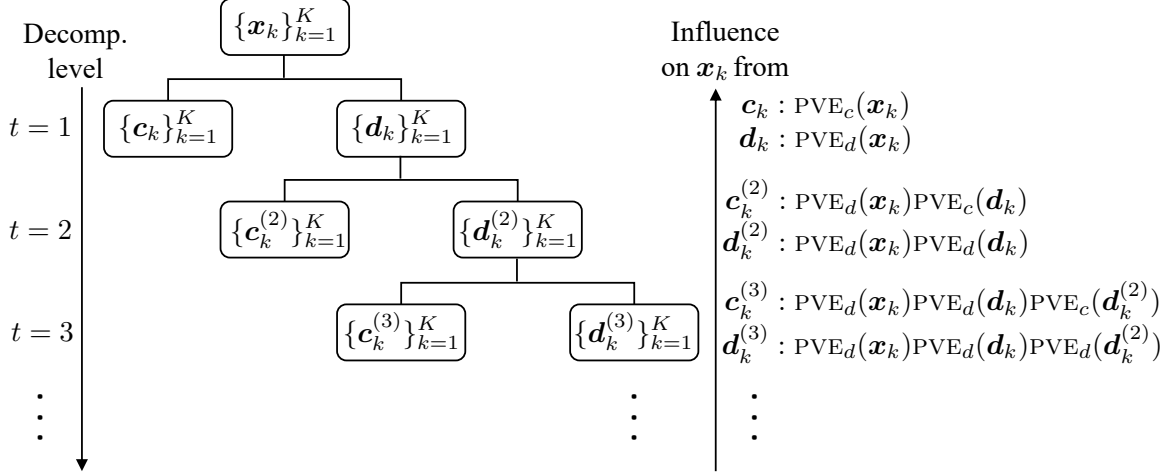


Figure 8: A hierarchical extension of D-GCCA.

For the $(t+1)$ th-level decomposition ($t \geq 1$), recall that the view-level explained proportion of $\mathbf{d}_k^{(t)}$'s variance $\text{PVE}_c(\mathbf{d}_k^{(t)}) = 1 - \text{PVE}_d(\mathbf{d}_k^{(t)}) := \text{tr}\{\text{cov}(\mathbf{c}_k^{(t+1)})\}/\text{tr}\{\text{cov}(\mathbf{d}_k^{(t)})\}$, and the variable-level explained proportion of variance $\text{PVE}_c([\mathbf{d}_k^{(t)}]^{[i]}) = 1 - \text{PVE}_d([\mathbf{d}_k^{(t)}]^{[i]}) := \text{var}([\mathbf{c}_k^{(t+1)}]^{[i]})/\text{var}([\mathbf{d}_k^{(t)}]^{[i]})$. Denote the sample matrices and their estimators of $(\mathbf{c}_k^{(t)}, \mathbf{d}_k^{(t)})$ by $(\mathbf{C}_k^{(t)}, \mathbf{D}_k^{(t)})$ and $(\widehat{\mathbf{C}}_k^{(t)}, \widehat{\mathbf{D}}_k^{(t)})$, and the estimators of $(\text{PVE}_c(\mathbf{d}_k^{(t)}), \text{PVE}_d(\mathbf{d}_k^{(t)}), \text{PVE}_c([\mathbf{d}_k^{(t)}]^{[i]}), \text{PVE}_d([\mathbf{d}_k^{(t)}]^{[i]}))$ by $(\widehat{\text{PVE}}_c(\mathbf{d}_k^{(t)}), \widehat{\text{PVE}}_d(\mathbf{d}_k^{(t)}), \widehat{\text{PVE}}_c([\mathbf{d}_k^{(t)}]^{[i]}), \widehat{\text{PVE}}_d([\mathbf{d}_k^{(t)}]^{[i]}))$. We define estimators $(\widehat{\mathbf{C}}_k^{(t+1)}, \widehat{\mathbf{D}}_k^{(t+1)})$ in the same way as $(\widehat{\mathbf{C}}_k, \widehat{\mathbf{D}}_k)$ given in Section 3.1 by replacing $\widehat{\mathbf{X}}_k$ with $\widehat{\mathbf{D}}_k^{(t)}$, where $\widehat{\mathbf{D}}_k^{(1)} = \widehat{\mathbf{D}}_k$, and define $\widehat{\text{PVE}}_c(\mathbf{d}_k^{(t)}) = 1 - \widehat{\text{PVE}}_d(\mathbf{d}_k^{(t)}) = \|\widehat{\mathbf{C}}_k^{(t+1)}\|_F^2/\|\widehat{\mathbf{D}}_k^{(t)}\|_F^2$ and $\widehat{\text{PVE}}_c([\mathbf{d}_k^{(t)}]^{[i]}) = 1 - \widehat{\text{PVE}}_d([\mathbf{d}_k^{(t)}]^{[i]}) = \|[\widehat{\mathbf{C}}_k^{(t+1)}]^{[i,:]}\|_F^2/\|[\widehat{\mathbf{D}}_k^{(t)}]^{[i,:]}\|_F^2$. The corresponding nuisance parameters are selected in the same fashion as in Section 3.3.

We have the following asymptotic properties for the above estimators.

Corollary 1 Suppose that Assumption 1 holds and the other conditions on $\{\mathbf{x}_k\}_{k=1}^K$ for (28)-(29) in Theorem 5 are also satisfied on $\{\mathbf{d}_k^{(t)}\}_{k=1}^K$ for all $0 \leq t \leq T$ with a fixed number $T \geq 1$. For all $1 \leq k \leq K$ and $1 \leq t \leq T$, further assume that the distinct eigenvalues of $\text{cov}(\mathbf{d}_k^{(t)})$, denoted by $\lambda_{k,1}^{(t)} > \dots > \lambda_{k,m_k^{(t)}}^{(t)} = 0$, satisfy $\lambda_{k,1}^{(t)} > \kappa^{(t)} \lambda_{r_k}(\text{cov}(\mathbf{x}_k))$, $\lambda_{k,1}^{(t)} \asymp \lambda_{k,m_k^{(t)}}^{(t)}$, and $(\lambda_{k,\ell}^{(t)} - \lambda_{k,\ell+1}^{(t)})/\lambda_{k,\ell}^{(t)} \geq \delta^{(t)}$ for $1 \leq \ell \leq m_k^{(t)}$ with constants $\kappa^{(t)}, \delta^{(t)} > 0$. If $\delta_\eta = o(1)$, then

$$\max \left\{ \frac{\|\widehat{\mathbf{C}}_k^{(T+1)} - \mathbf{C}_k^{(T+1)}\|_*^2}{\|\mathbf{D}_k^{(T)}\|_*^2}, \frac{\|\widehat{\mathbf{D}}_k^{(T+1)} - \mathbf{D}_k^{(T+1)}\|_*^2}{\|\mathbf{D}_k^{(T)}\|_*^2} \right\} = O_P(\delta_\eta^2) \quad (31)$$

and

$$|\widehat{\text{PVE}}_c(\mathbf{d}_k^{(T)}) - \text{PVE}_c(\mathbf{d}_k^{(T)})| = O_P(\delta_\eta). \quad (32)$$

Additionally, if the nonzero eigenvalues of $\text{cov}(\mathbf{d}_k^{(T)})$ are distinct, a basis of $\text{span}([\mathbf{d}_k^{(T)}]^\top)$ has all elements with the sub-Gaussian norm bounded from above, $\min_{i \leq p_k} \text{var}([\mathbf{d}_k^{(T)}]^{[i]}) \geq M_k^{(T)} \lambda_{k, m_k^{(T)}}^{(T)} / p_k$ with a constant $M_k^{(T)} > 0$, and $\delta_k = o(1)$, then we have

$$\max_{1 \leq i \leq p_k} \left| \widehat{\text{PVE}}_c([\mathbf{d}_k^{(T)}]^{[i]}) - \text{PVE}_c([\mathbf{d}_k^{(T)}]^{[i]}) \right| = O_P(\delta_\eta + \delta_k). \quad (33)$$

In Corollary 1, the condition $\lambda_{k,1}^{(t)} > \kappa^{(t)} \lambda_{r_k}(\text{cov}(\mathbf{x}_k))$ implies that the variance ratio $\text{tr}\{\text{cov}(\mathbf{d}_k^{(t)})\} / \text{tr}\{\text{cov}(\mathbf{x}_k)\}$ is bounded away from zero and hence is worth the $(t+1)$ th-level decomposition. The other conditions on $\{\mathbf{d}_k^{(t)}\}_{k=1}^K$ are similar to those in Assumption 1 and Theorem 5.

Appendix B. Theoretical Proofs

Proof of Theorem 1. Consider stage $\ell \leq r_f$. If $w \perp \text{span}(\mathbf{f}^\top)$, then $\sum_{k=1}^K \cos^2\{\theta(w, z_k)\} = 0$, and thus this w is not optimal because there always exists another $w \in \text{span}(\mathbf{f}^\top)$ and $z_k \in \text{span}(\mathbf{x}_k^\top)$, $k = 1, \dots, K$, such that $\sum_{k=1}^K \cos^2\{\theta(w, z_k)\} > 0$ for stage $\ell \leq r_f$. When $w \not\perp \text{span}(\mathbf{f}^\top)$, since $\cos\{\theta(w, z_k)\} = \cos\{\theta(w, w_0)\} \cos\{\theta(w_0, z_k)\}$, where w_0 denotes the projection of w onto $\text{span}(\mathbf{f}^\top)$, we only need to consider $w \in \text{span}(\mathbf{f}^\top)$. Then there exists a vector $\mathbf{b} = (b_1, \dots, b_K)^\top$ such that $w = \mathbf{b}^\top \mathbf{f}$ and $\text{cov}(w) = \mathbf{b}^\top \text{cov}(\mathbf{f}) \mathbf{b} = 1$. Let z_k^* be the projection of w onto $\text{span}(\mathbf{x}_k^\top)$. We only need to consider z_k such that

$$z_k \begin{cases} = \text{any standardized variable in } \text{span}(\mathbf{x}_k^\top), & \text{if } z_k^* = 0, \\ \propto z_k^*, & \text{if } z_k^* \neq 0. \end{cases}$$

Define $\Phi_k = (\mathbf{0}_{r_k \times \sum_{j=1}^{k-1} r_j}, \mathbf{I}_{r_k \times r_k}, \mathbf{0}_{r_k \times \sum_{j=k+1}^K r_j})$. Then $\mathbf{f}_k = \Phi_k \mathbf{f}$ and $\mathbf{I}_{\sum_{k=1}^K r_k \times \sum_{k=1}^K r_k} = \sum_{k=1}^K \Phi_k^\top \Phi_k$. Note that the inner product $\langle w, \mathbf{f}_k \rangle = \text{cov}(w, \mathbf{f}_k) = \text{cov}(\mathbf{b}^\top \mathbf{f}, \Phi_k \mathbf{f}) = \mathbf{b}^\top \text{cov}(\mathbf{f}) \Phi_k^\top$, which is zero if $z_k^* = 0$. We have

$$z_k^* = \langle w, \mathbf{f}_k \rangle \mathbf{f}_k = \mathbf{b}^\top \text{cov}(\mathbf{f}) \Phi_k^\top \Phi_k \mathbf{f}, \quad (34)$$

$$\text{var}(z_k^*) = \langle w, \mathbf{f}_k \rangle \text{cov}(\mathbf{f}_k) \langle w, \mathbf{f}_k \rangle^\top = \mathbf{b}^\top \text{cov}(\mathbf{f}) \Phi_k^\top \Phi_k \text{cov}(\mathbf{f}) \mathbf{b},$$

$$\text{cov}(w, z_k^*) = \mathbf{b}^\top \text{cov}(\mathbf{f}) \Phi_k^\top \Phi_k \text{cov}(\mathbf{f}) \mathbf{b},$$

$$\text{corr}^2(w, z_k^*) = \mathbf{b}^\top \text{cov}(\mathbf{f}) \Phi_k^\top \Phi_k \text{cov}(\mathbf{f}) \mathbf{b}, \quad (35)$$

and then

$$\sum_{k=1}^K \cos^2\{\theta(w, z_k)\} = \sum_{k=1}^K \text{corr}^2(w, z_k^*) = \mathbf{b}^\top \text{cov}^2(\mathbf{f}) \mathbf{b}. \quad (36)$$

Let $w^{(\ell)} = (\mathbf{b}^{(\ell)})^\top \mathbf{f}$. To maximize (36) with respect to \mathbf{b} under the constraints $\mathbf{b}^\top \text{cov}(\mathbf{f}) \mathbf{b} = 1$ and $\mathbf{b}^\top \text{cov}(\mathbf{f}) \mathbf{b}^{(j)} = 0$ for $j \leq \ell - 1$, the associated Lagrange function from the method of Lagrange multipliers is

$$\mathcal{L}(\mathbf{b}, l_1, \dots, l_\ell) = \mathbf{b}^\top \text{cov}^2(\mathbf{f}) \mathbf{b} - l_\ell (\mathbf{b}^\top \text{cov}(\mathbf{f}) \mathbf{b} - 1) - \sum_{j=1}^{\ell-1} l_j \mathbf{b}^\top \text{cov}(\mathbf{f}) \mathbf{b}^{(j)}.$$

There exist $l_1^{(\ell)}, \dots, l_\ell^{(\ell)}$ such that $\nabla \mathcal{L}(\mathbf{b}^{(\ell)}, l_1^{(\ell)}, \dots, l_\ell^{(\ell)}) = \mathbf{0}$, which yields

$$\begin{cases} 2 \operatorname{cov}^2(\mathbf{f}) \mathbf{b}^{(\ell)} = 2l_\ell^{(\ell)} \operatorname{cov}(\mathbf{f}) \mathbf{b}^{(\ell)} + \sum_{j=1}^{\ell-1} l_j^{(\ell)} \operatorname{cov}(\mathbf{f}) \mathbf{b}^{(j)}, \end{cases} \quad (37a)$$

$$(\mathbf{b}^{(\ell)})^\top \operatorname{cov}(\mathbf{f}) \mathbf{b}^{(\ell)} = 1, \quad (37b)$$

$$(\mathbf{b}^{(\ell)})^\top \operatorname{cov}(\mathbf{f}) \mathbf{b}^{(j)} = 0, \quad \text{for } j = 1, \dots, \ell - 1. \quad (37c)$$

When $\ell = 1$, (37a) becomes $\operatorname{cov}^2(\mathbf{f}) \mathbf{b}^{(1)} = l_1^{(1)} \operatorname{cov}(\mathbf{f}) \mathbf{b}^{(1)}$. Then by (37b), we have $l_1^{(1)} = (\mathbf{b}^{(1)})^\top \operatorname{cov}^2(\mathbf{f}) \mathbf{b}^{(1)}$. Thus, the maximum of (36) when $\ell = 1$, i.e., the maximum of $l_1^{(1)}$ is $l_{f,1} := \lambda_1(\operatorname{cov}(\mathbf{f}))$. We have $l_{f,1}^{-1/2} \operatorname{cov}(\mathbf{f}) \mathbf{b}^{(1)} = \boldsymbol{\eta}^{(1)}$. Hence, $\mathbf{b}^{(1)} = l_{f,1}^{1/2} [\operatorname{cov}(\mathbf{f})]^\dagger \boldsymbol{\eta}^{(1)} + \boldsymbol{\zeta}$ for any vector $\boldsymbol{\zeta}$ satisfying $\mathbf{V}_f^\top \boldsymbol{\zeta} = \mathbf{0}$, where $\operatorname{cov}(\mathbf{f}) = \mathbf{V}_f \boldsymbol{\Lambda}_f \mathbf{V}_f^\top$ is a compact SVD of $\operatorname{cov}(\mathbf{f})$, and $[\operatorname{cov}(\mathbf{f})]^\dagger = \mathbf{V}_f \boldsymbol{\Lambda}_f^{-1} \mathbf{V}_f^\top$ is the pseudo-inverse of $\operatorname{cov}(\mathbf{f})$. Let $\mathbf{u} = \boldsymbol{\Lambda}_f^{-1/2} \mathbf{V}_f^\top \mathbf{f}$. Then $\mathbf{f} = \operatorname{cov}(\mathbf{f}, \mathbf{u}) \mathbf{u} = \mathbf{V}_f \boldsymbol{\Lambda}_f^{1/2} \mathbf{u}$. We have

$$\begin{aligned} w^{(1)} &= (\mathbf{b}^{(1)})^\top \mathbf{f} = (l_{f,1}^{1/2} (\boldsymbol{\eta}^{(1)})^\top [\operatorname{cov}(\mathbf{f})]^\dagger + \boldsymbol{\zeta}^\top) \mathbf{V}_f \boldsymbol{\Lambda}_f^{1/2} \mathbf{u} \\ &= l_{f,1}^{1/2} (\boldsymbol{\eta}^{(1)})^\top [\operatorname{cov}(\mathbf{f})]^\dagger \mathbf{V}_f \boldsymbol{\Lambda}_f^{1/2} \mathbf{u} \\ &= l_{f,1}^{-1/2} (\boldsymbol{\eta}^{(1)})^\top \operatorname{cov}(\mathbf{f}) [\operatorname{cov}(\mathbf{f})]^\dagger \mathbf{V}_f \boldsymbol{\Lambda}_f^{1/2} \mathbf{u} \\ &= l_{f,1}^{-1/2} (\boldsymbol{\eta}^{(1)})^\top \mathbf{V}_f \boldsymbol{\Lambda}_f^{1/2} \mathbf{u} \\ &= l_{f,1}^{-1/2} (\boldsymbol{\eta}^{(1)})^\top \mathbf{f}. \end{aligned}$$

Hence, we can simply let $\mathbf{b}^{(1)} = l_{f,1}^{-1/2} \boldsymbol{\eta}^{(1)}$. When $\ell = 2$, left-multiplying (37a) by $\mathbf{b}^{(1)}$ yields $l_1^{(2)} = 0$. Then (37) becomes

$$\begin{cases} \operatorname{cov}^2(\mathbf{f}) \mathbf{b}^{(2)} = l_2^{(2)} \operatorname{cov}(\mathbf{f}) \mathbf{b}^{(2)}, \\ (\mathbf{b}^{(2)})^\top \operatorname{cov}(\mathbf{f}) \mathbf{b}^{(2)} = 1, \\ (\mathbf{b}^{(2)})^\top \operatorname{cov}(\mathbf{f}) \mathbf{b}^{(1)} = 0. \end{cases}$$

Thus, we have $[\lambda_2(\operatorname{cov}(\mathbf{f}))]^{-1/2} \operatorname{cov}(\mathbf{f}) \mathbf{b}^{(2)} = \boldsymbol{\eta}^{(2)}$. Then using the same skill for obtaining $\mathbf{b}^{(1)}$, we can simply let $\mathbf{b}^{(2)} = [\lambda_2(\operatorname{cov}(\mathbf{f}))]^{-1/2} \boldsymbol{\eta}^{(2)}$ and have $\sum_{k=1}^K \cos^2\{\theta(w^{(2)}, z_k^{(2)})\} = \lambda_2(\operatorname{cov}(\mathbf{f}))$. Similarly, for $2 < \ell \leq r_f$, we can simply let $\mathbf{b}^{(\ell)} = [\lambda_\ell(\operatorname{cov}(\mathbf{f}))]^{-1/2} \boldsymbol{\eta}^{(\ell)}$ and have $\sum_{k=1}^K \cos^2\{\theta(w^{(\ell)}, z_k^{(\ell)})\} = \lambda_\ell(\operatorname{cov}(\mathbf{f}))$.

For $\ell \leq r_f$, by (34), the projection of $w^{(\ell)}$ onto space $\operatorname{span}(\mathbf{x}_k^\top)$ is $z_k^{*(\ell)} = [\lambda_\ell(\operatorname{cov}(\mathbf{f}))]^{1/2} (\boldsymbol{\eta}_k^{(\ell)})^\top \mathbf{f}_k$ with $\operatorname{var}(z_k^{*(\ell)}) = \lambda_\ell(\operatorname{cov}(\mathbf{f})) \|\boldsymbol{\eta}_k^{(\ell)}\|_F^2$. Thus,

$$z_k^{(\ell)} = \begin{cases} \text{any standardized variable in } \operatorname{span}(\mathbf{x}^\top), & \text{if } \boldsymbol{\eta}_k^{(\ell)} = \mathbf{0}, \\ \pm (\boldsymbol{\eta}_k^{(\ell)} / \|\boldsymbol{\eta}_k^{(\ell)}\|_F)^\top \mathbf{f}_k, & \text{if } \boldsymbol{\eta}_k^{(\ell)} \neq \mathbf{0}. \end{cases}$$

From equation (35), we have $\operatorname{cov}(w^{(\ell)}, z_k^{*(\ell)}) = \lambda_\ell(\operatorname{cov}(\mathbf{f})) \|\boldsymbol{\eta}_k^{(\ell)}\|_F^2$. Then, $\cos\{\theta(w^{(\ell)}, z_k^{(\ell)})\} = \pm [\lambda_\ell(\operatorname{cov}(\mathbf{f}))]^{1/2} \|\boldsymbol{\eta}_k^{(\ell)}\|_F$.

To prove $\sum_{k=1}^K \text{span}(\mathbf{x}_k^\top) = \text{span}(\{w^{(\ell)}\}_{\ell=1}^{r_f})$, since $w^{(\ell)} \in \text{span}(\mathbf{f}^\top)$, we only need to show $\dim(\text{span}(\{w^{(\ell)}\}_{\ell=1}^{r_f})) = \dim(\text{span}(\mathbf{f}^\top)) = r_f$, which is true because the r_f nonzero variables $\{w^{(\ell)}\}_{\ell=1}^{r_f}$ are orthogonal.

Now consider the revised $z_k^{(\ell)}$ in (8) for result (ii). By $\cos\{\theta(w^{(\ell)}, z_k^{(\ell)})\} = [\lambda_\ell(\text{cov}(\mathbf{f}))]^{1/2} \|\boldsymbol{\eta}_k^{(\ell)}\|_F \geq 0$, we have $\theta(w^{(\ell)}, z_k^{(\ell)}) \in [0, \pi/2]$. Since $\text{span}(\{z_k^{(\ell)}\}_{\ell=1}^{r_f})$ is the projection of $\text{span}(\{w^{(\ell)}\}_{\ell=1}^{r_f})$ onto $\text{span}(\mathbf{x}_k^\top) \subseteq \text{span}(\{w^{(\ell)}\}_{\ell=1}^{r_f}) = \sum_{k=1}^K \text{span}(\mathbf{x}_k^\top)$, we have $\text{span}(\{z_k^{(\ell)}\}_{\ell=1}^{r_f}) = \text{span}(\mathbf{x}_k^\top)$.

Next, consider result (iii). For some k and ℓ , since $\text{span}(\{z_k^{(m)}\}_{m=1}^{\ell-1}) \neq \text{span}(\mathbf{x}_k^\top)$, there exists a unit-variance variable $v \in \text{span}(\mathbf{x}_k^\top)$ such that $v \perp \text{span}(\{z_k^{(m)}\}_{m=1}^{\ell-1})$. Moreover, $v \perp w^{(m)}$ for all $m \leq \ell - 1$, because v is orthogonal to both the projection of $w^{(m)}$ onto $\text{span}(\mathbf{x}_k^\top)$ and the rejection of $w^{(m)}$ from $\text{span}(\mathbf{x}_k^\top)$. Thus, we just let $w^{(\ell)} = v$. Then, $\cos^2\{\theta(w^{(\ell)}, z_k^{(\ell)})\} = 1$. By $\sum_{k=1}^K \cos^2\{\theta(w^{(\ell)}, z_k^{(\ell)})\} = \lambda_\ell(\text{cov}(\mathbf{f})) \leq 1$, we have $\sum_{j \neq k} \cos^2\{\theta(w^{(\ell)}, z_j^{(\ell)})\} = 0$, which implies $w^{(\ell)} \perp \sum_{1 \leq j \neq k \leq K} \text{span}(\mathbf{x}_j^\top)$. \blacksquare

Proof of Theorem 2. If $z_k^{(\ell)} = 0$ for some k , it is easy to see $\alpha^{(\ell)} = 0$. We only consider that for all $k \leq K$, $z_k^{(\ell)} \neq 0$, i.e., $\theta(w^{(\ell)}, z_k^{(\ell)}) \in [0, \pi/2]$. If $d_j^{(\ell)} \perp d_k^{(\ell)}$, then $\|d_j^{(\ell)}\|^2 + \|d_k^{(\ell)}\|^2 = \|z_j^{(\ell)} - z_k^{(\ell)}\|^2$, and consequently by the law of cosines we have

$$\begin{aligned} & \left(\|z_j^{(\ell)}\|^2 + \|c^{(\ell)}\|^2 - 2\|z_j^{(\ell)}\| \|c^{(\ell)}\| \text{sign}(\alpha^{(\ell)}) \cos\{\theta(z_j^{(\ell)}, w^{(\ell)})\} \right) \\ & + \left(\|z_k^{(\ell)}\|^2 + \|c^{(\ell)}\|^2 - 2\|z_k^{(\ell)}\| \|c^{(\ell)}\| \text{sign}(\alpha^{(\ell)}) \cos\{\theta(z_k^{(\ell)}, w^{(\ell)})\} \right) \\ & = \|z_j^{(\ell)}\|^2 + \|z_k^{(\ell)}\|^2 - 2\|z_j^{(\ell)}\| \|z_k^{(\ell)}\| \cos\{\theta(z_j^{(\ell)}, z_k^{(\ell)})\} \end{aligned}$$

which gives $\alpha^{(\ell)} = \frac{1}{2} \left[\cos\{\theta(z_j^{(\ell)}, w^{(\ell)})\} + \cos\{\theta(z_k^{(\ell)}, w^{(\ell)})\} \pm (\Delta_{jk}^{(\ell)})^{1/2} \right]$. Hence, the desired value of $\alpha^{(\ell)}$ is the one given in Theorem 2.

To prove the existence of $\alpha^{(\ell)}$, we only need to show that there exists a $\Delta_{jk}^{(\ell)} \geq 0$ with $j \neq k$. Denote $\lambda_\ell = \lambda_\ell(\text{cov}(\mathbf{f}))$, and $\boldsymbol{\nu}_\ell = (\nu_{\ell,1}, \dots, \nu_{\ell,K})^\top$ with $\nu_{\ell,k} = \|\boldsymbol{\eta}_k^{(\ell)}\|_F$. We have

$$\text{cov}(\mathbf{z}^{(\ell)}) = \text{diag} \left(\frac{(\boldsymbol{\eta}_1^{(\ell)})^\top}{\|\boldsymbol{\eta}_1^{(\ell)}\|_F}, \dots, \frac{(\boldsymbol{\eta}_K^{(\ell)})^\top}{\|\boldsymbol{\eta}_K^{(\ell)}\|_F} \right) \text{cov}(\mathbf{f}) \text{diag} \left(\frac{\boldsymbol{\eta}_1^{(\ell)}}{\|\boldsymbol{\eta}_1^{(\ell)}\|_F}, \dots, \frac{\boldsymbol{\eta}_K^{(\ell)}}{\|\boldsymbol{\eta}_K^{(\ell)}\|_F} \right),$$

$$\boldsymbol{\nu}_\ell^\top \text{cov}(\mathbf{z}^{(\ell)}) \boldsymbol{\nu}_\ell = \lambda_\ell, \quad \cos\{\theta(w^{(\ell)}, z_k^{(\ell)})\} = \lambda_\ell^{1/2} \nu_{\ell,k},$$

and for all $j, k \leq K$, $\Delta_{jk}^{(\ell)} = \lambda_\ell \nu_{\ell,j}^2 + \lambda_\ell \nu_{\ell,k}^2 + 2\lambda_\ell \nu_{\ell,j} \nu_{\ell,k} - 4 \text{cov}(z_j^{(\ell)}, z_k^{(\ell)})$. Then, we have

$$\begin{aligned}
 & \sum_{j=1}^K \sum_{k=1}^K \cos\{\theta(w^{(\ell)}, z_j^{(\ell)})\} \Delta_{jk}^{(\ell)} \cos\{\theta(w^{(\ell)}, z_k^{(\ell)})\} \\
 &= \sum_{j=1}^K \sum_{k=1}^K \text{cov}(w^{(\ell)}, z_j^{(\ell)}) \Delta_{jk}^{(\ell)} \text{cov}(w^{(\ell)}, z_k^{(\ell)}) \\
 &= \sum_{j=1}^K \sum_{k=1}^K \lambda_\ell^{1/2} \nu_{\ell,j} \left(\lambda_\ell \nu_{\ell,j}^2 + \lambda_\ell \nu_{\ell,k}^2 + 2\lambda_\ell \nu_{\ell,j} \nu_{\ell,k} - 4 \text{cov}(z_j^{(\ell)}, z_k^{(\ell)}) \right) \lambda_\ell^{1/2} \nu_{\ell,k} \\
 &= \left[\sum_{j=1}^K \sum_{k=1}^K \lambda_\ell^{1/2} \nu_{\ell,j} (\lambda_\ell \nu_{\ell,j}^2 + \lambda_\ell \nu_{\ell,k}^2 + 2\lambda_\ell \nu_{\ell,j} \nu_{\ell,k}) \lambda_\ell^{1/2} \nu_{\ell,k} \right] - 4\lambda_\ell \boldsymbol{\nu}_\ell^\top \text{cov}(\mathbf{z}^{(\ell)}) \boldsymbol{\nu}_\ell \\
 &= \left[\sum_{j=1}^K \sum_{k=1}^K \lambda_\ell^{1/2} \nu_{\ell,j} (\lambda_\ell \nu_{\ell,j}^2 + \lambda_\ell \nu_{\ell,k}^2 + 2\lambda_\ell \nu_{\ell,j} \nu_{\ell,k}) \lambda_\ell^{1/2} \nu_{\ell,k} \right] - 4\lambda_\ell^2 \boldsymbol{\nu}_\ell^\top (\boldsymbol{\nu}_\ell \boldsymbol{\nu}_\ell^\top) \boldsymbol{\nu}_\ell \\
 &= \sum_{j=1}^K \sum_{k=1}^K \lambda_\ell^{1/2} \nu_{\ell,j} (\lambda_\ell \nu_{\ell,j}^2 + \lambda_\ell \nu_{\ell,k}^2 + 2\lambda_\ell \nu_{\ell,j} \nu_{\ell,k} - 4\lambda_\ell \nu_{\ell,j} \nu_{\ell,k}) \lambda_\ell^{1/2} \nu_{\ell,k} \\
 &= \sum_{j=1}^K \sum_{k=1}^K \cos\{\theta(w^{(\ell)}, z_j^{(\ell)})\} (\lambda_\ell^{1/2} \nu_{\ell,j} - \lambda_\ell^{1/2} \nu_{\ell,k})^2 \cos\{\theta(w^{(\ell)}, z_k^{(\ell)})\} \\
 &\geq 0. \tag{38}
 \end{aligned}$$

For all $k < K$, $\cos\{\theta(w^{(\ell)}, z_k^{(\ell)})\} > 0$ for $\theta(w^{(\ell)}, z_k^{(\ell)}) \in [0, \pi/2)$, and moreover, we have $\Delta_{kk}^{(\ell)} = 4 \cos^2\{\theta(w^{(\ell)}, z_k^{(\ell)})\} - 4 \leq 0$. Hence, by (38), we have at least one $\Delta_{jk}^{(\ell)} \geq 0$ with $j \neq k$. \blacksquare

Proof of Theorem 3. When $K = 2$, by Lemma 2 in Kettenring (1971), L is equal to the number of positive canonical correlations between \mathbf{x}_1 and \mathbf{x}_2 . Then following the constructions of these two decomposition methods, the proof is easy to complete. The details are omitted. \blacksquare

Proof of Theorem 4. Let $\tilde{\mathbf{f}}_k^\top$ be another orthonormal basis of $\text{span}(\mathbf{x}_k^\top)$. Then, there exists an orthogonal matrix \mathbf{O}_k such that $\tilde{\mathbf{f}}_k = \mathbf{O}_k \mathbf{f}_k$. Define $\tilde{\mathbf{f}} = [\tilde{\mathbf{f}}_1; \dots; \tilde{\mathbf{f}}_K]$. We have $\tilde{\mathbf{f}} = \mathbf{O}\mathbf{f}$ and $\text{cov}(\tilde{\mathbf{f}}) = \mathbf{O} \text{cov}(\mathbf{f}) \mathbf{O}^\top$ with $\mathbf{O} = \text{diag}(\mathbf{O}_1, \dots, \mathbf{O}_K)$. Hence, $\lambda_\ell(\text{cov}(\tilde{\mathbf{f}})) = \lambda_\ell(\text{cov}(\mathbf{f}))$ for $\ell \leq \sum_{k=1}^K r_k$. Denote $\tilde{\boldsymbol{\eta}}^{(\ell)} = [\tilde{\boldsymbol{\eta}}_1^{(\ell)}; \dots; \tilde{\boldsymbol{\eta}}_K^{(\ell)}]$, with $\tilde{\boldsymbol{\eta}}_k^{(\ell)} \in \mathbb{R}^{r_k}$, to be a normalized eigenvector of $\text{cov}(\tilde{\mathbf{f}})$ corresponding to $\lambda_\ell(\text{cov}(\tilde{\mathbf{f}}))$ for $\ell \leq L$. Now, from the assumption that $\lambda_1(\text{cov}(\mathbf{f})), \dots, \lambda_L(\text{cov}(\mathbf{f}))$ are distinct, we have $\tilde{\boldsymbol{\eta}}^{(\ell)} = \pm \mathbf{O} \boldsymbol{\eta}^{(\ell)}$ and $\tilde{\boldsymbol{\eta}}_k^{(\ell)} = \pm \mathbf{O}_k \boldsymbol{\eta}_k^{(\ell)}$. Denote $\tilde{w}^{(\ell)}, \tilde{z}_k^{(\ell)}, \tilde{\alpha}^{(\ell)}$ and $\tilde{c}^{(\ell)}$ to be the counterparts of $w^{(\ell)}, z_k^{(\ell)}, \alpha^{(\ell)}$ and $c^{(\ell)}$ that are defined in (5), (8) and (11) by using $\tilde{\mathbf{f}}$ and $\tilde{\boldsymbol{\eta}}^{(\ell)}$ instead of \mathbf{f} and $\boldsymbol{\eta}^{(\ell)}$. We have $\tilde{w}^{(\ell)} = \pm w^{(\ell)}$, $\tilde{z}_k^{(\ell)} = \pm z_k^{(\ell)}$, $\tilde{\alpha}^{(\ell)} = \alpha^{(\ell)}$ due to the formula in Theorem 2, and then $\tilde{c}^{(\ell)} = \pm c^{(\ell)}$. Let

$\tilde{\mathbf{z}}_k^{\mathcal{I}_0} = (\tilde{z}_k^{(\ell)})_{\ell \in \mathcal{I}_0}^\top$ and $\tilde{\mathbf{c}}^{\mathcal{I}_0} = (\tilde{c}^{(\ell)})_{\ell \in \mathcal{I}_0}^\top$. There exists a diagonal matrix \mathbf{D} with diagonal entries being either 1 or -1 such that $\tilde{\mathbf{z}}_k^{\mathcal{I}_0} = \mathbf{D}\mathbf{z}_k^{\mathcal{I}_0}$ and $\tilde{\mathbf{c}}^{\mathcal{I}_0} = \mathbf{D}\mathbf{c}^{\mathcal{I}_0}$. Then,

$$\begin{aligned} \text{cov}(\mathbf{x}_k, \tilde{\mathbf{z}}_k^{\mathcal{I}_0})[\text{cov}(\tilde{\mathbf{z}}_k^{\mathcal{I}_0})]^\dagger \tilde{\mathbf{c}}^{\mathcal{I}_0} &= \text{cov}(\mathbf{x}_k, \mathbf{z}_k^{\mathcal{I}_0})\mathbf{D}[\mathbf{D} \text{cov}(\mathbf{z}_k^{\mathcal{I}_0})\mathbf{D}]^\dagger \mathbf{D}\mathbf{c}^{\mathcal{I}_0} \\ &= \text{cov}(\mathbf{x}_k, \mathbf{z}_k^{\mathcal{I}_0})\mathbf{D}[\mathbf{D}\mathbf{V}_{zk}\Lambda_{zk}\mathbf{V}_{zk}^\top\mathbf{D}]^\dagger \mathbf{D}\mathbf{c}^{\mathcal{I}_0} \\ &= \text{cov}(\mathbf{x}_k, \mathbf{z}_k^{\mathcal{I}_0})\mathbf{D}[\mathbf{D}\mathbf{V}_{zk}\Lambda_{zk}^{-1}\mathbf{V}_{zk}^\top\mathbf{D}]\mathbf{D}\mathbf{c}^{\mathcal{I}_0} \\ &= \text{cov}(\mathbf{x}_k, \mathbf{z}_k^{\mathcal{I}_0})[\text{cov}(\mathbf{z}_k^{\mathcal{I}_0})]^\dagger \mathbf{c}^{\mathcal{I}_0} = \mathbf{c}_k. \end{aligned}$$

The proof is complete. \blacksquare

Proof of Theorem 5. First of all, it is worth mentioning that $\hat{\mathbf{X}}_k$ is rank- r_k with probability tending to 1. This is because we have

$$\lambda_{r_k}(\widehat{\text{cov}}(\mathbf{x}_k)) \geq (1 - o_P(1)) \lambda_{r_k}(\text{cov}(\mathbf{x}_k))$$

from (S.17) in the supplement of Shu et al. (2020). Due to their Lemma S.1, in the rest of the proof we simply assume that $\hat{\mathbf{X}}_k$ is rank- r_k .

For the convergence results of $\{\hat{\mathbf{X}}_k, \hat{\mathbf{C}}_k, \hat{\mathbf{D}}_k\}$, we will follow the similar proof techniques of Theorem 3 in Shu et al. (2020). The key difference is that our \mathbf{C}_k and $\hat{\mathbf{C}}_k$ are defined from Carroll's GCCA for $K \geq 2$ which are more complex than those in Shu et al. (2020) from CCA for $K = 2$. Hence, our proof needs extra effort to establish the error bounds of each component in $\hat{\mathbf{C}}_k$ defined in (24) and then combine them together to yield the final error bound for $\hat{\mathbf{C}}_k$. Moreover, to the best of our knowledge, the results in (29)-(30) are the first work to show the high-dimensional estimation consistency of the view-level and variable-level proportions of explained signal variance for the decomposition model in (1)-(2) for $K \geq 2$, which are not seen in Shu et al. (2020) even when $K = 2$. In particular, the uniform consistency of the variable-level proportions of explained signal variance given in (30) will be derived from the ℓ_∞ eigenvector perturbation bound recently given in Fan et al. (2018).

1. We first consider the error bounds of $\hat{\mathbf{X}}_k$.

By (S.13) and (S.14) in Shu et al. (2020), there exists a constant $\kappa_x > 0$ such that

$$\kappa_x + o_P(1) \leq \frac{\|\mathbf{X}_k\|_2}{[n \lambda_1(\text{cov}(\mathbf{x}_k))]^{1/2}} \leq \frac{\|\mathbf{X}_k\|_F}{[n \lambda_1(\text{cov}(\mathbf{x}_k))]^{1/2}} \leq r_k^{1/2} + o_P(1). \quad (39)$$

From their (S.15), we have

$$\begin{aligned} \|\hat{\mathbf{X}}_k - \mathbf{X}_k\|_2 &\leq \|\hat{\mathbf{X}}_k - \mathbf{X}_k\|_F \\ &\lesssim_P \min \left\{ \left[\frac{\lambda_1(\text{cov}(\mathbf{x}_k))}{n} \right]^{1/2} + (p_k \log p_k)^{1/2}, [n \lambda_1(\text{cov}(\mathbf{x}_k))]^{1/2} \right\}. \end{aligned} \quad (40)$$

From (S.7) of Shu et al. (2020), we have $\lambda_1(\text{cov}(\mathbf{x}_k)) \asymp \lambda_{r_k}(\text{cov}(\mathbf{x}_k))$. By Weyl's inequality (see Theorem 3.3.16(a) in Horn and Johnson (1994)) as well as Assumption 1 (i) and (v), $\kappa_x \leq \lambda_{k,p_k} = \lambda_{k,(r_k+1)+(p_k-r_k)-1} - \lambda_{r_k+1}(\text{cov}(\mathbf{x}_k)) \leq \lambda_{p_k-r_k}(\text{cov}(\mathbf{e}_k)) \leq \lambda_1(\text{cov}(\mathbf{e}_k)) = \|\text{cov}(\mathbf{e}_k)\|_2 \leq \|\text{cov}(\mathbf{e}_k)\|_\infty \leq s_0$. Thus,

$$\frac{\lambda_1(\text{cov}(\mathbf{x}_k))}{p_k} \asymp \frac{\text{tr}(\text{cov}(\mathbf{x}_k))}{\text{tr}(\text{cov}(\mathbf{e}_k))} = \text{SNR}_k. \quad (41)$$

By (39), (40) and (41), we obtain

$$\max \left\{ \frac{\|\widehat{\mathbf{X}}_k - \mathbf{X}_k\|_2^2}{\|\mathbf{X}_k\|_2^2}, \frac{\|\widehat{\mathbf{X}}_k - \mathbf{X}_k\|_F^2}{\|\mathbf{X}_k\|_F^2} \right\} \lesssim_P \min \left\{ \frac{1}{n^2} + \frac{\log p_k}{n \text{SNR}_k}, 1 \right\}. \quad (42)$$

2. We next consider the error bounds of $\widehat{\mathbf{C}}_k$ and $\widehat{\mathbf{D}}_k$.

Simply choose $\mathbf{f}_k = \Lambda_{xk}^{-1/2} \mathbf{V}_{xk}^\top \mathbf{x}_k$, where $\text{cov}(\mathbf{x}_k) = \mathbf{V}_{xk} \Lambda_{xk} \mathbf{V}_{xk}^\top$ is a compact SVD. Then, we have $\mathbf{z}_k^{\mathcal{I}_0} = \mathbf{H}_k \mathbf{f}_k = \mathbf{H}_k \Lambda_{xk}^{-1/2} \mathbf{V}_{xk}^\top \mathbf{x}_k$ with $\mathbf{H}_k = (\boldsymbol{\eta}_k^{(\ell)} / \|\boldsymbol{\eta}_k^{(\ell)}\|_F)_{\ell \in \mathcal{I}_0}^\top$. From (13), it follows that we can write the common-source matrix \mathbf{C}_k as

$$\mathbf{C}_k = \text{cov}(\mathbf{x}_k, \mathbf{z}_k^{\mathcal{I}_0}) \{ \text{cov}(\mathbf{z}_k^{\mathcal{I}_0}) \}^\dagger \mathbf{C}^{\mathcal{I}_0}, \quad (43)$$

where the three components are formulated by $\text{cov}(\mathbf{x}_k, \mathbf{z}_k^{\mathcal{I}_0}) = \mathbf{V}_{xk} \Lambda_{xk}^{1/2} \mathbf{H}_k^\top$, $\text{cov}(\mathbf{z}_k^{\mathcal{I}_0}) = \mathbf{H}_k \mathbf{H}_k^\top$, and $\mathbf{C}^{\mathcal{I}_0} = \mathbf{ANF}$ with $\mathbf{A} = \text{diag}\{(\alpha^{(\ell)} [\lambda_\ell \{\text{cov}(\mathbf{f})\}]^{-1/2})_{\ell \in \mathcal{I}_0}\}$, $\mathbf{N} = (\boldsymbol{\eta}_k^{(\ell)})_{\ell \in \mathcal{I}_0}^\top$, and $\mathbf{F} = [\mathbf{F}_1; \dots; \mathbf{F}_K]$ in which $\mathbf{F}_k = \Lambda_{xk}^{-1/2} \mathbf{V}_{xk}^\top \mathbf{X}_k$.

Since K is a constant and each $\text{span}(\mathbf{x}_k^\top)$ is a fixed space independent of n and $\{p_k\}_{k=1}^K$, we have that r_1, \dots, r_K are constants and there exist positive constants κ_z , κ_η , κ_Δ and κ_{zz} such that $\min_{k \leq K} \lambda_{r_k^*}(\text{cov}(\mathbf{z}_k^{\mathcal{I}_0})) > \kappa_z$, $\min_{k \leq K, \ell \in \mathcal{I}_0} \|\boldsymbol{\eta}_k^{(\ell)}\|_F > \kappa_\eta$, $\min_{(j,k) \in \mathcal{I}_{\Delta+}^{(\ell)}, \ell \in \mathcal{I}_0} \Delta_{jk}^{(\ell)} > \kappa_\Delta$, and $\min_{(j,k) \in \mathcal{I}_{\Delta+}^{(\ell)} \cup \mathcal{I}_{\Delta_0}^{(\ell)}, \ell \in \mathcal{I}_0} |\cos\{\theta(z_j^{(\ell)}, z_k^{(\ell)})\}| > \kappa_{zz}$.

From Shu et al. (2020), using their (S.8), (S.30) and the first inequality on page 10 of their supplement, we have that for all $j, k \leq K$,

$$\lambda_1(\widehat{\text{cov}}(\mathbf{x}_k)) \lesssim_P \lambda_1(\text{cov}(\mathbf{x}_k)), \quad (44)$$

$$\|\widehat{\mathbf{V}}_{xk} \widehat{\Lambda}_{xk}^{1/2} - \mathbf{V}_{xk} \Lambda_{xk}^{1/2}\|_2 \lesssim_P \lambda_1^{1/2}(\text{cov}(\mathbf{x}_k)) n^{-1/2}, \quad (45)$$

and

$$\begin{aligned} \|\widehat{\text{cov}}(\mathbf{f}_j, \mathbf{f}_k) - \text{cov}(\mathbf{f}_j, \mathbf{f}_k)\|_F &\leq [\max(r_j, r_k)]^{1/2} \|\widehat{\text{cov}}(\mathbf{f}_j, \mathbf{f}_k) - \text{cov}(\mathbf{f}_j, \mathbf{f}_k)\|_2 \\ &\lesssim_P \min \left\{ n^{-1/2} + \left(\frac{p_j \log p_j}{n \lambda_1(\text{cov}(\mathbf{x}_j))} \right)^{1/2} + \left(\frac{p_k \log p_k}{n \lambda_1(\text{cov}(\mathbf{x}_k))} \right)^{1/2}, 1 \right\}, \end{aligned}$$

where $\widehat{\text{cov}}(\mathbf{f}_j, \mathbf{f}_k) = n^{-1} \widehat{\mathbf{F}}_j \widehat{\mathbf{F}}_k^\top$ is a submatrix of $\widehat{\text{cov}}(\mathbf{f})$. Then,

$$\begin{aligned} \|\widehat{\text{cov}}(\mathbf{f}) - \text{cov}(\mathbf{f})\|_F &= \left(\sum_{1 \leq j, k \leq K} \|\widehat{\text{cov}}(\mathbf{f}_j, \mathbf{f}_k) - \text{cov}(\mathbf{f}_j, \mathbf{f}_k)\|_F^2 \right)^{1/2} \\ &\lesssim_P \min \left\{ n^{-1/2} + \sum_{k=1}^K \left(\frac{p_k \log p_k}{n \lambda_1(\text{cov}(\mathbf{x}_k))} \right)^{1/2}, 1 \right\} \\ &\lesssim_P \delta_\eta. \end{aligned} \quad (46)$$

By the uniqueness given in Theorem 4, we let $\boldsymbol{\eta}^{(\ell)}$ satisfy $(\boldsymbol{\eta}^{(\ell)})^\top \hat{\boldsymbol{\eta}}^{(\ell)} \geq 0$ for all $\ell \in \mathcal{I}_0$. By Corollary 1 in Yu et al. (2015), $\delta_\eta = o(1)$, and the condition that $\{\lambda_\ell(\text{cov}(f))\}_{\ell=1}^L$ are distinct, we have

$$\begin{aligned} \max_{\ell \in \mathcal{I}_0} \|\hat{\boldsymbol{\eta}}^{(\ell)} - \boldsymbol{\eta}^{(\ell)}\|_F &\lesssim_P \frac{\delta_\eta}{\min_{\ell \in \mathcal{I}_0} \{\lambda_{\ell-1}(\text{cov}(\mathbf{f})) - \lambda_\ell(\text{cov}(\mathbf{f})), \lambda_\ell(\text{cov}(\mathbf{f})) - \lambda_{\ell+1}(\text{cov}(\mathbf{f}))\}} \\ &\lesssim_P \delta_\eta. \end{aligned} \quad (47)$$

Since $\delta_\eta = o(1)$ and $\min_{k \leq K, \ell \in \mathcal{I}_0} \|\boldsymbol{\eta}_k^{(\ell)}\|_F > \kappa_\eta$, then by (47) we have

$$\min_{k \leq K, \ell \in \mathcal{I}_0} \|\hat{\boldsymbol{\eta}}_k^{(\ell)}\|_F \geq \kappa_\eta - o_P(1), \quad (48)$$

and thus

$$\begin{aligned} \|\hat{\mathbf{H}}_k - \mathbf{H}_k\|_2 &\leq \|\hat{\mathbf{H}}_k - \mathbf{H}_k\|_F \lesssim_P L^{1/2} \max_{\ell \in \mathcal{I}_0} \left\| \hat{\boldsymbol{\eta}}_k^{(\ell)} / \|\hat{\boldsymbol{\eta}}_k^{(\ell)}\|_F - \boldsymbol{\eta}_k^{(\ell)} / \|\boldsymbol{\eta}_k^{(\ell)}\|_F \right\|_F \\ &\lesssim_P L^{1/2} \max_{\ell \in \mathcal{I}_0} \left\| \hat{\boldsymbol{\eta}}_k^{(\ell)} (\|\boldsymbol{\eta}_k^{(\ell)}\|_F - \|\hat{\boldsymbol{\eta}}_k^{(\ell)}\|_F) + (\hat{\boldsymbol{\eta}}_k^{(\ell)} - \boldsymbol{\eta}_k^{(\ell)}) \|\hat{\boldsymbol{\eta}}_k^{(\ell)}\|_F \right\|_F / (\|\hat{\boldsymbol{\eta}}_k^{(\ell)}\|_F \|\boldsymbol{\eta}_k^{(\ell)}\|_F) \\ &\lesssim_P 2L^{1/2} \max_{\ell \in \mathcal{I}_0} \|\hat{\boldsymbol{\eta}}_k^{(\ell)} - \boldsymbol{\eta}_k^{(\ell)}\|_F / \|\boldsymbol{\eta}_k^{(\ell)}\|_F \\ &\lesssim_P \delta_\eta. \end{aligned} \quad (49)$$

We will frequently use the following matrix inequality:

$$\|\widehat{\mathbf{M}}_1 \widehat{\mathbf{M}}_2 - \mathbf{M}_1 \mathbf{M}_2\|_2 \leq \begin{cases} \|\widehat{\mathbf{M}}_1\|_2 \|\widehat{\mathbf{M}}_2 - \mathbf{M}_2\|_2 + \|\mathbf{M}_2\|_2 \|\widehat{\mathbf{M}}_1 - \mathbf{M}_1\|_2, \\ \|\widehat{\mathbf{M}}_2\|_2 \|\widehat{\mathbf{M}}_1 - \mathbf{M}_1\|_2 + \|\mathbf{M}_1\|_2 \|\widehat{\mathbf{M}}_2 - \mathbf{M}_2\|_2. \end{cases} \quad (50)$$

Then together with $\max_{k \leq K} \{\|\mathbf{H}_k\|_F, \|\hat{\mathbf{H}}_k\|_F\} \leq L^{1/2}$, we have

$$\|\widetilde{\text{cov}}(\mathbf{z}_k^{\mathcal{I}_0}) - \text{cov}(\mathbf{z}_k^{\mathcal{I}_0})\|_2 = \|\hat{\mathbf{H}}_k \hat{\mathbf{H}}_k^\top - \mathbf{H}_k \mathbf{H}_k^\top\|_2 \leq (\|\hat{\mathbf{H}}_k\|_2 + \|\mathbf{H}_k\|_2) \|\hat{\mathbf{H}}_k - \mathbf{H}_k\|_2 \lesssim_P \delta_\eta. \quad (51)$$

Recall that $\min_{k \leq K} \lambda_{r_k^*}(\text{cov}(\mathbf{z}_k^{\mathcal{I}_0})) > \kappa_z$. Let $\text{cov}(\mathbf{z}_k^{\mathcal{I}_0}) = \mathbf{V}_{zk} \boldsymbol{\Lambda}_{zk} \mathbf{V}_{zk}^\top$ be its compact SVD, where $\boldsymbol{\Lambda}_{zk}$ has nonincreasing diagonal elements. Let $\widehat{\boldsymbol{\Lambda}}_{zk}^{[j,j]} = 0$ for $j > \tilde{r}_k := \text{rank}(\widetilde{\text{cov}}(\mathbf{z}_k^{\mathcal{I}_0}))$, and $\boldsymbol{\Lambda}_{zk}^{[j,j]} = 0$ for $j > r_k^*$. By Weyl's inequality (see Theorem 3.3.16(c) in Horn and Johnson (1994)), for all j ,

$$|\widehat{\boldsymbol{\Lambda}}_{zk}^{[j,j]} - \boldsymbol{\Lambda}_{zk}^{[j,j]}| \leq \|\widetilde{\text{cov}}(\mathbf{z}_k^{\mathcal{I}_0}) - \text{cov}(\mathbf{z}_k^{\mathcal{I}_0})\|_2 \lesssim_P \delta_\eta.$$

Hence,

$$\widehat{\boldsymbol{\Lambda}}_{zk}^{[\tilde{r}_k, \tilde{r}_k]} \geq \boldsymbol{\Lambda}_{zk}^{[\tilde{r}_k, \tilde{r}_k]} - O_P(\delta_\eta) \geq \kappa_z - o_P(1) \quad (52)$$

and

$$\max_{j > r_k^*} \widehat{\boldsymbol{\Lambda}}_{zk}^{[j,j]} \lesssim_P \delta_\eta.$$

Then,

$$\begin{aligned}
 \|\widehat{\text{cov}}(\mathbf{z}_k^{\mathcal{I}_0}) - \text{cov}(\mathbf{z}_k^{\mathcal{I}_0})\|_2 &= \left\| \sum_{j=1}^{\check{r}_k} \widehat{\boldsymbol{\Lambda}}_{zk}^{[j,j]} \widehat{\mathbf{V}}_{zk}^{[j]} (\widehat{\mathbf{V}}_{zk}^{[j]})^\top - \sum_{j=1}^{r_k^*} \boldsymbol{\Lambda}_{zk}^{[j,j]} \mathbf{V}_{zk}^{[j]} (\mathbf{V}_{zk}^{[j]})^\top \right\|_2 \\
 &\leq \left\| \sum_{j=1}^{\check{r}_k} \widehat{\boldsymbol{\Lambda}}_{zk}^{[j,j]} \widehat{\mathbf{V}}_{zk}^{[j]} (\widehat{\mathbf{V}}_{zk}^{[j]})^\top - \sum_{j=1}^{r_k^*} \boldsymbol{\Lambda}_{zk}^{[j,j]} \mathbf{V}_{zk}^{[j]} (\mathbf{V}_{zk}^{[j]})^\top \right\|_2 + \sum_{j=\check{r}_k+1}^{\tilde{r}_k} \|\widehat{\boldsymbol{\Lambda}}_{zk}^{[j,j]} \widehat{\mathbf{V}}_{zk}^{[j]} (\widehat{\mathbf{V}}_{zk}^{[j]})^\top\|_2 \\
 &= \|\widehat{\text{cov}}(\mathbf{z}_k^{\mathcal{I}_0}) - \text{cov}(\mathbf{z}_k^{\mathcal{I}_0})\|_2 + \sum_{j=\check{r}_k+1}^{\tilde{r}_k} \|\widehat{\boldsymbol{\Lambda}}_{zk}^{[j,j]}\| \\
 &\lesssim_P \delta_\eta + \max(\tilde{r}_k - r_k^*, 0) \delta_\eta \\
 &\lesssim_P \delta_\eta. \tag{53}
 \end{aligned}$$

By Theorem 2.1 in Meng and Zheng (2010), (52), and $\min_{k \leq K} \lambda_{r_k^*}(\text{cov}(\mathbf{z}_k^{\mathcal{I}_0})) > \kappa_z$,

$$\begin{aligned}
 \left\| [\widehat{\text{cov}}(\mathbf{z}_k^{\mathcal{I}_0})]^\dagger - [\text{cov}(\mathbf{z}_k^{\mathcal{I}_0})]^\dagger \right\|_2 &\leq \left\| [\widehat{\text{cov}}(\mathbf{z}_k^{\mathcal{I}_0})]^\dagger - [\text{cov}(\mathbf{z}_k^{\mathcal{I}_0})]^\dagger \right\|_F \\
 &\leq \max \left\{ \left\| [\widehat{\text{cov}}(\mathbf{z}_k^{\mathcal{I}_0})]^\dagger \right\|_2^2, \left\| [\text{cov}(\mathbf{z}_k^{\mathcal{I}_0})]^\dagger \right\|_2^2 \right\} \left\| \widehat{\text{cov}}(\mathbf{z}_k^{\mathcal{I}_0}) - \text{cov}(\mathbf{z}_k^{\mathcal{I}_0}) \right\|_F \\
 &\leq \max \left\{ \left\| [\widehat{\text{cov}}(\mathbf{z}_k^{\mathcal{I}_0})]^\dagger \right\|_2^2, \left\| [\text{cov}(\mathbf{z}_k^{\mathcal{I}_0})]^\dagger \right\|_2^2 \right\} L^{1/2} \left\| \widehat{\text{cov}}(\mathbf{z}_k^{\mathcal{I}_0}) - \text{cov}(\mathbf{z}_k^{\mathcal{I}_0}) \right\|_2 \\
 &\lesssim_P \delta_\eta. \tag{54}
 \end{aligned}$$

By (50), (49), and (45), we have

$$\begin{aligned}
 \|\widehat{\mathbf{V}}_{xk} \widehat{\boldsymbol{\Lambda}}_{xk}^{1/2} \widehat{\mathbf{H}}_k^\top - \mathbf{V}_{xk} \boldsymbol{\Lambda}_{xk}^{1/2} \mathbf{H}_k^\top\|_2 &\leq \|\mathbf{V}_{xk} \boldsymbol{\Lambda}_{xk}^{1/2}\|_2 \|\widehat{\mathbf{H}}_k - \mathbf{H}_k\|_2 + \|\widehat{\mathbf{H}}_k\|_2 \|\widehat{\mathbf{V}}_{xk} \widehat{\boldsymbol{\Lambda}}_{xk}^{1/2} - \mathbf{V}_{xk} \boldsymbol{\Lambda}_{xk}^{1/2}\|_2 \\
 &\lesssim_P \lambda_1^{1/2}(\text{cov}(\mathbf{x}_k)) \delta_\eta + \lambda_1^{1/2}(\text{cov}(\mathbf{x}_k)) n^{-1/2} \\
 &\lesssim_P \lambda_1^{1/2}(\text{cov}(\mathbf{x}_k)) \delta_\eta.
 \end{aligned}$$

Using (50) again together with the above inequality, (54), and (52) yields

$$\begin{aligned}
 &\left\| \widehat{\mathbf{V}}_{xk} \widehat{\boldsymbol{\Lambda}}_{xk}^{1/2} \widehat{\mathbf{H}}_k^\top [\widehat{\text{cov}}(\mathbf{z}_k^{\mathcal{I}_0})]^\dagger - \mathbf{V}_{xk} \boldsymbol{\Lambda}_{xk}^{1/2} \mathbf{H}_k^\top [\text{cov}(\mathbf{z}_k^{\mathcal{I}_0})]^\dagger \right\|_2 \\
 &\leq \left\| \mathbf{V}_{xk} \boldsymbol{\Lambda}_{xk}^{1/2} \mathbf{H}_k \right\|_2 \left\| [\widehat{\text{cov}}(\mathbf{z}_k^{\mathcal{I}_0})]^\dagger - [\text{cov}(\mathbf{z}_k^{\mathcal{I}_0})]^\dagger \right\|_2 \\
 &\quad + \left\| [\widehat{\text{cov}}(\mathbf{z}_k^{\mathcal{I}_0})]^\dagger \right\|_2 \left\| \widehat{\mathbf{V}}_{xk} \widehat{\boldsymbol{\Lambda}}_{xk}^{1/2} \widehat{\mathbf{H}}_k^\top - \mathbf{V}_{xk} \boldsymbol{\Lambda}_{xk}^{1/2} \mathbf{H}_k^\top \right\|_2 \\
 &\lesssim_P \lambda_1^{1/2}(\text{cov}(\mathbf{x}_k)) \delta_\eta. \tag{55}
 \end{aligned}$$

By Weyl's inequality (see Theorem 3.3.16(c) in Horn and Johnson (1994)) and (46), for all $\ell \in \mathcal{I}_0$ we have

$$|\lambda_\ell(\widehat{\text{cov}}(\mathbf{f})) - \lambda_\ell(\text{cov}(\mathbf{f}))| \leq \|\widehat{\text{cov}}(\mathbf{f}) - \text{cov}(\mathbf{f})\|_2 \lesssim_P \delta_\eta.$$

Then by $\delta_\eta = o(1)$ and $\lambda_L(\text{cov}(\mathbf{f})) > 1$, for all $\ell \in \mathcal{I}_0$ we have

$$\begin{aligned} \left| \lambda_\ell^{1/2}(\widehat{\text{cov}}(\mathbf{f})) - \lambda_\ell^{1/2}(\text{cov}(\mathbf{f})) \right| &= \left| \lambda_\ell^{1/2}(\widehat{\text{cov}}(\mathbf{f})) + \lambda_\ell^{1/2}(\text{cov}(\mathbf{f})) \right|^{-1} |\lambda_\ell(\widehat{\text{cov}}(\mathbf{f})) - \lambda_\ell(\text{cov}(\mathbf{f}))| \\ &\leq \lambda_\ell^{-1/2}(\text{cov}(\mathbf{f})) \|\widehat{\text{cov}}(\mathbf{f}) - \text{cov}(\mathbf{f})\|_2 \\ &\lesssim_P \delta_\eta = o(1). \end{aligned} \quad (56)$$

Thus, for all $\ell \in \mathcal{I}_0$,

$$\lambda_\ell^{1/2}(\widehat{\text{cov}}(\mathbf{f})) \geq \lambda_\ell^{1/2}(\text{cov}(\mathbf{f})) - \left| \lambda_\ell^{1/2}(\widehat{\text{cov}}(\mathbf{f})) - \lambda_\ell^{1/2}(\text{cov}(\mathbf{f})) \right| \geq 1 - o_P(1),$$

and then

$$\begin{aligned} \left| \lambda_\ell^{-1/2}(\widehat{\text{cov}}(\mathbf{f})) - \lambda_\ell^{-1/2}(\text{cov}(\mathbf{f})) \right| &= \left| \lambda_\ell^{1/2}(\widehat{\text{cov}}(\mathbf{f})) - \lambda_\ell^{1/2}(\text{cov}(\mathbf{f})) \right| \lambda_\ell^{-\frac{1}{2}}(\widehat{\text{cov}}(\mathbf{f})) \lambda_\ell^{-\frac{1}{2}}(\text{cov}(\mathbf{f})) \\ &\lesssim_P \delta_\eta. \end{aligned} \quad (57)$$

For all $k \leq K$ and $\ell \in \mathcal{I}_0$, by (50), $\lambda_1(\text{cov}(\mathbf{f})) \leq \text{tr}(\text{cov}(\mathbf{f})) \leq \sum_{k=1}^K r_k$, (47), $\|\widehat{\boldsymbol{\eta}}_k^{(\ell)}\|_F \leq \|\widehat{\boldsymbol{\eta}}^{(\ell)}\|_F = 1$, and (56), we obtain

$$\begin{aligned} \left| \widehat{\cos}\{\theta(w^{(\ell)}, z_k^{(\ell)})\} - \cos\{\theta(w^{(\ell)}, z_k^{(\ell)})\} \right| &= \left| \lambda_\ell^{1/2}(\widehat{\text{cov}}(\mathbf{f})) \|\widehat{\boldsymbol{\eta}}_k^{(\ell)}\|_F - \lambda_\ell^{1/2}(\text{cov}(\mathbf{f})) \|\boldsymbol{\eta}_k^{(\ell)}\|_F \right| \\ &\leq |\lambda_\ell^{1/2}(\text{cov}(\mathbf{f}))| \left| \|\widehat{\boldsymbol{\eta}}_k^{(\ell)}\|_F - \|\boldsymbol{\eta}_k^{(\ell)}\|_F \right| + \|\widehat{\boldsymbol{\eta}}_k^{(\ell)}\|_F \left| \lambda_\ell^{1/2}(\widehat{\text{cov}}(\mathbf{f})) - \lambda_\ell^{1/2}(\text{cov}(\mathbf{f})) \right| \\ &\lesssim_P \delta_\eta. \end{aligned} \quad (58)$$

For all $\ell \in \mathcal{I}_0$ and $j, k \leq K$,

$$\cos\{\theta(z_j^{(\ell)}, z_k^{(\ell)})\} = \frac{(\boldsymbol{\eta}_j^{(\ell)})^\top \text{cov}(\mathbf{f}_j, \mathbf{f}_k) \boldsymbol{\eta}_k^{(\ell)}}{\|\boldsymbol{\eta}_j^{(\ell)}\|_F \|\boldsymbol{\eta}_k^{(\ell)}\|_F}.$$

By (50), (48), (46), and (49),

$$\begin{aligned} &\left\| (\widehat{\boldsymbol{\eta}}_j^{(\ell)})^\top \|\widehat{\boldsymbol{\eta}}_j^{(\ell)}\|_F^{-1} \widehat{\text{cov}}(\mathbf{f}_j, \mathbf{f}_k) - (\boldsymbol{\eta}_j^{(\ell)})^\top \|\boldsymbol{\eta}_j^{(\ell)}\|_F^{-1} \text{cov}(\mathbf{f}_j, \mathbf{f}_k) \right\|_2 \\ &\leq \left\| (\widehat{\boldsymbol{\eta}}_j^{(\ell)})^\top \|\widehat{\boldsymbol{\eta}}_j^{(\ell)}\|_F^{-1} \right\|_2 \left\| \widehat{\text{cov}}(\mathbf{f}_j, \mathbf{f}_k) - \text{cov}(\mathbf{f}_j, \mathbf{f}_k) \right\|_2 \\ &\quad + \left\| \text{cov}(\mathbf{f}_j, \mathbf{f}_k) \right\|_2 \left\| (\widehat{\boldsymbol{\eta}}_j^{(\ell)})^\top \|\widehat{\boldsymbol{\eta}}_j^{(\ell)}\|_F^{-1} - (\boldsymbol{\eta}_j^{(\ell)})^\top \|\boldsymbol{\eta}_j^{(\ell)}\|_F^{-1} \right\|_2 \\ &\lesssim_P \delta_\eta, \end{aligned}$$

and then,

$$\begin{aligned} &\left| \widehat{\cos}\{\theta(z_j^{(\ell)}, z_k^{(\ell)})\} - \cos\{\theta(z_j^{(\ell)}, z_k^{(\ell)})\} \right| \\ &\leq \left\| \widehat{\boldsymbol{\eta}}_k^{(\ell)} \|\widehat{\boldsymbol{\eta}}_k^{(\ell)}\|_F^{-1} \right\|_2 \left\| (\widehat{\boldsymbol{\eta}}_j^{(\ell)})^\top \|\widehat{\boldsymbol{\eta}}_j^{(\ell)}\|_F^{-1} \widehat{\text{cov}}(\mathbf{f}_j, \mathbf{f}_k) - (\boldsymbol{\eta}_j^{(\ell)})^\top \|\boldsymbol{\eta}_j^{(\ell)}\|_F^{-1} \text{cov}(\mathbf{f}_j, \mathbf{f}_k) \right\|_2 \\ &\quad + \left\| (\boldsymbol{\eta}_j^{(\ell)})^\top \|\boldsymbol{\eta}_j^{(\ell)}\|_F^{-1} \text{cov}(\mathbf{f}_j, \mathbf{f}_k) \right\|_2 \left\| \widehat{\boldsymbol{\eta}}_k^{(\ell)} \|\widehat{\boldsymbol{\eta}}_k^{(\ell)}\|_F^{-1} - \boldsymbol{\eta}_k^{(\ell)} \|\boldsymbol{\eta}_k^{(\ell)}\|_F^{-1} \right\|_2 \\ &\lesssim_P \delta_\eta. \end{aligned} \quad (59)$$

Consider $\ell \in \mathcal{I}_0$ and $(j, k) \in \mathcal{I}_{\Delta_+}^{(\ell)}$. By (58) and (59),

$$\begin{aligned}
 & \left| \tilde{\Delta}_{jk}^{(\ell)} - \Delta_{jk}^{(\ell)} \right| \\
 & \leq \left| [\widehat{\cos}\{\theta(w^{(\ell)}, z_j^{(\ell)})\} + \widehat{\cos}\{\theta(w^{(\ell)}, z_k^{(\ell)})\}]^2 - [\cos\{\theta(w^{(\ell)}, z_j^{(\ell)})\} + \cos\{\theta(w^{(\ell)}, z_k^{(\ell)})\}]^2 \right| \\
 & \quad + 4 \left| \widehat{\cos}\{\theta(z_j^{(\ell)}, z_k^{(\ell)})\} - \cos\{\theta(z_j^{(\ell)}, z_k^{(\ell)})\} \right| \\
 & \leq 4 \left| [\widehat{\cos}\{\theta(w^{(\ell)}, z_j^{(\ell)})\} + \widehat{\cos}\{\theta(w^{(\ell)}, z_k^{(\ell)})\}] - [\cos\{\theta(w^{(\ell)}, z_j^{(\ell)})\} + \cos\{\theta(w^{(\ell)}, z_k^{(\ell)})\}] \right| \\
 & \quad + 4 \left| \widehat{\cos}\{\theta(z_j^{(\ell)}, z_k^{(\ell)})\} - \cos\{\theta(z_j^{(\ell)}, z_k^{(\ell)})\} \right| \\
 & \leq 8 \max_{1 \leq k \leq K} \left| \widehat{\cos}\{\theta(w^{(\ell)}, z_k^{(\ell)})\} - \cos\{\theta(w^{(\ell)}, z_k^{(\ell)})\} \right| + 4 \left| \widehat{\cos}\{\theta(z_j^{(\ell)}, z_k^{(\ell)})\} - \cos\{\theta(z_j^{(\ell)}, z_k^{(\ell)})\} \right| \\
 & \lesssim_P \delta_\eta.
 \end{aligned} \tag{60}$$

By (60), $\Delta_{jk}^{(\ell)} > \kappa_\Delta$ and $\delta_\eta = o(1)$, we have $\tilde{\Delta}_{jk}^{(\ell)} > \kappa_\Delta - o_P(1)$. Then by the mean value theorem, we have

$$\begin{aligned}
 \left| (\widehat{\Delta}_{jk}^{(\ell)})^{1/2} - (\Delta_{jk}^{(\ell)})^{1/2} \right| & \leq \frac{1}{2} [\min(\widehat{\Delta}_{jk}^{(\ell)}, \Delta_{jk}^{(\ell)})]^{-1/2} \left| \widehat{\Delta}_{jk}^{(\ell)} - \Delta_{jk}^{(\ell)} \right| \\
 & \leq \frac{1}{2} [\kappa_\Delta - o_P(1)]^{-1/2} \left| \tilde{\Delta}_{jk}^{(\ell)} - \Delta_{jk}^{(\ell)} \right| \\
 & \lesssim_P \delta_\eta.
 \end{aligned} \tag{61}$$

Now consider $\ell \in \mathcal{I}_0$ and $(j, k) \in \mathcal{I}_\Delta^{(\ell)} := \mathcal{I}_{\Delta_+}^{(\ell)} \cup \mathcal{I}_{\Delta_0}^{(\ell)}$. From (58) and (61),

$$|\widehat{\alpha}_{jk}^{(\ell)} - \alpha_{jk}^{(\ell)}| \lesssim_P \delta_\eta. \tag{62}$$

Recall that $\min_{(j,k) \in \mathcal{I}_\Delta^{(\ell)}, \ell \in \mathcal{I}_0} |\cos\{\theta(z_j^{(\ell)}, z_k^{(\ell)})\}| > \kappa_{zz}$. By (59) and $\delta_\eta = o(1)$, with probability tending to 1 we have that $\widehat{\cos}\{\theta(z_j^{(\ell)}, z_k^{(\ell)})\} \cos\{\theta(z_j^{(\ell)}, z_k^{(\ell)})\} > 0$ and thus $\widehat{\alpha}_{jk}^{(\ell)} \alpha_{jk}^{(\ell)} > 0$. Without loss of generality, we assume $\alpha^{(\ell)} > 0$. Let $\mathcal{I}_+^{(\ell)} = \{(j, k) \in \mathcal{I}_\Delta^{(\ell)} : \alpha_{jk}^{(\ell)} > 0\}$, then $\alpha^{(\ell)} = \min\{\alpha_{jk}^{(\ell)} : \alpha_{jk}^{(\ell)} > 0, (j, k) \in \mathcal{I}_+^{(\ell)}\}$. With probability tending to 1, $\widehat{\alpha}^{(\ell)} = \min\{\widehat{\alpha}_{jk}^{(\ell)} : \widehat{\alpha}_{jk}^{(\ell)} > 0, (j, k) \in \mathcal{I}_+^{(\ell)}\}$. Due to Lemma S.1 in Shu et al. (2020), we simply assume $\widehat{\alpha}^{(\ell)} = \min\{\widehat{\alpha}_{jk}^{(\ell)} : \widehat{\alpha}_{jk}^{(\ell)} > 0, (j, k) \in \mathcal{I}_+^{(\ell)}\}$ in the rest of the proof. Without loss of generality, denote $\alpha_{12}^{(\ell)} = \alpha^{(\ell)}$. If $\widehat{\alpha}_{12}^{(\ell)} = \widehat{\alpha}^{(\ell)}$, then $|\widehat{\alpha}^{(\ell)} - \alpha^{(\ell)}| \lesssim_P \delta_\eta$. Otherwise, without loss of generality we assume $\widehat{\alpha}^{(\ell)} = \widehat{\alpha}_{23}^{(\ell)} < \widehat{\alpha}_{12}^{(\ell)}$ and $\alpha^{(\ell)} = \alpha_{12}^{(\ell)} < \alpha_{23}^{(\ell)}$. Then by (62) and $\delta_\eta = o(1)$, $\widehat{\alpha}_{23}^{(\ell)} - \widehat{\alpha}_{12}^{(\ell)} \geq \alpha_{23}^{(\ell)} - \alpha_{12}^{(\ell)} - o_P(1)$, which contradicts $\widehat{\alpha}_{12}^{(\ell)} > \widehat{\alpha}_{23}^{(\ell)} = \widehat{\alpha}^{(\ell)}$. Hence,

$$|\widehat{\alpha}^{(\ell)} - \alpha^{(\ell)}| \lesssim_P \delta_\eta. \tag{63}$$

By (50), (57) and (63), for all $\ell \in \mathcal{I}_0$,

$$\begin{aligned}
 & \left| \widehat{\alpha}^{(\ell)} \lambda_\ell^{-1/2} (\widehat{\text{cov}}(\mathbf{f})) - \alpha^{(\ell)} \lambda_\ell^{-1/2} (\text{cov}(\mathbf{f})) \right| \\
 & \leq \widehat{\alpha}^{(\ell)} \left| \lambda_\ell^{-1/2} (\widehat{\text{cov}}(\mathbf{f})) - \lambda_\ell^{-1/2} (\text{cov}(\mathbf{f})) \right| + \lambda_\ell^{-1/2} (\text{cov}(\mathbf{f})) |\widehat{\alpha}^{(\ell)} - \alpha^{(\ell)}| \\
 & \lesssim_P \delta_\eta.
 \end{aligned}$$

Then together with (50) and (47) gives

$$\|\widehat{\mathbf{A}}\widehat{\mathbf{N}} - \mathbf{AN}\|_2 \leq \|\mathbf{A}\|_2 \|\widehat{\mathbf{N}} - \mathbf{N}\|_F + \|\widehat{\mathbf{N}}\|_F \|\widehat{\mathbf{A}} - \mathbf{A}\|_2 \lesssim_P \delta_\eta, \quad (64)$$

where $\widehat{\mathbf{A}} := \text{diag}\{(\widehat{\alpha}^{(\ell)}[\lambda_\ell(\widehat{\text{cov}}(\mathbf{f}))]^{-1/2})_{\ell \in \mathcal{I}_0}\}$ with $0/0 := 0$, and $\widehat{\mathbf{N}} := (\widehat{\boldsymbol{\eta}}^{(\ell)})_{\ell \in \mathcal{I}_0}^\top$. From the inequalities respectively below (S.12) and (S.22) in the supplement of Shu et al. (2020), we obtain

$$n^{-1}\|\mathbf{F}_k\|_F^2 = r_k + O_P(n^{-1/2})$$

and

$$\|\widehat{\mathbf{F}}_k - \mathbf{F}_k\|_F \leq r_k^{1/2} \|\widehat{\mathbf{F}}_k - \mathbf{F}_k\|_2 \lesssim_P \min \left\{ 1 + [p_k \lambda_1^{-1}(\text{cov}(\mathbf{x}_k)) \log p_k]^{1/2}, n^{1/2} \right\} =: \delta_{F_k}.$$

Hence,

$$\|\mathbf{F}\|_F = \left(\sum_{k=1}^K \|\mathbf{F}_k\|_F^2 \right)^{1/2} = O_P(n^{1/2}) \quad (65)$$

and

$$\|\widehat{\mathbf{F}} - \mathbf{F}\|_F = \left(\sum_{k=1}^K \|\widehat{\mathbf{F}}_k - \mathbf{F}_k\|_F^2 \right)^{1/2} \lesssim_P \sum_{k=1}^K \delta_{F_k}. \quad (66)$$

By (50), (65), (64) and (66), we obtain

$$\begin{aligned} \|\widehat{\mathbf{C}}^{\mathcal{I}_0} - \mathbf{C}^{\mathcal{I}_0}\|_2 &\leq \|\mathbf{F}\|_F \|\widehat{\mathbf{A}}\widehat{\mathbf{N}} - \mathbf{AN}\|_2 + \|\widehat{\mathbf{A}}\|_2 \|\widehat{\mathbf{N}}\|_F \|\widehat{\mathbf{F}} - \mathbf{F}\|_F \\ &\lesssim_P n^{1/2} \delta_\eta + \sum_{k=1}^K \delta_{F_k} \lesssim_P n^{1/2} \delta_\eta. \end{aligned} \quad (67)$$

Using (50), (65), (55), (44), (52) and (67) yields

$$\begin{aligned} &\|\widehat{\mathbf{C}}_k - \mathbf{C}_k\|_2 \\ &\leq \|\mathbf{ANF}\|_2 \left\| \widehat{\mathbf{V}}_{xk} \widehat{\boldsymbol{\Lambda}}_{xk}^{1/2} \widehat{\mathbf{H}}_k^\top [\widehat{\text{cov}}(\mathbf{z}_k^{\mathcal{I}_0})]^\dagger - \mathbf{V}_{xk} \boldsymbol{\Lambda}_{xk}^{1/2} \mathbf{H}_k^\top [\text{cov}(\mathbf{z}_k^{\mathcal{I}_0})]^\dagger \right\|_2 \\ &\quad + \left\| \widehat{\mathbf{V}}_{xk} \widehat{\boldsymbol{\Lambda}}_{xk}^{1/2} \widehat{\mathbf{H}}_k^\top [\widehat{\text{cov}}(\mathbf{z}_k^{\mathcal{I}_0})]^\dagger \right\|_2 \|\widehat{\mathbf{C}}^{\mathcal{I}_0} - \mathbf{C}^{\mathcal{I}_0}\|_2 \\ &\lesssim_P n^{1/2} [\lambda_1^{1/2}(\text{cov}(\mathbf{x}_k)) \delta_\eta + \lambda_1^{1/2}(\text{cov}(\mathbf{x}_k)) n^{-1/2}] + \lambda_1^{1/2}(\text{cov}(\mathbf{x}_k)) n^{1/2} \delta_\eta \\ &\lesssim_P \lambda_1^{1/2}(\text{cov}(\mathbf{x}_k)) n^{1/2} \delta_\eta. \end{aligned} \quad (68)$$

By $\text{rank}(\mathbf{M}_1 \mathbf{M}_2) \leq \min(\text{rank}(\mathbf{M}_1), \text{rank}(\mathbf{M}_2))$ and $\text{rank}(\mathbf{M}_1 - \mathbf{M}_2) \leq \text{rank}(\mathbf{M}_1) + \text{rank}(\mathbf{M}_2)$ for any real matrices \mathbf{M}_1 and \mathbf{M}_2 with compatible sizes, we have $\text{rank}(\widehat{\mathbf{C}}_k - \mathbf{C}_k) \leq 2L$. Thus,

$$\|\widehat{\mathbf{C}}_k - \mathbf{C}_k\|_F \leq \|\widehat{\mathbf{C}}_k - \mathbf{C}_k\|_2 [\text{rank}(\widehat{\mathbf{C}}_k - \mathbf{C}_k)]^{1/2} \lesssim_P \lambda_1^{1/2}(\text{cov}(\mathbf{x}_k)) n^{1/2} \delta_\eta. \quad (69)$$

By (68), (69) and (39), we obtain

$$\max \left\{ \frac{\|\widehat{\mathbf{C}}_k - \mathbf{C}_k\|_2}{\|\mathbf{X}_k\|_2}, \frac{\|\widehat{\mathbf{C}}_k - \mathbf{C}_k\|_F}{\|\mathbf{X}_k\|_F} \right\} \lesssim_P \delta_\eta. \quad (70)$$

By $\|\widehat{\mathbf{D}}_k - \mathbf{D}_k\| \leq \|\widehat{\mathbf{X}}_k - \mathbf{X}_k\| + \|\widehat{\mathbf{C}}_k - \mathbf{C}_k\|$ for both the Frobenius norm and the spectral norm, (42) and (70), we obtain

$$\max \left\{ \frac{\|\widehat{\mathbf{D}}_k - \mathbf{D}_k\|_2}{\|\mathbf{X}_k\|_2}, \frac{\|\widehat{\mathbf{D}}_k - \mathbf{D}_k\|_F}{\|\mathbf{X}_k\|_F} \right\} \lesssim_P \delta_\eta. \quad (71)$$

3. Now we consider the estimated view-level proportion of explained signal variance.

Note that $\|\widehat{\mathbf{X}}_k\|_F^2/n = \text{tr}(\widehat{\mathbf{X}}_k \widehat{\mathbf{X}}_k^\top/n) = \text{tr}(\widehat{\text{cov}}(\mathbf{x}_k))$. By inequality (S.16) of Shu et al. (2020),

$$\begin{aligned} \left| \|\widehat{\mathbf{X}}_k\|_F^2/n - \text{tr}(\text{cov}(\mathbf{x}_k)) \right| &= \left| \text{tr}(\widehat{\text{cov}}(\mathbf{x}_k)) - \text{tr}(\text{cov}(\mathbf{x}_k)) \right| \leq \sum_{\ell=1}^{r_k} |\lambda_\ell(\widehat{\text{cov}}(\mathbf{x}_k)) - \lambda_\ell(\text{cov}(\mathbf{x}_k))| \\ &\lesssim_P \lambda_1(\text{cov}(\mathbf{x}_k)) n^{-1/2}, \end{aligned} \quad (72)$$

and by their (S.17),

$$\|\widehat{\mathbf{X}}_k\|_F^2/n = \text{tr}(\widehat{\text{cov}}(\mathbf{x}_k)) = \sum_{\ell=1}^{r_k} \lambda_\ell(\widehat{\text{cov}}(\mathbf{x}_k)) \geq r_k(1 - o_P(1)) \lambda_{r_k}(\text{cov}(\mathbf{x}_k)). \quad (73)$$

Since (69) and

$$\|\mathbf{C}_k\|_F \leq L^{1/2} \|\mathbf{C}_k\|_2 = L^{1/2} \|\mathbf{V}_{xk} \Lambda_{xk}^{1/2} \mathbf{H}_k^\top [\text{cov}(\mathbf{z}_k^{\mathcal{I}_0})]^\dagger \mathbf{ANF}\|_2 \lesssim_P \lambda_1^{1/2}(\text{cov}(\mathbf{x}_k)) n^{1/2},$$

we obtain

$$\|\widehat{\mathbf{C}}_k\|_F \leq \|\widehat{\mathbf{C}}_k - \mathbf{C}_k\|_F + \|\mathbf{C}_k\|_F \lesssim_P \lambda_1^{1/2}(\text{cov}(\mathbf{x}_k)) n^{1/2}. \quad (74)$$

Then,

$$\begin{aligned} \left| \|\widehat{\mathbf{C}}_k\|_F^2/n - \|\mathbf{C}_k\|_F^2/n \right| &= n^{-1} \left| \|\widehat{\mathbf{C}}_k\|_F - \|\mathbf{C}_k\|_F \right| (\|\widehat{\mathbf{C}}_k\|_F + \|\mathbf{C}_k\|_F) \\ &\leq n^{-1} \|\widehat{\mathbf{C}}_k - \mathbf{C}_k\|_F (\|\widehat{\mathbf{C}}_k\|_F + \|\mathbf{C}_k\|_F) \\ &\lesssim_P \lambda_1(\text{cov}(\mathbf{x}_k)) \delta_\eta. \end{aligned} \quad (75)$$

From the central limit theorem,

$$\left\| \mathbf{FF}^\top/n - \text{cov}(\mathbf{f}) \right\|_2 \leq \sum_{k=1}^K r_k \left\| \mathbf{FF}^\top/n - \text{cov}(\mathbf{f}) \right\|_{\max} \lesssim_P n^{-1/2}.$$

Let $\mathbf{Q}_k = \mathbf{V}_{xk} \Lambda_{xk}^{1/2} \mathbf{H}_k^\top [\text{cov}(\mathbf{z}_k^{\mathcal{I}_0})]^\dagger \mathbf{AN}$, then $\|\mathbf{Q}_k\|_2 \lesssim_P \lambda_1^{1/2}(\text{cov}(\mathbf{x}_k))$. By Weyl's inequality (see Theorem 3.3.16(c) in Horn and Johnson (1994)),

$$\begin{aligned} \max_{\ell \leq L} \left| \lambda_\ell(\mathbf{C}_k \mathbf{C}_k^\top/n) - \lambda_\ell(\text{cov}(\mathbf{c}_k)) \right| &\leq \left\| \mathbf{C}_k \mathbf{C}_k^\top/n - \text{cov}(\mathbf{c}_k) \right\|_2 \\ &= \left\| \mathbf{Q}_k n^{-1} \mathbf{FF}^\top \mathbf{Q}_k^\top - \mathbf{Q}_k \text{cov}(\mathbf{f}) \mathbf{Q}_k^\top \right\|_2 \leq \|\mathbf{Q}_k\|_2 \left\| \mathbf{FF}^\top/n - \text{cov}(\mathbf{f}) \right\|_2 \|\mathbf{Q}_k^\top\|_2 \\ &\lesssim_P \lambda_1(\text{cov}(\mathbf{x}_k)) n^{-1/2}. \end{aligned}$$

Then applying the same skill used for (72) yields

$$\left| \|\mathbf{C}_k\|_F^2/n - \text{tr}(\text{cov}(\mathbf{c}_k)) \right| \leq \sum_{\ell=1}^L \left| \lambda_\ell(\mathbf{C}_k \mathbf{C}_k^\top/n) - \lambda_\ell(\text{cov}(\mathbf{c}_k)) \right| \lesssim_P \lambda_1(\text{cov}(\mathbf{x}_k)) n^{-1/2}. \quad (76)$$

Combining (75) and (76) with the triangle inequality gives

$$\left| \|\widehat{\mathbf{C}}_k\|_F^2/n - \text{tr}(\text{cov}(\mathbf{c}_k)) \right| \lesssim_P \lambda_1(\text{cov}(\mathbf{x}_k)) \delta_\eta. \quad (77)$$

From (50), (72), (73), (74), (77) and (41), we have

$$\begin{aligned} & \left| \widehat{\text{PVE}}_c(\mathbf{x}_k) - \text{PVE}_c(\mathbf{x}_k) \right| = \left| \frac{\frac{1}{n} \|\widehat{\mathbf{C}}_k\|_F^2}{\frac{1}{n} \|\widehat{\mathbf{X}}_k\|_F^2} - \frac{\text{tr}(\text{cov}(\mathbf{c}_k))}{\text{tr}(\text{cov}(\mathbf{x}_k))} \right| \\ & \leq \left| \frac{1}{\frac{1}{n} \|\widehat{\mathbf{X}}_k\|_F^2} - \frac{1}{\text{tr}(\text{cov}(\mathbf{x}_k))} \right| \cdot \frac{1}{n} \|\widehat{\mathbf{C}}_k\|_F^2 + \left| \frac{1}{n} \|\widehat{\mathbf{C}}_k\|_F^2 - \text{tr}(\text{cov}(\mathbf{c}_k)) \right| \frac{1}{\text{tr}(\text{cov}(\mathbf{x}_k))} \\ & \leq \frac{\left| \text{tr}(\text{cov}(\mathbf{x}_k)) - \frac{1}{n} \|\widehat{\mathbf{X}}_k\|_F^2 \right|}{\frac{1}{n} \|\widehat{\mathbf{X}}_k\|_F^2 \text{tr}(\text{cov}(\mathbf{x}_k))} \cdot \frac{1}{n} \|\widehat{\mathbf{C}}_k\|_F^2 + \left| \frac{1}{n} \|\widehat{\mathbf{C}}_k\|_F^2 - \text{tr}(\text{cov}(\mathbf{c}_k)) \right| \frac{1}{\text{tr}(\text{cov}(\mathbf{x}_k))} \\ & \lesssim_P \delta_\eta. \end{aligned}$$

4. Next, we consider the estimated variable-level proportion of explained signal variance.

First consider the error of $\widehat{\mathbf{V}}_{xk}$ in the max norm. We will use Theorem 3 of Fan et al. (2018). Before applying the theorem, we need to check the conditions therein. By Assumption 1 (iv) and (v), we have $\|\text{cov}(\mathbf{y}_k)\|_{\max} \leq \|\text{cov}(\mathbf{x}_k)\|_{\max} + \|\text{cov}(\mathbf{e}_k)\|_{\max} \leq r_k \kappa_B^2 \lambda_{k,1}/p_k + s_0$. Then from the proof of Lemma A2 (i) in Shu et al. (2019) and Assumption 1 (iv), we obtain

$$\left\| \frac{1}{n} \mathbf{Y} \mathbf{Y}^\top - \text{cov}(\mathbf{y}_k) \right\|_{\max} \lesssim_P \|\text{cov}(\mathbf{y}_k)\|_{\max} \sqrt{\frac{\log p_k}{n}} \lesssim_P \left(\frac{\lambda_{k,1}}{p_k} + s_0 \right) \sqrt{\frac{\log p_k}{n}}.$$

Thus, in our context, their notation $\epsilon = 0$, $\mu(\mathbf{V}_{xk}) = \frac{p_k}{r_k} \max_{1 \leq i \leq p_k} \sum_{j=1}^{r_k} (\mathbf{V}_{xk}^{[i,j]})^2 = O(\frac{p_k}{r_k} r_k \frac{\kappa_B^2}{p_k}) = O(1)$ (by Assumption 1 (iv) and (ii)), and $\|E\|_\infty = \|\text{cov}(\mathbf{e}_k) + \frac{1}{n} \mathbf{Y} \mathbf{Y}^\top - \text{cov}(\mathbf{y}_k)\|_\infty \leq s_0 + p_k \|\frac{1}{n} \mathbf{Y} \mathbf{Y}^\top - \text{cov}(\mathbf{y}_k)\|_{\max} \lesssim_P 1 + (\lambda_{k,1} + p_k) \sqrt{(\log p_k)/n}$. Hence, by Assumption 1 (i) and letting their notation $\delta = \delta_0 \lambda_{r_k}(\text{cov}(\mathbf{x}_k))/2$, if $\lambda_{r_k}(\text{cov}(\mathbf{x}_k)) > \widetilde{M}_k (\lambda_{k,r_k} + p_k) \sqrt{(\log p_k)/n}$ with a sufficiently large constant $\widetilde{M}_k > 0$, which is satisfied due to $\delta_k = o(1)$ and (79), then from Theorem 3 of Fan et al. (2018), we have

$$\|\widehat{\mathbf{V}}_{xk} - \mathbf{V}_{xk}\|_{\max} = O\left(\frac{\|E\|_\infty}{\lambda_{k,r_k} \sqrt{p_k}}\right) = O_P\left(\left(\frac{1}{\sqrt{p_k}} + \frac{\sqrt{p_k}}{\lambda_{k,r_k}}\right) \sqrt{\frac{\log p_k}{n}}\right) := O_P(\delta_{V_k}). \quad (78)$$

From (S.6), (S.16) and (S.18) in Shu et al. (2020), we have

$$\lambda_{k,\ell}/\lambda_\ell(\text{cov}(\mathbf{x}_k)) \rightarrow 1 \quad \text{for } 1 \leq \ell \leq r_k, \quad (79)$$

$$\|\widehat{\boldsymbol{\Lambda}}_{xk} - \boldsymbol{\Lambda}_{xk}\|_{\max} \lesssim_P \lambda_{k,1}/\sqrt{n}, \quad (80)$$

and

$$\|\widehat{\boldsymbol{\Lambda}}_{xk}^{1/2} - \boldsymbol{\Lambda}_{xk}^{1/2}\|_{\max} \lesssim_P \sqrt{\lambda_{k,1}/n}. \quad (81)$$

Then by (78), (80), (81), and Assumption 1 (iv), we obtain

$$\begin{aligned} \|\widehat{\mathbf{V}}_{xk}\widehat{\boldsymbol{\Lambda}}_{xk} - \mathbf{V}_{xk}\boldsymbol{\Lambda}_{xk}\|_{\max} &\leq \|(\widehat{\mathbf{V}}_{xk} - \mathbf{V}_{xk})\widehat{\boldsymbol{\Lambda}}_{xk}\|_{\max} + \|\mathbf{V}_{xk}(\widehat{\boldsymbol{\Lambda}}_{xk} - \boldsymbol{\Lambda}_{xk})\|_{\max} \\ &\lesssim_P \delta_{V_k}\lambda_{k,1} + \sqrt{1/p_k}\lambda_{k,1}/\sqrt{n} \lesssim_P \delta_{V_k}\lambda_{k,1}, \end{aligned}$$

$$\begin{aligned} \|\widehat{\text{cov}}(\mathbf{x}_k) - \text{cov}(\mathbf{x}_k)\|_{\max} &= \|\widehat{\mathbf{V}}_{xk}\widehat{\boldsymbol{\Lambda}}_{xk}\widehat{\mathbf{V}}_{xk}^{\top} - \mathbf{V}_{xk}\boldsymbol{\Lambda}_{xk}\mathbf{V}_{xk}^{\top}\|_{\max} \\ &\leq \|(\widehat{\mathbf{V}}_{xk}\widehat{\boldsymbol{\Lambda}}_{xk} - \mathbf{V}_{xk}\boldsymbol{\Lambda}_{xk})\widehat{\mathbf{V}}_{xk}^{\top}\|_{\max} + \|\mathbf{V}_{xk}\boldsymbol{\Lambda}_{xk}(\widehat{\mathbf{V}}_{xk} - \mathbf{V}_{xk})^{\top}\|_{\max} \\ &\leq \|\widehat{\mathbf{V}}_{xk}\widehat{\boldsymbol{\Lambda}}_{xk} - \mathbf{V}_{xk}\boldsymbol{\Lambda}_{xk}\|_{\max}\|\widehat{\mathbf{V}}_{xk}^{\top}\|_1 + \|\widehat{\mathbf{V}}_{xk} - \mathbf{V}_{xk}\|_{\max}\|\boldsymbol{\Lambda}_{xk}\mathbf{V}_{xk}^{\top}\|_1 \\ &\lesssim_P \delta_{V_k}\lambda_{k,1}/\sqrt{p_k}, \end{aligned} \quad (82)$$

and

$$\begin{aligned} \|\widehat{\mathbf{V}}_{xk}\widehat{\boldsymbol{\Lambda}}_{xk}^{1/2} - \mathbf{V}_{xk}\boldsymbol{\Lambda}_{xk}^{1/2}\|_{\max} &\leq \|(\widehat{\mathbf{V}}_{xk} - \mathbf{V}_{xk})\widehat{\boldsymbol{\Lambda}}_{xk}^{1/2}\|_{\max} + \|\mathbf{V}_{xk}(\widehat{\boldsymbol{\Lambda}}_{xk}^{1/2} - \boldsymbol{\Lambda}_{xk}^{1/2})\|_{\max} \\ &\lesssim_P \delta_{V_k}\lambda_{k,1}^{1/2} + \sqrt{1/p_k}\sqrt{\lambda_{k,1}/n} \lesssim_P \delta_{V_k}\lambda_{k,1}^{1/2}. \end{aligned}$$

By the last inequality, Assumption 1 (iv), and (49),

$$\begin{aligned} \|\widehat{\text{cov}}(\mathbf{x}_k, \mathbf{z}_k^{\mathcal{I}_0}) - \text{cov}(\mathbf{x}_k, \mathbf{z}_k^{\mathcal{I}_0})\|_{\max} &= \|\widehat{\mathbf{V}}_{xk}\widehat{\boldsymbol{\Lambda}}_{xk}^{1/2}\widehat{\mathbf{H}}_k^{\top} - \mathbf{V}_{xk}\boldsymbol{\Lambda}_{xk}^{1/2}\mathbf{H}_k^{\top}\|_{\max} \\ &\leq \|\mathbf{V}_{xk}\boldsymbol{\Lambda}_{xk}^{1/2}(\widehat{\mathbf{H}}_k^{\top} - \mathbf{H}_k^{\top})\|_{\max} + \|(\widehat{\mathbf{V}}_{xk}\widehat{\boldsymbol{\Lambda}}_{xk}^{1/2} - \mathbf{V}_{xk}\boldsymbol{\Lambda}_{xk}^{1/2})\widehat{\mathbf{H}}_k^{\top}\|_{\max} \\ &\leq \|\mathbf{V}_{xk}\boldsymbol{\Lambda}_{xk}^{1/2}\|_{\max}\sqrt{r_k}\|\widehat{\mathbf{H}}_k^{\top} - \mathbf{H}_k^{\top}\|_2 + \|\widehat{\mathbf{V}}_{xk}\widehat{\boldsymbol{\Lambda}}_{xk}^{1/2} - \mathbf{V}_{xk}\boldsymbol{\Lambda}_{xk}^{1/2}\|_{\max}\sqrt{r_k}\|\widehat{\mathbf{H}}_k^{\top}\|_2 \\ &\lesssim_P (\lambda_{k,1}/p_k)^{1/2}\delta_{\eta} + \delta_{V_k}\lambda_{k,1}^{1/2}. \end{aligned}$$

Then by (54), $\min_{k \leq K} \lambda_{r_k^*}(\text{cov}(\mathbf{z}_k^{\mathcal{I}_0})) > \kappa_z$, and $\delta_{\eta} = o(1)$, we similarly have

$$\begin{aligned} \delta_{B_k} &:= \|\widehat{\text{cov}}(\mathbf{x}_k, \mathbf{z}_k^{\mathcal{I}_0})\{\widehat{\text{cov}}(\mathbf{z}_k^{\mathcal{I}_0})\}^{\dagger} - \text{cov}(\mathbf{x}_k, \mathbf{z}_k^{\mathcal{I}_0})\{\text{cov}(\mathbf{z}_k^{\mathcal{I}_0})\}^{\dagger}\|_{\max} \\ &\leq \|\text{cov}(\mathbf{x}_k, \mathbf{z}_k^{\mathcal{I}_0})\|_{\max}\sqrt{|\mathcal{I}_0|}\|\{\widehat{\text{cov}}(\mathbf{z}_k^{\mathcal{I}_0})\}^{\dagger} - \{\text{cov}(\mathbf{z}_k^{\mathcal{I}_0})\}^{\dagger}\|_2 \\ &\quad + \|\widehat{\text{cov}}(\mathbf{x}_k, \mathbf{z}_k^{\mathcal{I}_0}) - \text{cov}(\mathbf{x}_k, \mathbf{z}_k^{\mathcal{I}_0})\|_{\max}\sqrt{|\mathcal{I}_0|}\|\{\widehat{\text{cov}}(\mathbf{z}_k^{\mathcal{I}_0})\}^{\dagger}\|_2 \\ &\leq \|\mathbf{V}_{xk}\boldsymbol{\Lambda}_{xk}^{1/2}\|_{\max}\sqrt{r_k}\|\mathbf{H}_k^{\top}\|_2\sqrt{|\mathcal{I}_0|}\|\{\widehat{\text{cov}}(\mathbf{z}_k^{\mathcal{I}_0})\}^{\dagger} - \{\text{cov}(\mathbf{z}_k^{\mathcal{I}_0})\}^{\dagger}\|_2 \\ &\quad + \|\widehat{\text{cov}}(\mathbf{x}_k, \mathbf{z}_k^{\mathcal{I}_0}) - \text{cov}(\mathbf{x}_k, \mathbf{z}_k^{\mathcal{I}_0})\|_{\max}\sqrt{|\mathcal{I}_0|}(\|[\text{cov}(\mathbf{z}_k^{\mathcal{I}_0})]^{\dagger}\|_2 + \|[\widehat{\text{cov}}(\mathbf{z}_k^{\mathcal{I}_0})]^{\dagger} - [\text{cov}(\mathbf{z}_k^{\mathcal{I}_0})]^{\dagger}\|_2) \\ &\lesssim_P (\lambda_{k,1}/p_k)^{1/2}\delta_{\eta} + \delta_{V_k}\lambda_{k,1}^{1/2}. \end{aligned} \quad (83)$$

From (50) and (67), $\|\frac{1}{n}\widehat{\mathbf{C}}^{\mathcal{I}_0}(\widehat{\mathbf{C}}^{\mathcal{I}_0})^{\top} - \frac{1}{n}\mathbf{C}^{\mathcal{I}_0}(\mathbf{C}^{\mathcal{I}_0})^{\top}\|_2 \lesssim_P \delta_{\eta}$. Besides, by the central limit theorem, $\|\frac{1}{n}\mathbf{C}^{\mathcal{I}_0}(\mathbf{C}^{\mathcal{I}_0})^{\top} - \text{cov}(\mathbf{c}^{\mathcal{I}_0})\|_2 \leq |\mathcal{I}_0|\|\frac{1}{n}\mathbf{C}^{\mathcal{I}_0}(\mathbf{C}^{\mathcal{I}_0})^{\top} - \text{cov}(\mathbf{c}^{\mathcal{I}_0})\|_{\max} \lesssim_P n^{-1/2}$. Thus, by the triangle inequality,

$$\left\| \widehat{\mathbf{C}}^{\mathcal{I}_0}(\widehat{\mathbf{C}}^{\mathcal{I}_0})^{\top}/n - \text{cov}(\mathbf{c}^{\mathcal{I}_0}) \right\|_2 \lesssim_P \delta_{\eta}. \quad (84)$$

By (83) and (84),

$$\begin{aligned}
\delta_{B_k \Sigma_c} &:= \left\| \widehat{\text{cov}}(\mathbf{x}_k, \mathbf{z}_k^{\mathcal{I}_0}) \{ \widehat{\text{cov}}(\mathbf{z}_k^{\mathcal{I}_0}) \}^\dagger \widehat{\mathbf{C}}^{\mathcal{I}_0} (\widehat{\mathbf{C}}^{\mathcal{I}_0})^\top / n - \text{cov}(\mathbf{x}_k, \mathbf{z}_k^{\mathcal{I}_0}) \{ \text{cov}(\mathbf{z}_k^{\mathcal{I}_0}) \}^\dagger \text{cov}(\mathbf{c}^{\mathcal{I}_0}) \right\|_{\max} \\
&\leq \| \text{cov}(\mathbf{x}_k, \mathbf{z}_k^{\mathcal{I}_0}) \{ \text{cov}(\mathbf{z}_k^{\mathcal{I}_0}) \}^\dagger \|_{\max} \sqrt{|\mathcal{I}_0|} \left\| \widehat{\mathbf{C}}^{\mathcal{I}_0} (\widehat{\mathbf{C}}^{\mathcal{I}_0})^\top / n - \text{cov}(\mathbf{c}^{\mathcal{I}_0}) \right\|_2 \\
&\quad + \| \widehat{\text{cov}}(\mathbf{x}_k, \mathbf{z}_k^{\mathcal{I}_0}) \{ \widehat{\text{cov}}(\mathbf{z}_k^{\mathcal{I}_0}) \}^\dagger - \text{cov}(\mathbf{x}_k, \mathbf{z}_k^{\mathcal{I}_0}) \{ \text{cov}(\mathbf{z}_k^{\mathcal{I}_0}) \}^\dagger \|_{\max} \sqrt{|\mathcal{I}_0|} \left\| \widehat{\mathbf{C}}^{\mathcal{I}_0} (\widehat{\mathbf{C}}^{\mathcal{I}_0})^\top / n \right\|_2 \\
&\lesssim_P (\lambda_{k,1}/p_k)^{1/2} \delta_\eta + (\lambda_{k,1}/p_k)^{1/2} \delta_\eta + \delta_{V_k} \lambda_{k,1}^{1/2} \\
&\lesssim_P (\lambda_{k,1}/p_k)^{1/2} \delta_\eta + \delta_{V_k} \lambda_{k,1}^{1/2},
\end{aligned}$$

and thus,

$$\begin{aligned}
&\| \widehat{\text{cov}}(\mathbf{c}_k) - \text{cov}(\mathbf{c}_k) \|_{\max} \\
&= \| \widehat{\text{cov}}(\mathbf{x}_k, \mathbf{z}_k^{\mathcal{I}_0}) \{ \widehat{\text{cov}}(\mathbf{z}_k^{\mathcal{I}_0}) \}^\dagger n^{-1} \widehat{\mathbf{C}}^{\mathcal{I}_0} (\widehat{\mathbf{C}}^{\mathcal{I}_0})^\top (\widehat{\text{cov}}(\mathbf{x}_k, \mathbf{z}_k^{\mathcal{I}_0}) \{ \widehat{\text{cov}}(\mathbf{z}_k^{\mathcal{I}_0}) \}^\dagger)^\top \\
&\quad - \text{cov}(\mathbf{x}_k, \mathbf{z}_k^{\mathcal{I}_0}) \{ \text{cov}(\mathbf{z}_k^{\mathcal{I}_0}) \}^\dagger \text{cov}(\mathbf{c}^{\mathcal{I}_0}) (\text{cov}(\mathbf{x}_k, \mathbf{z}_k^{\mathcal{I}_0}) \{ \text{cov}(\mathbf{z}_k^{\mathcal{I}_0}) \}^\dagger)^\top \|_{\max} \\
&\leq \| \text{cov}(\mathbf{x}_k, \mathbf{z}_k^{\mathcal{I}_0}) \{ \text{cov}(\mathbf{z}_k^{\mathcal{I}_0}) \}^\dagger \text{cov}(\mathbf{c}^{\mathcal{I}_0}) \|_{\max} |\mathcal{I}_0| \delta_{B_k} + \delta_{B_k \Sigma_c} |\mathcal{I}_0| \| \widehat{\text{cov}}(\mathbf{x}_k, \mathbf{z}_k^{\mathcal{I}_0}) \{ \widehat{\text{cov}}(\mathbf{z}_k^{\mathcal{I}_0}) \}^\dagger \|_{\max} \\
&\lesssim_P (\lambda_{k,1}/p_k)^{1/2} [(\lambda_{k,1}/p_k)^{1/2} \delta_\eta + \delta_{V_k} \lambda_{k,1}^{1/2}] \\
&\quad + [(\lambda_{k,1}/p_k)^{1/2} \delta_\eta + \delta_{V_k} \lambda_{k,1}^{1/2}] [(\lambda_{k,1}/p_k)^{1/2} + (\lambda_{k,1}/p_k)^{1/2} \delta_\eta + \delta_{V_k} \lambda_{k,1}^{1/2}] \\
&\lesssim_P [(\lambda_{k,1}/p_k)^{1/2} \delta_\eta + \delta_{V_k} \lambda_{k,1}^{1/2}] (\lambda_{k,1}/p_k)^{1/2}.
\end{aligned} \tag{85}$$

From Assumption 1 (iv),

$$\begin{aligned}
\| \text{cov}(\mathbf{c}_k) \|_{\max} &\leq \max_{1 \leq i \leq p_k} | \text{var}(\mathbf{c}_k^{[i]}) | \\
&= \max_{1 \leq i \leq p_k} | \mathbf{V}_{xk}^{[i,:]} \boldsymbol{\Lambda}_{xk}^{1/2} \mathbf{H}_k^\top [\text{cov}(\mathbf{z}_k^{\mathcal{I}_0})]^\dagger \mathbf{A} \mathbf{N} \text{cov}(\mathbf{f}) (\mathbf{V}_{xk}^{[i,:]} \boldsymbol{\Lambda}_{xk}^{1/2} \mathbf{H}_k^\top [\text{cov}(\mathbf{z}_k^{\mathcal{I}_0})]^\dagger \mathbf{A} \mathbf{N})^\top | \\
&\leq \max_{1 \leq i \leq p_k} \{ \| \mathbf{V}_{xk}^{[i,:]} \boldsymbol{\Lambda}_{xk}^{1/2} \|_2^2 \| \mathbf{H}_k^\top [\text{cov}(\mathbf{z}_k^{\mathcal{I}_0})]^\dagger \mathbf{A} \mathbf{N} \text{cov}(\mathbf{f}) (\mathbf{H}_k^\top [\text{cov}(\mathbf{z}_k^{\mathcal{I}_0})]^\dagger \mathbf{A} \mathbf{N})^\top \|_2 \\
&\lesssim_P \max_{1 \leq i \leq p_k} \| \mathbf{V}_{xk}^{[i,:]} \boldsymbol{\Lambda}_{xk}^{1/2} \|_2^2 \leq \max_{1 \leq i \leq p_k} \| \mathbf{V}_{xk}^{[i,:]} \boldsymbol{\Lambda}_{xk}^{1/2} \|_{\max}^2 r_k \\
&\lesssim_P \lambda_{k,1}/p_k.
\end{aligned} \tag{86}$$

Denote $\widehat{\text{var}}(\mathbf{c}_k^{[i]}) = \|\widehat{\mathbf{C}}_k^{[i,:]}\|_F^2/n$ and $\widehat{\text{var}}(\mathbf{x}_k^{[i]}) = \|\widehat{\mathbf{X}}_k^{[i,:]}\|_F^2/n$. By the triangle inequality, (85), (86), $\delta_\eta = o(1)$, and $o(1) = \delta_k \asymp \delta_{V_k} \sqrt{p_k}$ (from (41), (79), and $\lambda_{k,1} \asymp \lambda_{k,r_k}$ in Assumption 1 (ii)), we have $\max_{i \leq p_k} \widehat{\text{var}}(\mathbf{c}_k^{[i]}) \leq \|\widehat{\text{cov}}(\mathbf{c}_k)\|_{\max} \lesssim_P \lambda_{k,1}/p_k$. By (82) and $\min_{i \leq p_k} \text{var}(\mathbf{x}_k^{[i]}) \geq M_k \lambda_{r_k} (\text{cov}(\mathbf{x}_k))/p_k$, we obtain $\min_{i \leq p_k} \widehat{\text{var}}(\mathbf{x}_k^{[i]}) \geq M_k \lambda_{r_k} (\text{cov}(\mathbf{x}_k))/p_k -$

$o_P(\lambda_{k,1}/p_k)$. Then together with (82) and (85), we have that, uniformly for all $i = 1, \dots, p_k$,

$$\begin{aligned}
 & \left| \widehat{\text{PVE}}_c(\mathbf{x}_k^{[i]}) - \text{PVE}_c(\mathbf{x}_k^{[i]}) \right| = \left| \frac{\text{var}(\mathbf{c}_k^{[i]})}{\text{var}(\mathbf{x}_k^{[i]})} - \frac{\widehat{\text{var}}(\mathbf{c}_k^{[i]})}{\widehat{\text{var}}(\mathbf{x}_k^{[i]})} \right| \\
 & \leq \frac{|\widehat{\text{var}}(\mathbf{x}_k^{[i]}) - \text{var}(\mathbf{x}_k^{[i]})|}{\widehat{\text{var}}(\mathbf{x}_k^{[i]}) \text{var}(\mathbf{x}_k^{[i]})} \widehat{\text{var}}(\mathbf{c}_k^{[i]}) + \left| \widehat{\text{var}}(\mathbf{c}_k^{[i]}) - \text{var}(\mathbf{c}_k^{[i]}) \right| \frac{1}{\text{var}(\mathbf{x}_k^{[i]})} \\
 & \lesssim_P \frac{|\widehat{\text{var}}(\mathbf{x}_k^{[i]}) - \text{var}(\mathbf{x}_k^{[i]})|}{\text{var}(\mathbf{x}_k^{[i]})} + \left| \widehat{\text{var}}(\mathbf{c}_k^{[i]}) - \text{var}(\mathbf{c}_k^{[i]}) \right| \frac{1}{\text{var}(\mathbf{x}_k^{[i]})} \\
 & \lesssim_P \left\{ \delta_{V_k} \lambda_{k,1} / \sqrt{p_k} + [(\lambda_{k,1}/p_k)^{1/2} \delta_\eta + \delta_{V_k} \lambda_{k,1}^{1/2}] (\lambda_{k,1}/p_k)^{1/2} \right\} \frac{1}{\text{var}(\mathbf{x}_k^{[i]})} \\
 & \lesssim_P \delta_\eta + \delta_{V_k} p_k^{1/2} \\
 & \lesssim_P \delta_\eta + \delta_k.
 \end{aligned}$$

The proof is complete. \blacksquare

Proof of Corollary 1. Let $\text{cov}(\mathbf{d}_k^{(t)}) = \mathbf{V}_{d_k^{(t)}} \boldsymbol{\Lambda}_{d_k^{(t)}} \mathbf{V}_{d_k^{(t)}}^\top$ be its compact SVD, where $\boldsymbol{\Lambda}_{d_k^{(t)}}$ is a diagonal matrix with nonincreasing diagonal elements. Then, $\mathbf{f}_k^{(t)} = \boldsymbol{\Lambda}_{d_k^{(t)}}^{-1/2} \mathbf{V}_{d_k^{(t)}}^\top \mathbf{d}_k^{(t)}$ is an orthonormal basis of $\text{span}((\mathbf{d}_k^{(t)})^\top)$, and $\mathbf{d}_k^{(t)} = \mathbf{V}_{d_k^{(t)}} \boldsymbol{\Lambda}_{d_k^{(t)}}^{1/2} \mathbf{f}_k^{(t)}$. Denote $\mathbf{F}_k^{(t)}$ and $\mathbf{D}_k^{(t)}$ to be the sample matrices of $\mathbf{f}_k^{(t)}$ and $\mathbf{d}_k^{(t)}$, respectively. By the central limit theorem, we have

$$\|n^{-1} \mathbf{F}_j^{(1)} (\mathbf{F}_k^{(1)})^\top - \text{cov}(\mathbf{f}_j^{(1)}, \mathbf{f}_k^{(1)})\|_F = O_P(n^{-1/2}). \quad (87)$$

Consequently,

$$\begin{aligned}
 & \|n^{-1} \mathbf{D}_k^{(1)} (\mathbf{D}_k^{(1)})^\top - \text{cov}(\mathbf{d}_k^{(1)})\|_2 \leq \|n^{-1} \mathbf{D}_k^{(1)} (\mathbf{D}_k^{(1)})^\top - \text{cov}(\mathbf{d}_k^{(1)})\|_F \\
 & = \|\mathbf{V}_{d_k^{(t)}} \boldsymbol{\Lambda}_{d_k^{(t)}}^{1/2} n^{-1} \mathbf{F}_k^{(1)} (\mathbf{F}_k^{(1)})^\top \boldsymbol{\Lambda}_{d_k^{(t)}}^{1/2} \mathbf{V}_{d_k^{(t)}}^\top - \mathbf{V}_{d_k^{(t)}} \boldsymbol{\Lambda}_{d_k^{(t)}}^{1/2} \text{cov}(\mathbf{f}^{(1)}) \boldsymbol{\Lambda}_{d_k^{(t)}}^{1/2} \mathbf{V}_{d_k^{(t)}}^\top\|_F \\
 & \lesssim_P \lambda_1(\text{cov}(\mathbf{d}_k^{(1)})) n^{-1/2}.
 \end{aligned} \quad (88)$$

Moreover,

$$\begin{aligned}
 \|\mathbf{D}_k^{(1)}\|_2 &= \|\mathbf{D}_k^{(1)} (\mathbf{D}_k^{(1)})^\top\|_2^{1/2} \leq n^{1/2} (\|n^{-1} \mathbf{D}_k^{(1)} (\mathbf{D}_k^{(1)})^\top - \text{cov}(\mathbf{d}_k^{(1)})\|_2 + \|\text{cov}(\mathbf{d}_k^{(1)})\|_2)^{1/2} \\
 &\lesssim_P [n \lambda_1(\text{cov}(\mathbf{d}_k^{(1)}))]^{1/2}
 \end{aligned} \quad (89)$$

On the other hand, it follows from (39) and (71) that

$$\|\widehat{\mathbf{D}}_k^{(1)} - \mathbf{D}_k^{(1)}\|_2 \lesssim_P \delta_\eta [n \lambda_1(\text{cov}(\mathbf{x}_k))]^{1/2}. \quad (90)$$

Then by (71) and (89),

$$\begin{aligned} & \|\widehat{\mathbf{D}}_k^{(1)}(\widehat{\mathbf{D}}_k^{(1)})^\top - \mathbf{D}_k^{(1)}(\mathbf{D}_k^{(1)})^\top\|_F \\ & \lesssim_P \{[n\lambda_1(\text{cov}(\mathbf{d}_k^{(1)}))]^{1/2} + \delta_\eta[n\lambda_1(\text{cov}(\mathbf{x}_k))]^{1/2}\}\delta_\eta[n\lambda_1(\text{cov}(\mathbf{x}_k))]^{1/2}. \end{aligned}$$

Using the above inequality, (88) and the triangle inequality yields

$$\begin{aligned} & \|n^{-1}\widehat{\mathbf{D}}_k^{(1)}(\widehat{\mathbf{D}}_k^{(1)})^\top - \text{cov}(\mathbf{d}_k^{(1)})\|_F \\ & \leq \sqrt{3r_k}\|n^{-1}\widehat{\mathbf{D}}_k^{(1)}(\widehat{\mathbf{D}}_k^{(1)})^\top - \text{cov}(\mathbf{d}_k^{(1)})\|_2 \\ & \lesssim_P \{[n\lambda_1(\text{cov}(\mathbf{d}_k^{(1)}))]^{1/2} + \delta_\eta[n\lambda_1(\text{cov}(\mathbf{x}_k))]^{1/2}\}\delta_\eta[n\lambda_1(\text{cov}(\mathbf{x}_k))]^{1/2}/n + \lambda_1(\text{cov}(\mathbf{d}_k^{(1)}))n^{-1/2} \\ & \lesssim_P \delta_\eta\lambda_1(\text{cov}(\mathbf{x}_k)), \end{aligned} \quad (91)$$

where we used

$$\begin{aligned} \lambda_1(\text{cov}(\mathbf{d}_k)) & \leq \text{tr}(\text{cov}(\mathbf{d}_k)) = \text{tr}(\text{cov}(\mathbf{x}_k - \mathbf{c}_k)) \\ & \leq \text{tr}(\text{cov}(\mathbf{x}_k)) + \text{tr}(\text{cov}(\mathbf{c}_k)) + 2|\text{tr}(\text{cov}(\mathbf{x}_k, \mathbf{c}_k))| \\ & \lesssim_P \lambda_1(\text{cov}(\mathbf{x}_k)) \end{aligned} \quad (92)$$

following from

$$\begin{aligned} \text{tr}(\text{cov}(\mathbf{c}_k)) & \leq |\mathcal{I}_0|\|\text{cov}(\mathbf{c}_k)\|_2 \\ & = |\mathcal{I}_0|\|\mathbf{V}_{xk}\Lambda_{xk}^{1/2}\mathbf{H}_k^\top[\text{cov}(\mathbf{z}_k^{\mathcal{I}_0})]^\dagger\mathbf{A}\mathbf{N}\text{cov}(\mathbf{f})(\mathbf{V}_{xk}\Lambda_{xk}^{1/2}\mathbf{H}_k^\top[\text{cov}(\mathbf{z}_k^{\mathcal{I}_0})]^\dagger\mathbf{A}\mathbf{N})^\top\|_2 \\ & \lesssim_P \lambda_1(\text{cov}(\mathbf{x}_k)) \end{aligned}$$

and

$$\begin{aligned} |\text{tr}(\text{cov}(\mathbf{x}_k, \mathbf{c}_k))| & = \sum_{i=1}^{p_k} |\text{cov}(\mathbf{x}_k^{[i]}, \mathbf{c}_k^{[i]})| \leq \sum_{i=1}^{p_k} [\text{var}(\mathbf{x}_k^{[i]})]^{1/2}[\text{var}((\mathbf{c}_k^{[i]}))]^{1/2} \\ & \leq [\sum_{i=1}^{p_k} \text{var}(\mathbf{x}_k^{[i]})]^{1/2}[\sum_{i=1}^{p_k} \text{var}(\mathbf{c}_k^{[i]})]^{1/2} = [\text{tr}(\text{cov}(\mathbf{x}_k))\text{tr}(\text{cov}(\mathbf{c}_k))]^{1/2} \\ & \lesssim_P \lambda_1(\text{cov}(\mathbf{x}_k)). \end{aligned}$$

Denote $r_k^{(t)} = \text{rank}(\text{cov}(\mathbf{d}_k^{(t)}))$. By Theorem 2 in Yu et al. (2015), (91), and the condition that $\lambda_{k,1}^{(1)} > \kappa^{(1)}\lambda_{r_k}(\text{cov}(\mathbf{x}_k))$, $\lambda_{k,1}^{(1)} \asymp \lambda_{k,m_k^{(1)}}^{(1)}$, and $(\lambda_{k,\ell}^{(1)} - \lambda_{k,\ell+1}^{(1)})/\lambda_{k,\ell}^{(1)} \geq \delta^{(1)}$ for $1 \leq \ell \leq m_k^{(1)}$, we have that there exists $\widehat{\mathbf{V}}_{d_k^{(1)}} \in \mathbb{R}^{p_k \times r_k^{(1)}}$, whose columns are the left-singular vectors of $n^{-1}\widehat{\mathbf{D}}_k^{(1)}(\widehat{\mathbf{D}}_k^{(1)})^\top$ corresponding to its $r_k^{(1)}$ largest singular values, such that

$$\|\widehat{\mathbf{V}}_{d_k^{(1)}} - \mathbf{V}_{d_k^{(1)}}\|_F \lesssim_P \delta_\eta. \quad (93)$$

From Weyl's inequality and (91),

$$\|\widehat{\Lambda}_{d_k^{(1)}} - \Lambda_{d_k^{(1)}}\|_{\max} \leq \|n^{-1}\widehat{\mathbf{D}}_k^{(1)}(\widehat{\mathbf{D}}_k^{(1)})^\top - \text{cov}(\mathbf{d}_k^{(1)})\|_2 \lesssim_P \delta_\eta\lambda_1(\text{cov}(\mathbf{x}_k)), \quad (94)$$

where $\widehat{\Lambda}_{d_k^{(1)}} \in \mathbb{R}^{r_k^{(1)} \times r_k^{(1)}}$ is a diagonal matrix with nonincreasing diagonal elements being the $r_k^{(1)}$ largest singular values of $n^{-1}\widehat{\mathbf{D}}_k^{(1)}(\widehat{\mathbf{D}}_k^{(1)})^\top$. Then by $\delta_\eta = o(1)$ and $\lambda_{r_k^{(1)}}(\text{cov}(\mathbf{d}_k^{(1)})) \asymp \lambda_1(\text{cov}(\mathbf{d}_k^{(1)})) > \kappa_*^{(1)}\lambda_{r_k}(\text{cov}(\mathbf{x}_k)) \asymp \lambda_1(\text{cov}(\mathbf{x}_k))$, for $1 \leq \ell \leq r_k^{(1)}$ we have

$$\widehat{\Lambda}_{d_k^{(1)}}^{[\ell,\ell]} \geq \Lambda_{d_k^{(1)}}^{[\ell,\ell]} - |\widehat{\Lambda}_{d_k^{(1)}}^{[\ell,\ell]} - \Lambda_{d_k^{(1)}}^{[\ell,\ell]}| \geq \kappa_*^{(1)}(1 - o_P(1))\lambda_{r_k}(\text{cov}(\mathbf{x}_k)) \quad (95)$$

with a constant $\kappa_*^{(1)} > 0$, and consequently from the mean value theorem,

$$\begin{aligned} \|\widehat{\Lambda}_{d_k^{(1)}}^{1/2} - \Lambda_{d_k^{(1)}}^{1/2}\|_{\max} &\leq \frac{1}{2}[\kappa_*^{(1)}(1 - o_P(1))\lambda_{r_k}(\text{cov}(\mathbf{x}_k))]^{-1/2}\|\widehat{\Lambda}_{d_k^{(1)}} - \Lambda_{d_k^{(1)}}\|_{\max} \\ &\lesssim_P \delta_\eta \lambda_1^{1/2}(\text{cov}(\mathbf{x}_k)). \end{aligned} \quad (96)$$

and

$$\begin{aligned} \|(\widehat{\Lambda}_{d_k^{(1)}}^{1/2})^\dagger - \Lambda_{d_k^{(1)}}^{-1/2}\|_{\max} &\leq \frac{1}{2}[\kappa_*^{(1)}(1 - o_P(1))\lambda_{r_k}(\text{cov}(\mathbf{x}_k))]^{-3/2}\|\widehat{\Lambda}_{d_k^{(1)}} - \Lambda_{d_k^{(1)}}\|_{\max} \\ &\lesssim_P \delta_\eta \lambda_1^{-1/2}(\text{cov}(\mathbf{x}_k)). \end{aligned} \quad (97)$$

By (50), (93), (96) and (97),

$$\|\widehat{\mathbf{V}}_{d_k^{(1)}}\widehat{\Lambda}_{d_k^{(1)}}^{1/2} - \mathbf{V}_{d_k^{(1)}}\Lambda_{d_k^{(1)}}^{1/2}\|_2 \lesssim_P \delta_\eta \lambda_1^{1/2}(\text{cov}(\mathbf{x}_k)) \quad (98)$$

and

$$\|(\widehat{\Lambda}_{d_k^{(1)}}^{1/2})^\dagger \widehat{\mathbf{V}}_{d_k^{(1)}}^\top - \Lambda_{d_k^{(1)}}^{-1/2} \mathbf{V}_{d_k^{(1)}}^\top\|_2 \lesssim_P \delta_\eta \lambda_1^{-1/2}(\text{cov}(\mathbf{x}_k)). \quad (99)$$

Define $\widehat{\mathbf{F}}_k^{(t)} = (\widehat{\Lambda}_{d_k^{(t)}}^{1/2})^\dagger \widehat{\mathbf{V}}_{d_k^{(t)}}^\top \widehat{\mathbf{D}}_k^{(t)}$. By (50), (89), (90) and (99),

$$\|\widehat{\mathbf{F}}_k^{(1)} - \mathbf{F}_k^{(1)}\|_2 = \|(\widehat{\Lambda}_{d_k^{(1)}}^{1/2})^\dagger \widehat{\mathbf{V}}_{d_k^{(1)}}^\top \widehat{\mathbf{D}}_k^{(1)} - \Lambda_{d_k^{(1)}}^{-1/2} \mathbf{V}_{d_k^{(1)}}^\top \mathbf{D}_k^{(1)}\|_2 \lesssim_P \delta_\eta n^{1/2}. \quad (100)$$

Then by (50) again, $\|n^{-1}\widehat{\mathbf{F}}_j^{(1)}(\widehat{\mathbf{F}}_k^{(1)})^\top - n^{-1}\mathbf{F}_j^{(1)}(\mathbf{F}_k^{(1)})^\top\|_2 \lesssim_P \delta_\eta$. Using the above inequality, (87) and the triangle inequality yields

$$\|n^{-1}\widehat{\mathbf{F}}_j^{(1)}(\widehat{\mathbf{F}}_k^{(1)})^\top - \text{cov}(\mathbf{f}_j^{(1)}, \mathbf{f}_k^{(1)})\|_2 \lesssim_P \delta_\eta. \quad (101)$$

From the central limit theorem, $\|\mathbf{F}_k^{(1)}(\mathbf{F}_k^{(1)})^\top/n - \mathbf{I}_{r_k^{(1)} \times r_k^{(1)}}\|_{\max} = O_P(n^{-1/2})$ and thus

$$\|\mathbf{F}_k^{(1)}\|_F^2 = \text{tr}(\mathbf{F}_k^{(1)}(\mathbf{F}_k^{(1)})^\top) = O_P(\sqrt{n}). \quad (102)$$

Following parts 2 and 3 in the proof of Theorem 5 with (90), (91), (92), (94), (95), (98), (100), (101) and (102), we can obtain the error bounds given in (31) and (32) for $T = 1$.

Now we consider to prove (33) for $T = 1$. By $\|\text{cov}(\mathbf{x}_k)\|_{\max} \leq r_k \kappa_B^2 \lambda_{k,1}/p_k$ (from Assumption 1 (iv)) and (86), we have

$$\begin{aligned} \|\text{cov}(\mathbf{d}_k)\|_{\max} &= \|\text{cov}(\mathbf{x}_k - \mathbf{c}_k)\|_{\max} \leq \|\text{cov}(\mathbf{x}_k)\|_{\max} + \|\text{cov}(\mathbf{c}_k)\|_{\max} + 2\|\text{cov}(\mathbf{x}_k, \mathbf{c}_k)\|_{\max} \\ &\leq \|\text{cov}(\mathbf{x}_k)\|_{\max} + \|\text{cov}(\mathbf{c}_k)\|_{\max} + 2 \max_{1 \leq i, j \leq p_k} [\text{var}(\mathbf{x}_k^{[i]}) \text{var}(\mathbf{c}_k^{[j]})]^{1/2} \\ &\lesssim_P \lambda_{k,1}/p_k. \end{aligned} \quad (103)$$

Then by (79), $\lambda_{k,1} \asymp \lambda_{k,r_k}$, and $\kappa^{(1)}\lambda_{r_k}(\text{cov}(\mathbf{x}_k))\|\mathbf{V}_{d_k^{(1)}}\|_{\max}^2 \leq \lambda_1(\text{cov}(\mathbf{d}_k))\|\mathbf{V}_{d_k^{(1)}}\|_{\max}^2 \asymp \lambda_{r_k^{(1)}}(\text{cov}(\mathbf{d}_k))\|\mathbf{V}_{d_k^{(1)}}\|_{\max}^2 \leq \max_{1 \leq i \leq p_k} \sum_{j=1}^{r_k^{(1)}} (\mathbf{V}_{d_k^{(1)}}^{[i,j]})^2 \lambda_j(\text{cov}(\mathbf{d}_k)) = \max_{1 \leq i \leq p_k} \text{var}(\mathbf{d}_k^{[i]}) \lesssim_P \lambda_{k,1}/p_k$, we have

$$\|\mathbf{V}_{d_k^{(1)}}\|_{\max} \lesssim_P 1/\sqrt{p_k}. \quad (104)$$

Then following part 4 in the proof of Theorem 5 with (103), (104), (94), (96) and (92), we can obtain the error bound in (33) for $T = 1$.

The proof of (31)–(33) for any fixed $T \geq 1$ follows the same way as that for $T = 1$. ■

Appendix C. Additional Simulation Results

In Setup 1.1, the angle $\theta_z = 10^\circ, 20^\circ, 30^\circ, 40^\circ, 50^\circ, 60^\circ, 70^\circ$ corresponds to $\text{PVE}_c(\mathbf{x}_k) = 0.853, 0.702, 0.552, 0.409, 0.279, 0.167, 0.079$ for all $k \in \{1, 2, 3\}$. In Setup 2.1, the covariance matrix $\text{cov}(\mathbf{f}) \in \mathbb{R}^{15 \times 15}$ has blocks

$$\begin{aligned} & \text{cov}(\mathbf{f}_1, \mathbf{f}_2) \\ &= \begin{bmatrix} 0.02498103503160578 & -0.3734791596502449 & -0.1482674122573037 & -0.3913807076061239 & -0.05845072081373771 \\ 0.1298912403724416 & -0.2915966482089937 & -0.703223066831662 & -0.286977394728156 & -0.07037562289439672 \\ -0.4691315902716665 & -0.02216628581934877 & -0.05789731182102772 & -0.1224434530178697 & 0.7359965879693088 \\ -0.005270967060252731 & -0.1916047000827934 & 0.1572469950904809 & -0.1862928969932901 & 0.0648022978041196 \\ 0.3309749556233325 & 0.2910731038141944 & -0.2222302484678626 & 0.4183644600274041 & -0.09116219316544609 \end{bmatrix}, \\ & \text{cov}(\mathbf{f}_1, \mathbf{f}_3) \\ &= \begin{bmatrix} -0.1652455953442644 & 0.07288409202801582 & 0.4797927991048995 & -0.1974810941368655 & 0.2123320697504773 \\ -0.3889488816571995 & 0.05377416249857463 & 0.5653871787847853 & 0.03845218160536631 & -0.2069628634535125 \\ 0.4125592431747815 & -0.7372033575312142 & 0.2721804829221633 & -0.0862772040030661 & -0.2227478031028198 \\ -0.02345535210198419 & -0.1075518721538277 & 0.1394751370539585 & -0.1625882523272944 & 0.3301641568167817 \\ -0.3328426143159536 & -0.09361178321406048 & -0.4483940610130605 & 0.3455811570541347 & -0.09767404221183135 \end{bmatrix}, \\ & \text{cov}(\mathbf{f}_2, \mathbf{f}_3) \\ &= \begin{bmatrix} -0.1234093117538375 & 0.2223022967058531 & -0.3593383789512091 & 0.04344070064196999 & 0.2617381817815529 \\ -0.09993460814692552 & -0.008819786526375878 & -0.4039397802979183 & 0.2933537865045707 & -0.2650032054127345 \\ 0.5075563895372593 & -0.1098865559264541 & -0.4771360952896037 & -0.1119099874049149 & 0.2079731636733454 \\ -0.08232391689469482 & -0.01395485249078317 & -0.5724368834706903 & 0.3121430368957581 & -0.1821568224740747 \\ 0.3937761144502051 & -0.699822772013208 & 0.1161733947993463 & -0.04568041770157075 & -0.1795827017135321 \end{bmatrix}, \end{aligned}$$

and $\text{cov}(\mathbf{f}_k) = \mathbf{I}_{5 \times 5}$ for $k = 1, 2, 3$. Figures 9–14 show the additional simulation results for Setups 1.1–2.2. The result analysis described in Section 4.2 also holds here.

DECOMPOSITION-BASED GENERALIZED CANONICAL CORRELATION ANALYSIS

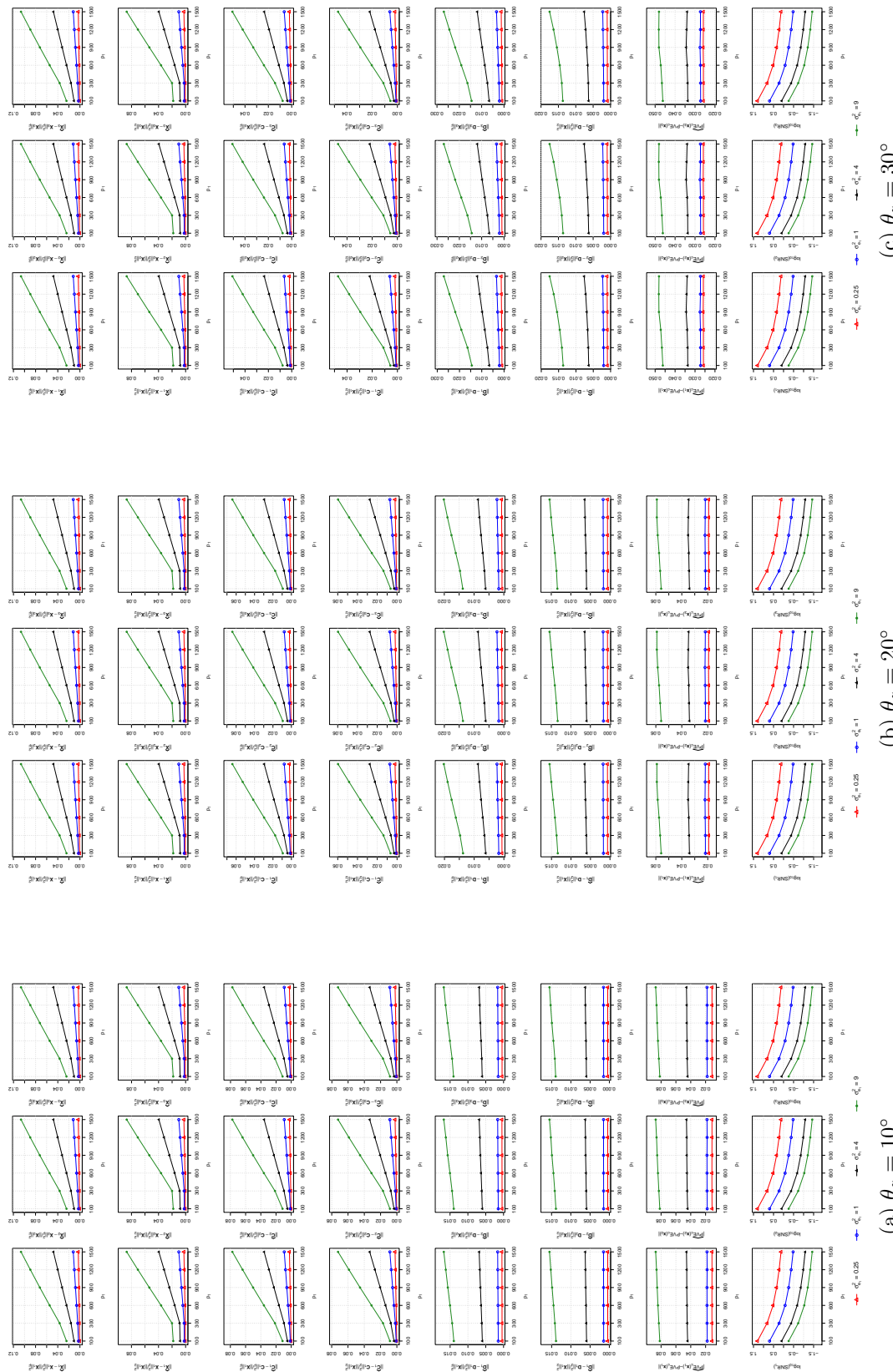


Figure 9: Average errors of D-GCCA estimates over 1000 replications for Setup 1.1 with $\theta_z \in \{10^\circ, 20^\circ, 30^\circ\}$.

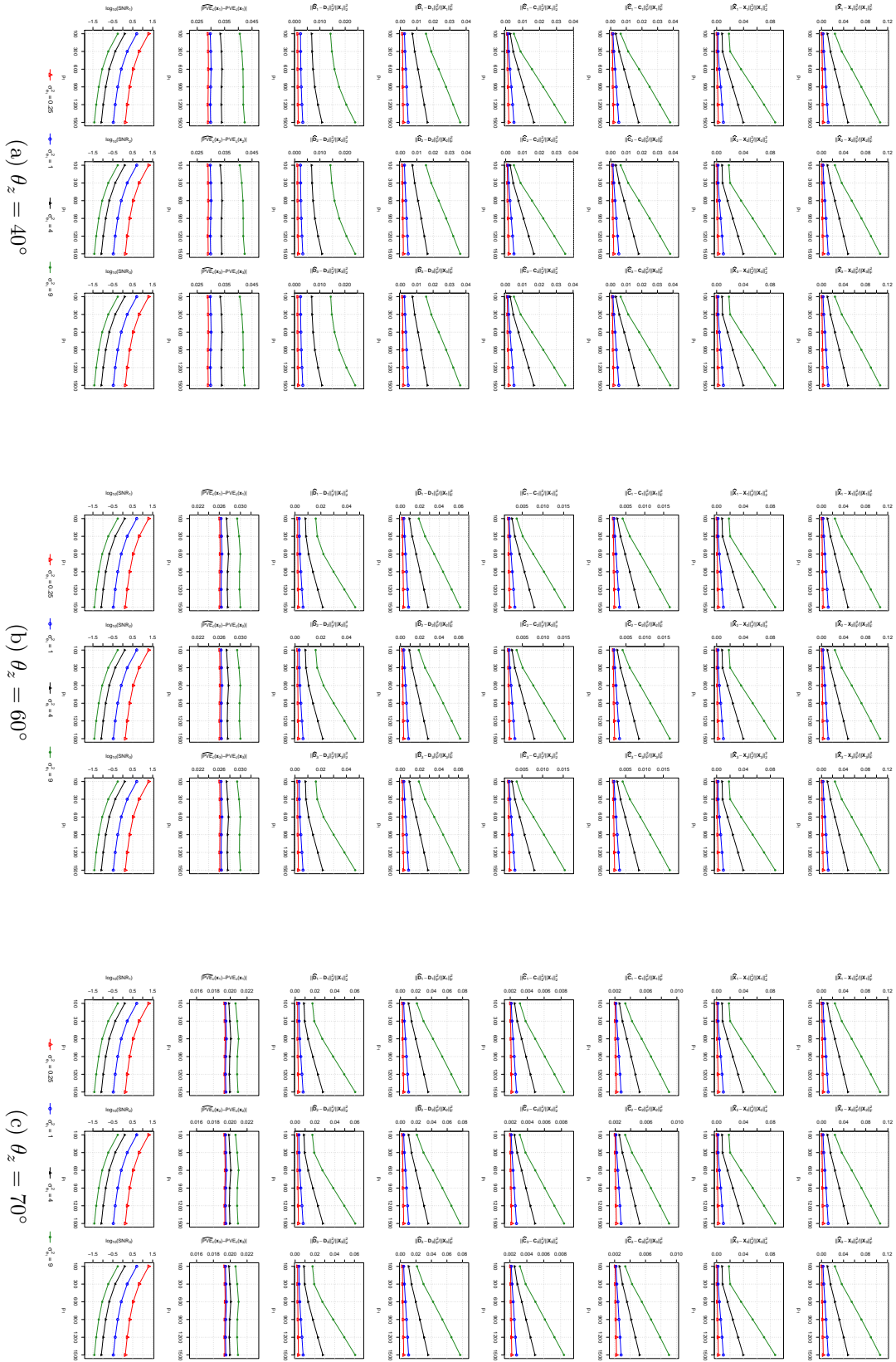


Figure 10: Average errors of D-GCCA estimates over 1000 replications for Setup 1.1 with $\theta_z \in \{40^\circ, 60^\circ, 70^\circ\}$.

DECOMPOSITION-BASED GENERALIZED CANONICAL CORRELATION ANALYSIS

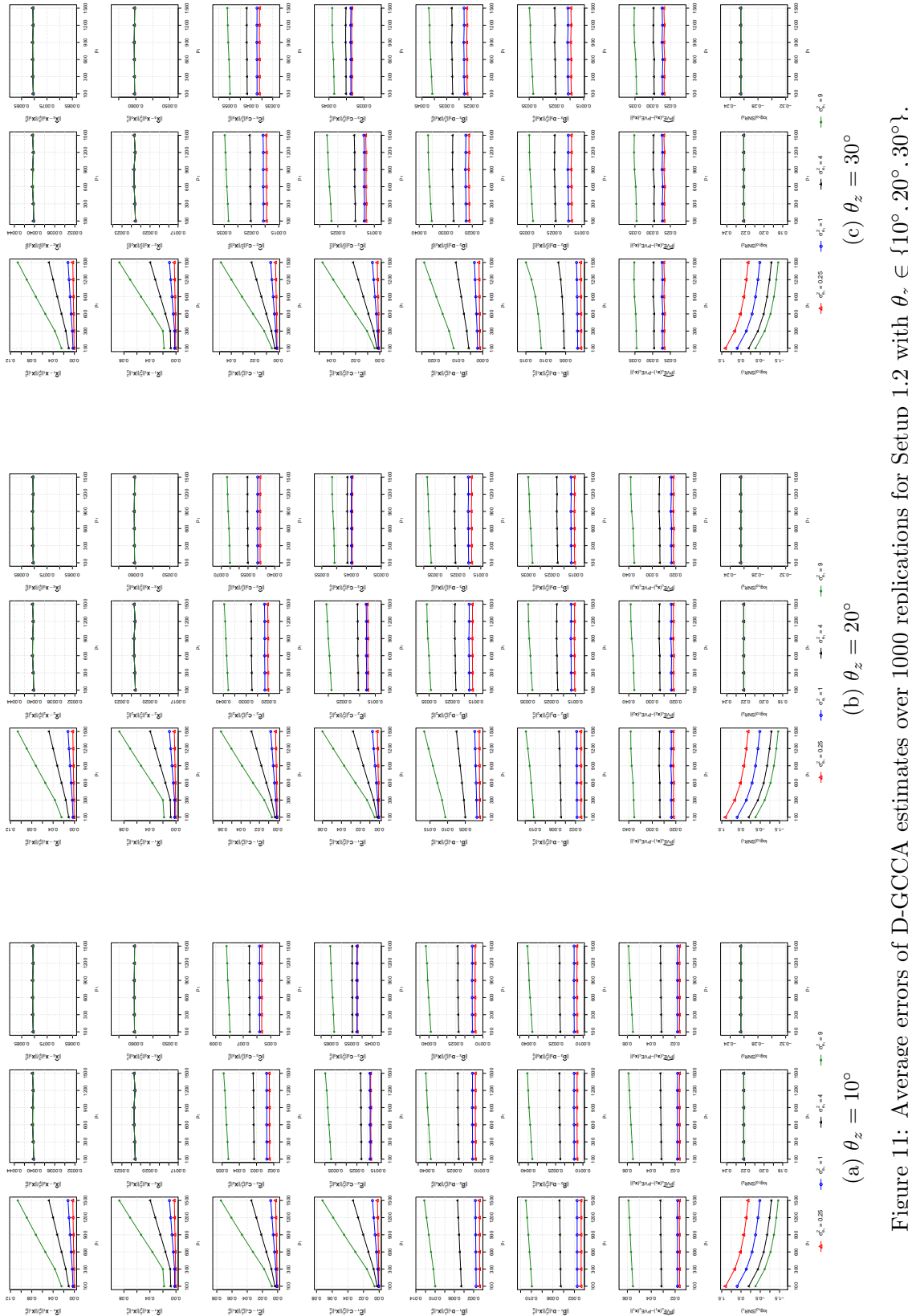


Figure 11: Average errors of D-GCCA estimates over 1000 replications for Setup 1.2 with $\theta_z \in \{10^\circ, 20^\circ, 30^\circ\}$.

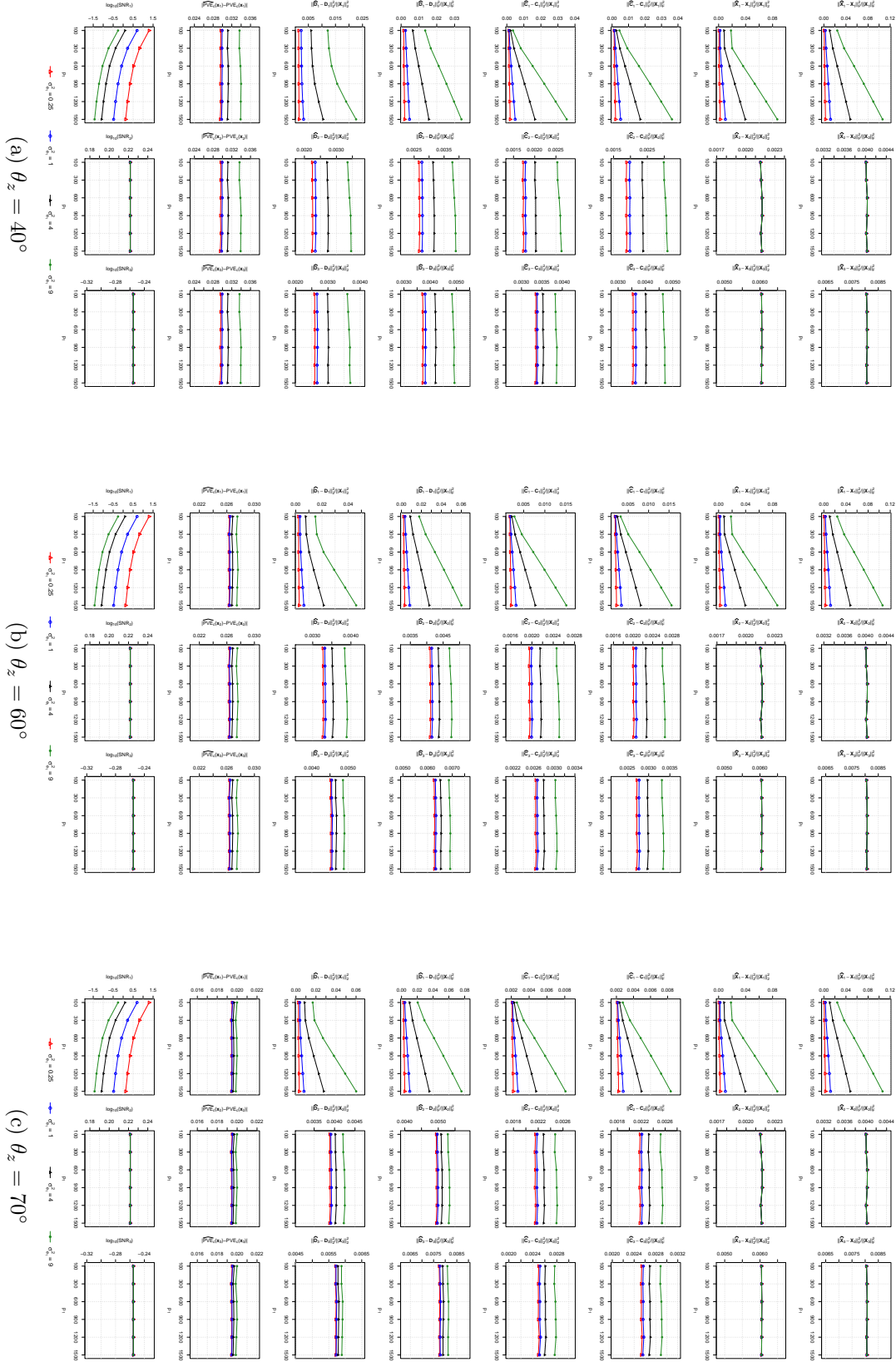


Figure 12: Average errors of D-GCCA estimates over 1000 replications for Setup 1.2 with $\theta_z \in \{40^\circ, 60^\circ, 70^\circ\}$.

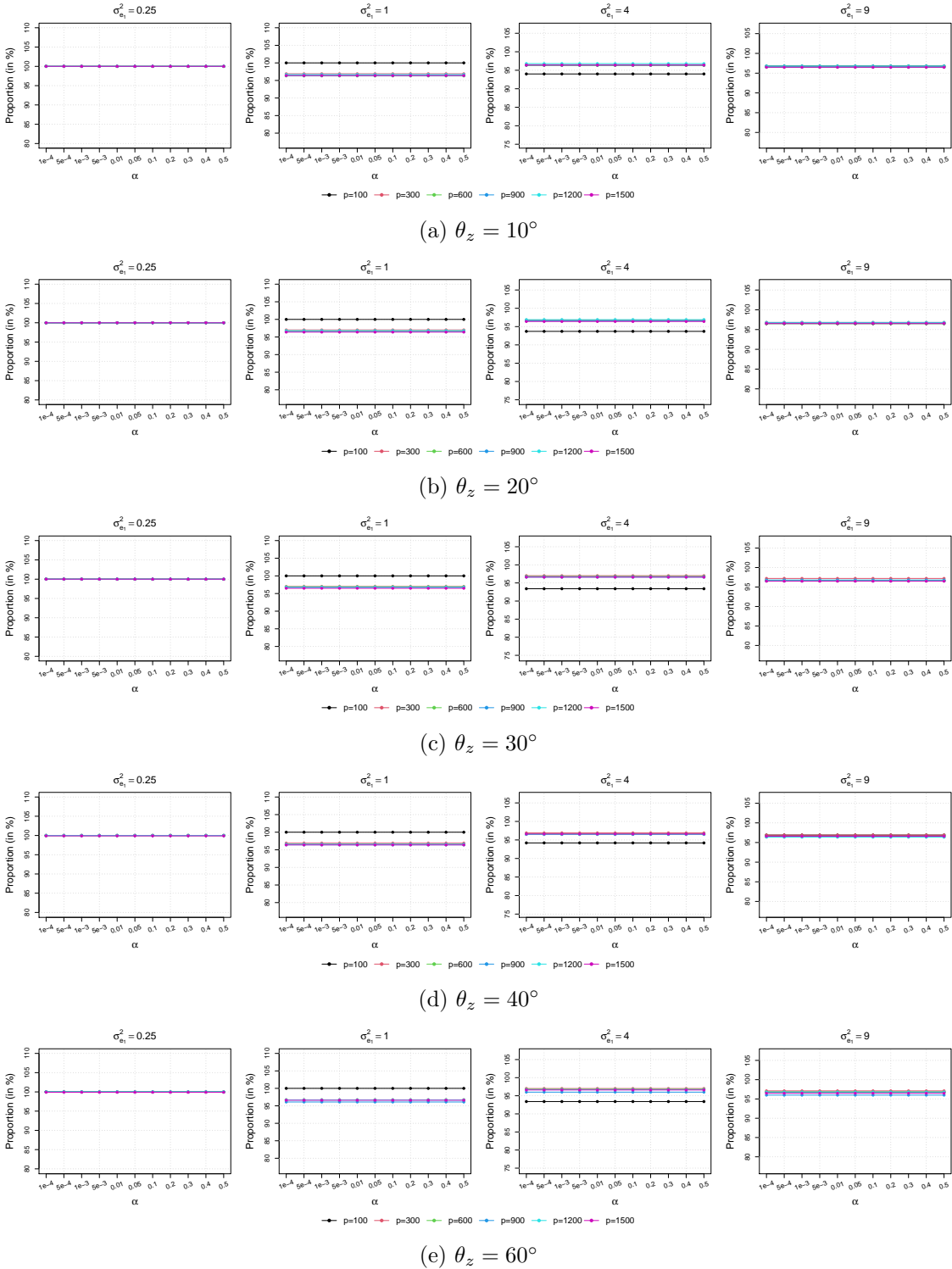


Figure 13: The proportion of 1000 simulation replications of Setup 1.1 where all nuisance parameters of D-GCCA are correctly selected. The nuisance parameters are selected using the approach in Section 3.3 with a significance level α uniformly applied to all tests.

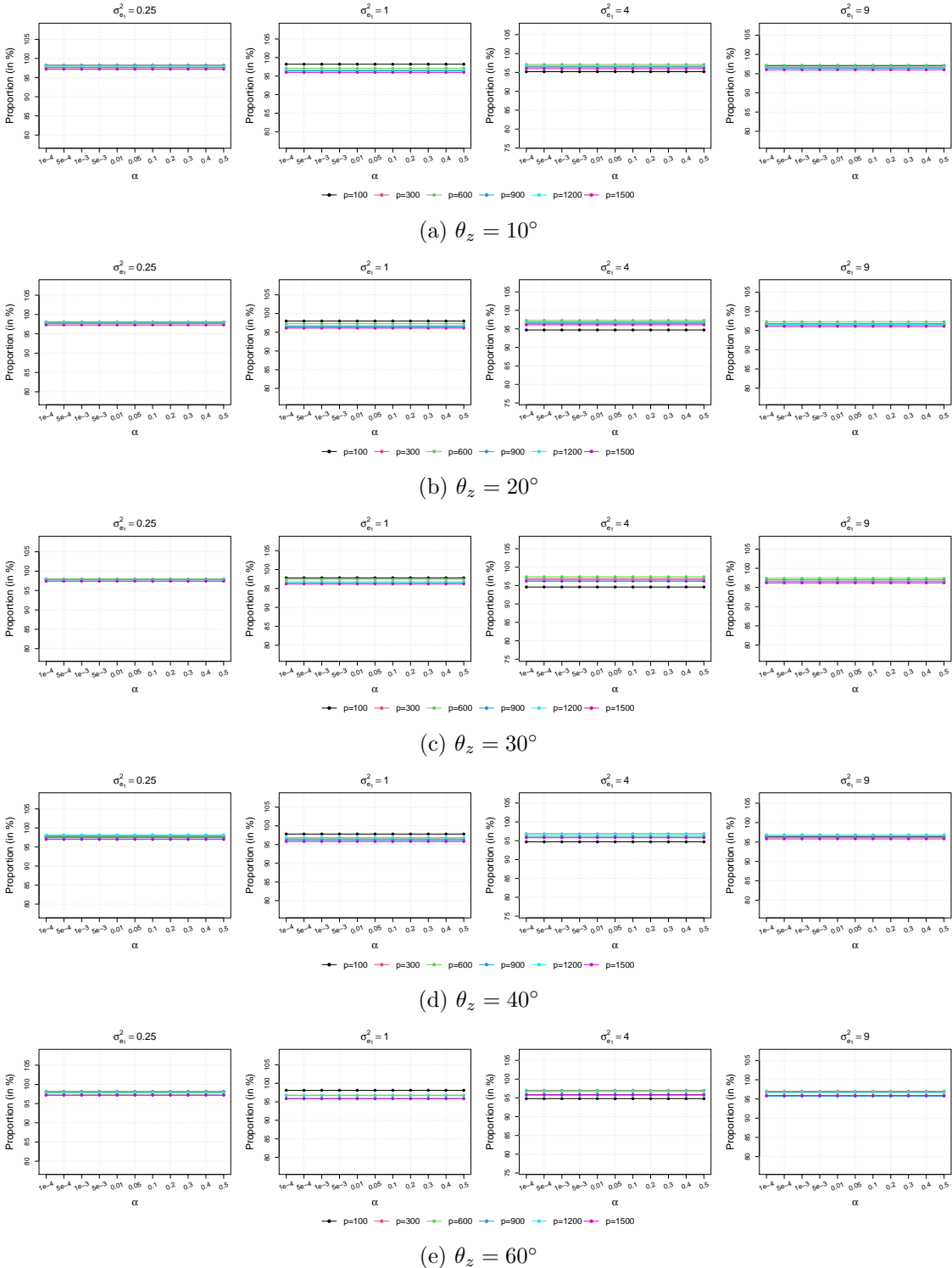


Figure 14: The proportion of 1000 simulation replications of Setup 1.2 where all nuisance parameters of D-GCCA are correctly selected. The nuisance parameters are selected using the approach in Section 3.3 with a significance level α uniformly applied to all tests.

References

- Jushan Bai. Inferential theory for factor models of large dimensions. *Econometrica*, 71(1):135–171, 2003.
- Jushan Bai, Serena Ng, et al. Large dimensional factor analysis. *Foundations and Trends in Econometrics*, 3(2):89–163, 2008.
- D. M. Barch, G. C. Burgess, M. P. Harms, S. E. Petersen, B. L. Schlaggar, M. Corbetta, M. F. Glasser, S. Curtiss, S. Dixit, C. Feldt, et al. Function in the human connectome: task-fMRI and individual differences in behavior. *Neuroimage*, 80:169–189, 2013.
- M. S. Bartlett. The statistical significance of canonical correlations. *Biometrika*, 32:29–37, 1941.
- Y. Benjamini and Y. Hochberg. Controlling the false discovery rate: a practical and powerful approach to multiple testing. *Journal of the Royal Statistical Society: Series B*, 57(1):289–300, 1995.
- A. Benton, H. Khayrallah, B. Gujral, D. A. Reisinger, S. Zhang, and R. Arora. Deep generalized canonical correlation analysis. In *Proceedings of the 4th Workshop on Representation Learning for NLP*, pages 1–6, 2019.
- Peter J Bickel and Elizaveta Levina. Covariance regularization by thresholding. *The Annals of Statistics*, 36(6):2577–2604, 2008.
- A. Birnbaum, I. M. Johnstone, B. Nadler, and D. Paul. Minimax bounds for sparse PCA with noisy high-dimensional data. *The Annals of Statistics*, 41(3):1055–1084, 2013.
- R. L. Buckner, F. M. Krienen, A. Castellanos, J. C. Diaz, and B. T. Thomas Yeo. The organization of the human cerebellum estimated by intrinsic functional connectivity. *Journal of Neurophysiology*, 106(5):2322–2345, 2011.
- C. R. Cabanski, Y. Qi, X. Yin, E. Bair, M. C. Hayward, C. Fan, J. Li, M. D. Wilkerson, J. S. Marron, C. M. Perou, and D. N. Hayes. SWISS MADE: Standardized within class sum of squares to evaluate methodologies and dataset elements. *PLoS ONE*, 5(3):e9905, 2010.
- Jia Cai and Junyi Huo. Sparse generalized canonical correlation analysis via linearized bregman method. *Communications on Pure & Applied Analysis*, 19(8):3933, 2020.
- T. Caliński and M. Krzyśko. A closed testing procedure for canonical correlations. *Communications in Statistics - Theory and Methods*, 34(5):1105–1116, 2005.
- J. D. Campbell, C. Yau, R. Bowlby, Y. Liu, K. Brennan, H. Fan, A. M. Taylor, C. Wang, V. Walter, R. Akbani, et al. Genomic, pathway network, and immunologic features distinguishing squamous carcinomas. *Cell Reports*, 23(1):194–212, 2018.
- J. D. Carroll. Generalization of canonical correlation analysis to three or more sets of variables. In *Proceedings of the 76th Annual Convention of the American Psychological Association*, pages 227–228, 1968.

- G. Chamberlain and M. Rothschild. Arbitrage, factor structure, and mean-variance analysis on large asset markets. *Econometrica*, 51:1281–1304, 1983.
- Q. Chen and Z. Fang. Improved inference on the rank of a matrix. *Quantitative Economics*, 10:1787–1824, 2019.
- G. Ciriello, M. L. Gatzka, A. H. Beck, M. D. Wilkerson, S. K. Rhie, A. Pastore, H. Zhang, M. McLellan, C. Yau, C. Kandoth, and R. Bowlby. Comprehensive molecular portraits of invasive lobular breast cancer. *Cell*, 163(2):506–519, 2015.
- K. L. Crawford, S. C. Neu, and A. W. Toga. The image and data archive at the laboratory of neuro imaging. *Neuroimage*, 124:1080–1083, 2016.
- Tobias Dahl and Tormod Næs. A bridge between tucker-1 and carroll’s generalized canonical analysis. *Computational Statistics & Data Analysis*, 50(11):3086–3098, 2006.
- C. J. DiCiccio and J. P. Romano. Robust permutation tests for correlation and regression coefficients. *Journal of the American Statistical Association*, 112:1211–1220, 2017.
- Leo Dorst, Daniel Fontijne, and Stephen Mann. *Geometric algebra for computer science: an object-oriented approach to geometry*. Elsevier, 2010.
- B. Draper, M. Kirby, J. Marks, T. Marrinan, and C. Peterson. A flag representation for finite collections of subspaces of mixed dimensions. *Linear Algebra and its Applications*, 451:15–32, 2014.
- B. Efron and R. J. Tibshirani. *An Introduction to the Bootstrap*. Chapman and Hall, New York, 1993.
- J. Fan, Y. Liao, and M. Mincheva. Large covariance estimation by thresholding principal orthogonal complements. *Journal of the Royal Statistical Society, Series B*, 75(4):603–680, 2013.
- Jianqing Fan, Weichen Wang, and Yiqiao Zhong. An ℓ_∞ eigenvector perturbation bound and its application to robust covariance estimation. *Journal of Machine Learning Research*, 18(207):1–42, 2018.
- Q. Feng, M. Jiang, J. Hannig, and J. S. Marron. Angle-based joint and individual variation explained. *Journal of Multivariate Analysis*, 166:241–265, 2018.
- Xiao Fu, Kejun Huang, Mingyi Hong, Nicholas D Sidiropoulos, and Anthony Man-Cho So. Scalable and flexible multiview max-var canonical correlation analysis. *IEEE Transactions on Signal Processing*, 65(16):4150–4165, 2017.
- Chenfeng Guo and Dongrui Wu. Canonical correlation analysis (cca) based multi-view learning: An overview. *arXiv preprint arXiv:1907.01693*, 2019.
- A. K. Gupta and T. Varga. Rank of a quadratic form in an elliptically contoured matrix random variable. *Statistics & probability letters*, 12(2):131–134, 1991.

- T. Hastie, R. Tibshirani, and J. Friedman. *The Elements of Statistical Learning: Data Mining, Inference, and Prediction*. Springer, New York, second edition, 2009.
- David Hestenes and Garret Sobczyk. *Clifford algebra to geometric calculus*. D. Reidel Publishing Co., Dordrecht, 1984.
- K. A. Hoadley, C. Yau, T. Hinoue, D. M. Wolf, A. J. Lazar, E. Drill, R. Shen, A. M. Taylor, A. D. Cherniack, V. Thorsson, et al. Cell-of-origin patterns dominate the molecular classification of 10,000 tumors from 33 types of cancer. *Cell*, 173(2):291–304, 2018.
- R. A. Horn and C. R. Johnson. *Topics in Matrix Analysis*. Cambridge University Press, Cambridge, 1994.
- Paul Horst. Relations among m sets of measures. *Psychometrika*, 26:129–149, 1961.
- H. Hotelling. Relations between two sets of variates. *Biometrika*, 28(3/4):321–377, 1936.
- H. Huang. Asymptotic behavior of support vector machine for spiked population model. *Journal of Machine Learning Research*, 18(45):1–21, 2017.
- M. A. Jensen, V. Ferretti, R. L. Grossman, and L. M. Staudt. The NCI Genomic Data Commons as an engine for precision medicine. *Blood*, 130:453–459, 2017.
- J. R. Kettenring. Canonical analysis of several sets of variables. *Biometrika*, 58(3):433–451, 1971.
- Henk AL Kiers, Robert Cleroux, and Jos MF Ten Berge. Generalized canonical analysis based on optimizing matrix correlations and a relation with idioscal. *Computational statistics & data analysis*, 18(3):331–340, 1994.
- N. Kishore Kumar and J. Schneider. Literature survey on low rank approximation of matrices. *Linear and Multilinear Algebra*, 65(11):2212–2244, 2017.
- D. C. Koboldt, R. S. Fulton, M. D. McLellan, Heather S., Joelle Kalicki-Veizer, J. F. McMichael, L. L. Fulton, D. J. Dooling, D. Li, et al. Comprehensive molecular portraits of human breast tumours. *Nature*, 490(7418):61–70, 2012.
- D. N. Lawley. Tests of significance in canonical analysis. *Biometrika*, 46(1/2):59–66, 1959.
- Y. Li, F. Wu, and A. Ngom. A review on machine learning principles for multi-view biological data integration. *Briefings in Bioinformatics*, 19:325–340, 2018.
- E. F. Lock and D. B. Dunson. Bayesian consensus clustering. *Bioinformatics*, 29(20):2610–2616, 2013.
- E. F. Lock, K. A. Hoadley, J. S. Marron, and A. B. Nobel. Joint and individual variation explained (JIVE) for integrated analysis of multiple data types. *Annals of Applied Statistics*, 7(1):523–542, 2013.
- T. Löfstedt and J. Trygg. OnPLS—a novel multiblock method for the modelling of predictive and orthogonal variation. *Journal of Chemometrics*, 25(8):441–455, 2011.

- L. Meng and B. Zheng. The optimal perturbation bounds of the Moore-Penrose inverse under the Frobenius norm. *Linear Algebra and its Applications*, 432(4):956–963, 2010.
- Puneet Mishra, Jean Michel Roger, Delphine Jouan-Rimbaud-Bouveresse, Alessandra Biancolillo, Federico Marini, Alison Nordon, and Douglas N Rutledge. Recent trends in multi-block data analysis in chemometrics for multi-source data integration. *TrAC Trends in Analytical Chemistry*, page 116206, 2021.
- R. R. Nadakuditi and J. W. Silverstein. Fundamental limit of sample generalized eigenvalue based detection of signals in noise using relatively few signal-bearing and noise-only samples. *IEEE Journal of Selected Topics in Signal Processing*, 4(3):468–480, 2010.
- M. J. O’Connell and E. F. Lock. R.JIVE for exploration of multi-source molecular data. *Bioinformatics*, 32(18):2877–2879, 2016.
- M. Okamoto. Distinctness of the eigenvalues of a quadratic form in a multivariate sample. *The Annals of Statistics*, 1(4):763–765, 1973.
- A. Onatski. Determining the number of factors from empirical distribution of eigenvalues. *The Review of Economics and Statistics*, 92(4):1004–1016, 2010.
- J. S. Parker, M. Mullins, M. C. Cheang, S. Leung, D. Voduc, T. Vickery, S. Davies, C. Fauzon, X. He, Z. Hu, and J. F. Quackenbush. Supervised risk predictor of breast cancer based on intrinsic subtypes. *Journal of Clinical Oncology*, 27(8):1160–1167, 2009.
- Vijay K. Rohatgi and A. K. Md. Ehsanes Saleh. *An introduction to probability and statistics*. John Wiley & Sons, Inc., Hoboken, NJ, third edition, 2015.
- Adam J Rothman, Elizaveta Levina, and Ji Zhu. Generalized thresholding of large covariance matrices. *Journal of the American Statistical Association*, 104(485):177–186, 2009.
- U. Saeed, J. Compagnone, R. I. Aviv, A. P. Strafella, S. E. Black, A. E. Lang, and M. Masellis. Imaging biomarkers in parkinson’s disease and parkinsonian syndromes: current and emerging concepts. *Translational Neurodegeneration*, 6(1):8, Mar 2017.
- Martijn Schouteden, Katrijn Van Deun, Sven Pattyn, and Iven Van Mechelen. Sca with rotation to distinguish common and distinctive information in linked data. *Behavior research methods*, 45(3):822–833, 2013.
- Hai Shu, Bin Nan, et al. Estimation of large covariance and precision matrices from temporally dependent observations. *The Annals of Statistics*, 47(3):1321–1350, 2019.
- Hai Shu, Xiao Wang, and Hongtu Zhu. D-cca: A decomposition-based canonical correlation analysis for high-dimensional datasets. *Journal of the American Statistical Association*, 115(529):292–306, 2020.
- A. K. Smilde, I. Måge, T. Næs, T. Hankemeier, M. A. Lips, H. A. L. Kiers, E. Acar, and R. Bro. Common and distinct components in data fusion. *Journal of Chemometrics*, 31(7):e2900, 2017. ISSN 1099-128X.

- Age K Smilde, Johan A Westerhuis, and Sijmen de Jong. A framework for sequential multi-block component methods. *Journal of Chemometrics: A Journal of the Chemometrics Society*, 17(6):323–337, 2003.
- Y. Song, P. J. Schreier, D. Ramírez, and T. Hasija. Canonical correlation analysis of high-dimensional data with very small sample support. *Signal Processing*, 128:449–458, 2016.
- Charles Spearman. The proof and measurement of association between two things. *The American Journal of Psychology*, 15(1):72–101, 1904.
- Arthur Tenenhaus and Michel Tenenhaus. Regularized generalized canonical correlation analysis. *Psychometrika*, 76(2):257, 2011.
- Arthur Tenenhaus and Michel Tenenhaus. Regularized generalized canonical correlation analysis for multiblock or multigroup data analysis. *European Journal of operational research*, 238(2):391–403, 2014.
- Arthur Tenenhaus, Cathy Philippe, Vincent Guillemot, Kim-Anh Le Cao, Jacques Grill, and Vincent Frouin. Variable selection for generalized canonical correlation analysis. *Biostatistics*, 15(3):569–583, 2014.
- M. Udell and A. Townsend. Why are big data matrices approximately low rank? *SIAM Journal on Mathematics of Data Science*, 1(1):144–160, 2019.
- M. van de Velden. On generalized canonical correlation analysis. In *Proceedings of the 58th World Statistical Congress*, pages 758—765, 2011.
- F. M. van der Kloet, P. Sebastián-León, A. Conesa, A. K. Smilde, and J. A. Westerhuis. Separating common from distinctive variation. *BMC bioinformatics*, 17(5):S195, 2016.
- D. C. Van Essen, S. M. Smith, D. M. Barch, T. E. J. Behrens, E. Yacoub, K. Ugurbil, and WU-Minn HCP Consortium. The WU-Minn human connectome project: an overview. *Neuroimage*, 80:62–79, 2013.
- R. Vershynin. Introduction to the non-asymptotic analysis of random matrices. In *Compressed Sensing*, pages 210–268. Cambridge University Press, Cambridge, 2012.
- W. Wang and J. Fan. Asymptotics of empirical eigenstructure for high dimensional spiked covariance. *Annals of Statistics*, 45(3):1342–1374, 2017.
- Yining Wang, Liwei Wang, Yuanzhi Li, Di He, and Tie-Yan Liu. A theoretical analysis of ndcg type ranking measures. In *Proceedings of the 26th Annual Conference on Learning Theory*, pages 25–54, 2013.
- M. W. Weiner, D. P. Veitch, P. S. Aisen, L. A. Beckett, N. J. Cairns, R. C. Green, D. Harvey, C. R. Jack, W. Jagust, E. Liu, et al. The alzheimer’s disease neuroimaging initiative: a review of papers published since its inception. *Alzheimer’s & Dementia*, 9(5):e111–e194, 2013.

- Hok Shing Wong, Li Wang, Raymond Chan, and Tieyong Zeng. Deep tensor cca for multi-view learning. *IEEE Transactions on Big Data*, 2021. doi: 10.1109/TBDBDATA.2021.3079234.
- Y. Yin, Z. Bai, and P. R. Krishnaiah. On the limit of the largest eigenvalue of the large dimensional sample covariance matrix. *Probability Theory and Related Fields*, 78(4):509–521, 1988.
- Y. Yu, T. Wang, and R. J. Samworth. A useful variant of the davis–kahan theorem for statisticians. *Biometrika*, 102(2):315–323, 2015.
- Jing Zhao, Xijiong Xie, Xin Xu, and Shiliang Sun. Multi-view learning overview: Recent progress and new challenges. *Information Fusion*, 38:43–54, 2017.
- G. Zhou, A. Cichocki, Y. Zhang, and D. P. Mandic. Group component analysis for multi-block data: Common and individual feature extraction. *IEEE Transactions on Neural Networks and Learning Systems*, 27(11):2426 – 2439, 2016.
- J. Zhou and X. He. Dimension reduction based on constrained canonical correlation and variable filtering. *The Annals of Statistics*, 36(4):1649–1668, 2008.